Offshore Energy Hub Island in the North Sea

The development of a hydrodynamic model to explore the ecological feasibility

J.V. Groot

TU Delft Delft University of Technology

Deltares Enabling Delta Life

Offshore Energy Hub Island in the North Sea

The development of a hydrodynamic model to explore the ecological feasibility

by

J.V. Groot

jvgroot@gmail.com
+316 11 09 02 08
Master of Science Student in Hydraulic Engineering
Specialisation in Coastal Engineering

Student number:	4204581	
Project duration:	01-03-2018 until 21-11-2018	
Thesis committee:	Prof. dr. ir. S.G.J. Aarninkhof	TU Delft, chair of committee
	Dr. C.A. Katsman	TU Delft
	Ir. R. Hoekstra	TU Delft & Deltares
	Ir. F. Zijl	Deltares
	Dr. L.A. van Duren	Deltares

This thesis is confidential and cannot be made public until November 21, 2018

TU Delft

Deltares
Enabling Delta Life

Preface

This thesis finalises my Master of Science program at the Delft University of Technology in 'Hydraulic Engineering', and was carried out as a graduation internship at Deltares in Delft.

I would like to express my gratitude to all members of my thesis committee for their profitable discussions and critical feedback during the entire project. A special thanks goes to Roderik, for introducing me to the available research topic and bringing me into contact with all the required expertise. Additionally, I would like to express my gratitude towards Deltares for its hospitality and all the helpful colleagues who aided me with any complication and assisted me with great hydraulic engineering expertise. In addition, I would like to thank fellow students Tim van Domburg and Lennart Keyzer for the motivational coffee breaks during the summer period.

Finally, thanks go out to my family, friends and girlfriend for the support they gave me during this research project.

Jeffrey Groot
Delft, November 2018

Abstract

To combat the emission of greenhouse gasses and the corresponding climate change, emission reduction goals have been established in the recent Paris Agreement. In order to meet these reduction goals and minimise the global average temperature increase, implementation of renewable energy sources is critical. Wind energy is one of the fastest growing renewable energy sources in the European Union, since Europe has the largest offshore wind energy capacity with its shallow shelf sea: the North Sea.

Over the last twenty years, the wind energy capacity has increased significantly to become the current second highest power generation form of the European Union. The downside to offshore wind energy however, are the high costs that come with its generation. Cable losses of alternating currents between the wind turbines and the shore become increasingly high, as the distances towards the shore increment. For long distances, this inefficiency becomes unacceptable and conversion to a direct current is deemed necessary.

A recently presented concept that aims to reduce the costs of offshore wind energy, is the concept of a large scale roll-out of interlinked offshore turbines, coordinated at an European level, including a so-called hub island. This artificial island facilitates converters, as well as a home base for engineers and large scale power storage. Technically, no big problems are expected with the construction of such artificial island. The major reason that could stop the hub island concept, is resistance from environmental organisations.

To predict ecological repercussions of an artificial island, the impact on hydrodynamic parameters most important to the bottom of the marine food chain are explored. The primary producers represent this foundation of the food chain, and are most affected by the island through changes in water stratification and residual currents. These parameters highly influence the light and nutrient availability, thereby regulating the primary production dynamics of the ecosystem.

By developing and applying the Three Dimensional Dutch Continental Shelf Flexible Mesh (3D DCSM-FM) model, the impact of an artificial island on the stratification and residual currents is explored for five case studies. Each case study comprises a $6km^2$ cylindrical island, for different North Sea locations with distinct hydrodynamic properties.

The implementation of an artificial island alters residual currents up to 10km from its position. The location determines the impact pattern, but influences remain local without any large scale North Sea impacts. Since changes in nutrient availability are only expected for large scale residual current impacts, no significant alterations in primary production dynamics are to be expected.

The impact on stratification however, can have a significant influence on the dynamics of primary production. The originally well-mixed areas remain mostly unchanged, while islands in the more stratified regions can cause significant changes in absolute stratification up to 20km from the banks, and alterations in regimes or the seasonal onset timing up to 2.5km. The location and its hydrodynamic properties are paramount to the type of expected stratification impact, and proves to be an important design parameter for ecology around an offshore energy hub island in the North Sea.

Contents

List of Figures

List of Tables

Nomenclature

Acronyms and abbreviations

3D	Three Dimensional
AC	Alternating Current
DC	Direct Current
DCSM	Dutch Continental Shelf Model
E	East
EU	European Union
FM	Flexible Mesh
GEM	Generic Ecological Model
GHG	Greenhouse Gasses
IS	Intermittently Stratified
MPIOM	Max Planck Institute Ocean Model
N	North
PM	Permanently Mixed
PS	Permanently Stratified
RMSD	Root Mean Squared Deviation
S	South
SPM	Suspended Particle Matter
SS	Seasonally Stratified
SWE	Shallow Water Equations
W	West
ZUNO	Zuiderlijke Noordzee

ρ	Density
q_0	Specific discharge
δ	Finite increment
k	Total turbulent kinetic energy
R	Reynolds number
U	Mean free stream velocity
h	Water depth
ν	Kinematic viscosity
$\overline{u}$	Tidal current amplitude
R	Radius of a cylinder
ω'	Tidal flow frequency

Units of measurement

cm	centimetre
m	metre
km	kilometre
pH	potential of hydrogen
kg	kilogram
PSU	practical salinity unit
C	Celsius
%	percentage
s	seconds
deg	degrees
mg	milligram

1 Introduction

"Environmental pollution is an incurable disease. It can only be prevented."
-Barry Commoner

Climate change is fundamentally different from most forms of pollution. Climate change does not have a direct effect on human health, does not smell and is not visible. Greenhouse gasses (GHG) cause long term pollution and affect the entire global environment. Mostly linked to the use of fossil fuels, GHG emissions have been proven to have a serious global impact (IPCC, 2013). The scientific evidence is deemed compelling and forms a basis for future emission reduction goals (Delbelke and Vis, 2016).

The fairly recent Paris Agreement aims to prevent future environmental catastrophes by decreasing the emission of GHG by "holding the increase in global average temperature to well below 2°C above pre-industrial levels and recognising that this would significantly reduce the risks and impacts of climate change" (United Nations, 2015).

The European Union (EU) is definitely on track to meet the GHG reduction targets of 2020, at which the emission must be reduced by 20%. However, the energy consumption shows a slight increase forcing the need of extra efforts to reach the near- and far-future goals of the EU (European Environment Agency, 2017).

1.1 Wind Energy

By implementing the use of renewable energy sources, the future GHG reduction goals can be met. Wind energy is one of the fastest growing renewable energy sources in the EU and currently holds second place for most used power generation form, as can be seen in Figure 1.1. The great popularity of wind energy follows from the fact that Europe has the largest offshore wind energy capacity around the world. As a result, the offshore wind energy installations show a considerable growth over the last twenty years. The downside however, are the costs that are associated with wind energy and especially offshore wind energy, it being one of the most expensive forms of renewable energy (Gerrits, 2017).

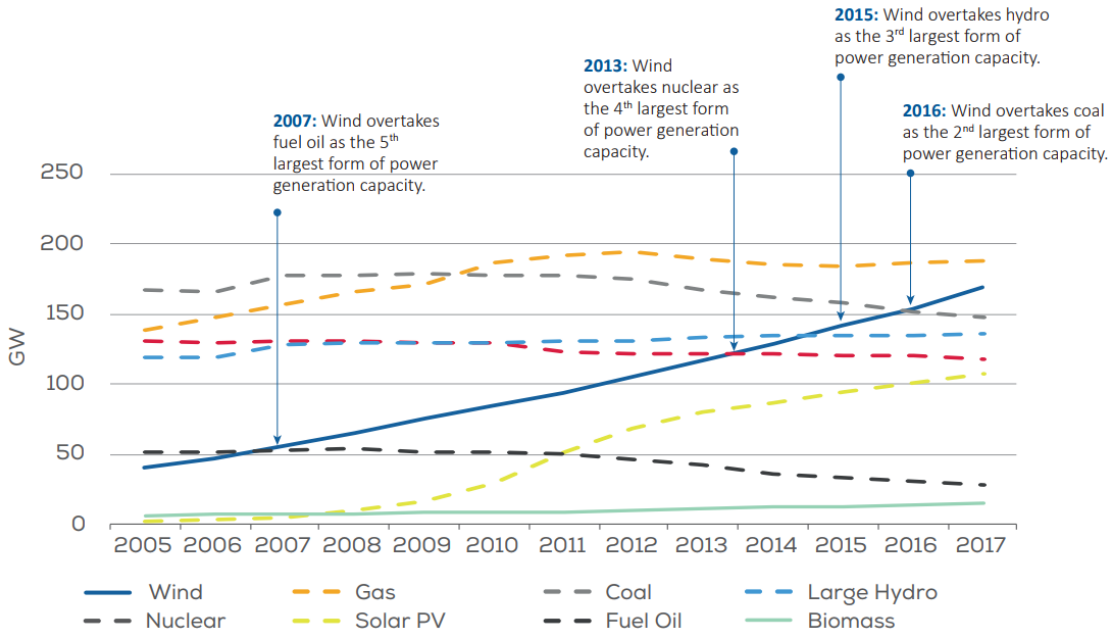

Figure 1.1: Power generation capacity in the European Union 2005-2017 (WindEurope, 2018).

The main reason behind the high costs of wind farms further away from the shore, is the type of infrastructure behind it. The generated alternating current (AC) electricity of offshore wind turbines is transported towards the shore with the use of cables, which have electricity cable losses that increase with higher cable distances. This means, that the costs of offshore wind energy increase with the distance from the shore. Direct current (DC) infrastructures have much lower amounts of cable losses and are preferred for long cable distances. These infrastructures however, are usually even more expensive due to their required conversion equipment and the strict offshore safety and maintenance regulations.

1.2 Artificial hub island

A recently introduced concept that aims to reduce the costs of offshore wind energy, is the concept of a large scale roll-out of interlinked offshore connectors, coordinated at an European level, including a so-called interconnected hub island. This vision includes many cost-saving aspects which help to make offshore wind energy in the North-Sea more attractive. By working together on an European level, an international shallow North-Sea area can be utilised which will reduce the construction costs of wind farms and improve the overall infrastructure efficiency (Meijden, 2016). Dutch transmission system operator TenneT presented this hub and spoke concept in 2016. An adjusted artist impression of the island by TenneT (2017) is found on the cover of this report.

The construction of an off-shore energy hub island has many advantages. An important aspect is the conversion from an alternating electricity current to a direct current. As a rule of thumb, Boveri (2012) describes that cable losses become unacceptable for distances over 60km using an AC infrastructure. This makes the conversion to a DC infrastructure expedient with the hub island as a great location for the installation of converters. By placing converters on the island the construction costs are decreased, as well as the maintenance costs as they are more easily accessible. More-over, the strict offshore safety regulations no longer apply to the converters, and the island can be utilised as storage area whenever there is a surplus in the energy supply.

To make the most out of the hub island concept, the location must satisfy some important characteristics. A logical location for the island is one where the national borders meet, where the depths are relatively limited and where the wind conditions are as good as possible since the good offshore wind conditions compensate for the increased costs as a result of large distances.

A location which meets many of the requirements is the Dogger Bank, presented by TenneT and located in the heart of the North Sea as can be seen in Figure 1.2. The Dogger Bank is a shallow sand bank of around 18,000km^2 that facilitates depths ranging from around 15m to 40m and adequate wind conditions (Meijden, 2016) simultaneously.

1.3 Ecology

The significant downside affiliated with this suggested location is that the Dogger Bank is a Natura 2000 conserved territory. Natura 2000 protected areas are considered to comprise the most threatened and valued species and habitats of Europe. In the designation of the Dogger Bank as protected area (Dam, 2016), the large contribution to the ecology of Europe is stressed as well as the need to conserve the habitat and species within the territory.

The Dogger Bank is a habitat labelled as permanently flooded sandbank and is the only one of its sort within Europe. Natura 2000 aims to preserve the surface area as much as possible. Simultaneously, animals such as the harbour porpoise and the grey seal make great use of the Dogger Bank, causing them (amongst others) to be included as protected species.

Since the Dogger bank is Nature 2000 protected, construction of an artificial hub island on the Dogger bank can only be realised in close co-operation with all involved stakeholder such as the managing province and ministry. The preservation of these areas was proven to be of high interest and developers often avoid Natura 2000 areas as they induce many additional impact assessments and construction requirements.

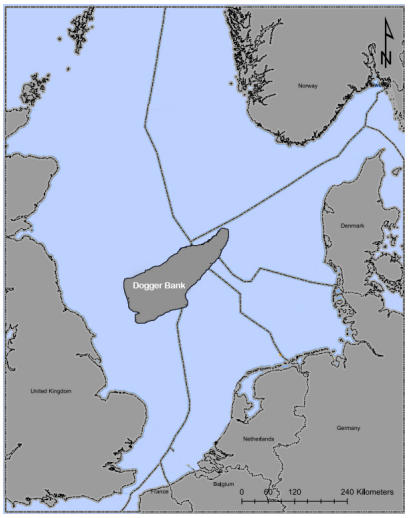

Figure 1.2: Location of the Dogger Bank within the North Sea (edited from Jongbloed et al. (2014)).

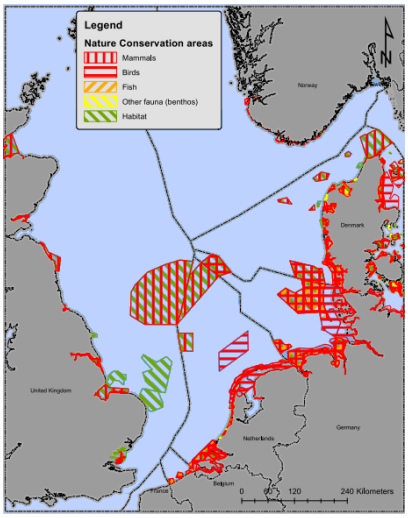

Figure 1.3: All types of Natura2000 protected areas (edited from Jongbloed et al. (2014)).

The construction of an artificial island on the Dogger Bank possibly affects the near-field ecology of the Dogger Bank. Constructing a large artificial island possibly even has an effect on the North Sea as a whole. It is unknown in what ways the presence of an island will affect the large scale and local hydrodynamics. The effects of the island could endanger the local habitat as well as the faraway ecology.

Natura 2000 aims to preserve the ecology as much as possible. However, it does not completely forbid human activity. In practice, human activity is allowed as long as current ecological values are maintained. Investigating the impact of constructing an artificial island helps to put the concept of the energy hub in perspective. The environmental impact of the island must be small compared to the advantages of a large sustainable power generation capacity, regardless of the location it is constructed at.

Technically there are some uncertainties, but no big problems are expected. The major reason which could stop the Hub and Spoke concept from being realised on the Dogger Bank is resistance from environmental organisations.

- Mart van der Meijden (TenneT); (Gerrits, 2017)

Since no substantial research has been published on the ecological impact and opportunities of an artificial energy hub facility in the North Sea, this research will serve as a first intervention-orientated design project. The impact of an artificial island on the Dogger Bank will be investigated, along side other shallow water location options in the North Sea.

1.4 Research objective

The construction of an artificial island is a permanent solution to the current expenses of offshore wind energy. Once constructed, the hydrodynamic environment is altered with all its possible effects on the local and far-field ecology. The hub island could be broken down in case it loses its function, but whether the area restores to its previous hydrodynamic and environmental equilibrium is debatable.

The effects of an artificial island in the North Sea on local and far away ecology have been explored earlier, based on specific parameters. Los et al. (2004), analysed the effect of sand mining activities and the island's presence on turbidity and ecology for the Flyland project near the Dutch coast. An artificial island is expected to affect many hydrodynamic characters and for this project, it is important to explore the most decisive parameters to the surrounding ecology.

More quantification research on relevant parameters is essential to justify the construction of a large scale hub-island in the North Sea. Moreover, the research can disclose opportunities for improving ecological values by responding properly to the changing hydrodynamic environment. This is a practice orientated research project, with the following objective.

Investigating the hydrodynamic effects, most important to ecological health, of an offshore wind energy hub-island on both the local and far-field environment of the North Sea.

The secondary objective follows from the intervention orientated form of practice research: While investigating possible design impacts, the potential of the hydrodynamic modelling software can be tested as a design tool for artificial islands in the North Sea.

1.4.1 Research scope

Since the marine ecosystems are highly variable systems, a straightforward framework is used to define the research scope. For this research project, the hydrodynamic environment of the North Sea (and more particularly around the artificial-island) is used as a basis for the ecological framework. The hydrodynamic environment determines the conditions organisms have to live in and adapt to.

Table 1.1 summarises the main hydrodynamic parameters that form the basic conditions for organisms to adept to. The importance of each parameter differs for different levels within the marine food chain. Section A.1 describes these parameters in more detail.

Table 1.1: Hydrodynamic parameters that affect the ecological dynamics.

Physical parameters	Water quality parameters
Flow velocity	Turbidity
Wave strength	Acidity
Water depth	Nutrient supply
Stratification	Oxygenation
Soil movement	
Salinity	
Temperature	

In order to determine the most important hydrodynamic parameters for the island impact exploration, the most important area of interest within the food web must be selected. For this exploratory research project, it is important to focus on the area within the food chain which best captures the impact on the complete food chain.

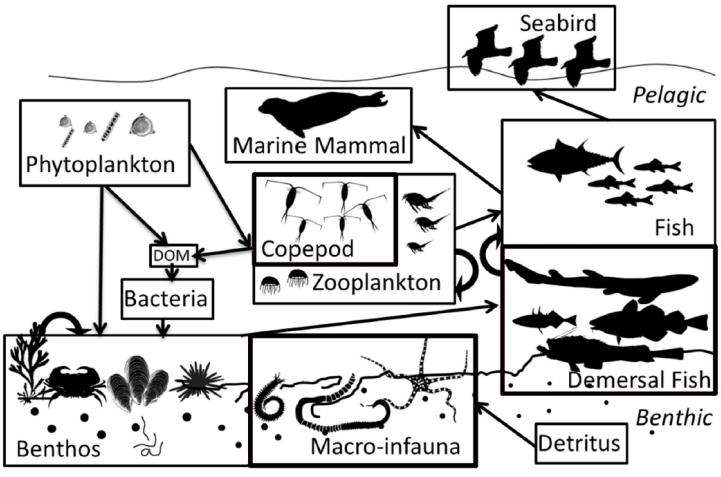

Figure 1.4: A schematic food web of the North Sea adapted from Pecuchet et al. (2018). Black arrows indicate a feeding link from one compartment to the other, while half-circle arrows represent intra-guild predation.

The main sections within the marine ecosystem of the North Sea, are presented in Figure 1.4. This food chain indicates the interactions between several species and visualises the feeding of the major compartments. The importance of phytoplankton, at the basis of all feeding processes is evident. Since food chains come in many forms and complexities, this research focusses on the most basic marine alternatives, as provided by Molony et al. (2010).

Figure 1.5 shows three possible forms of a generic marine food chain representation. Even though these simplistic food chains do not include the more detailed levels of the food chain and its processes, they do represent the general hierarchy. These food chains also highlight the importance of the (phytoplankton) primary producers within a marine ecosystem. The primary producers are found at the basis aquatic chain and dominate the biogeochemial cycles.

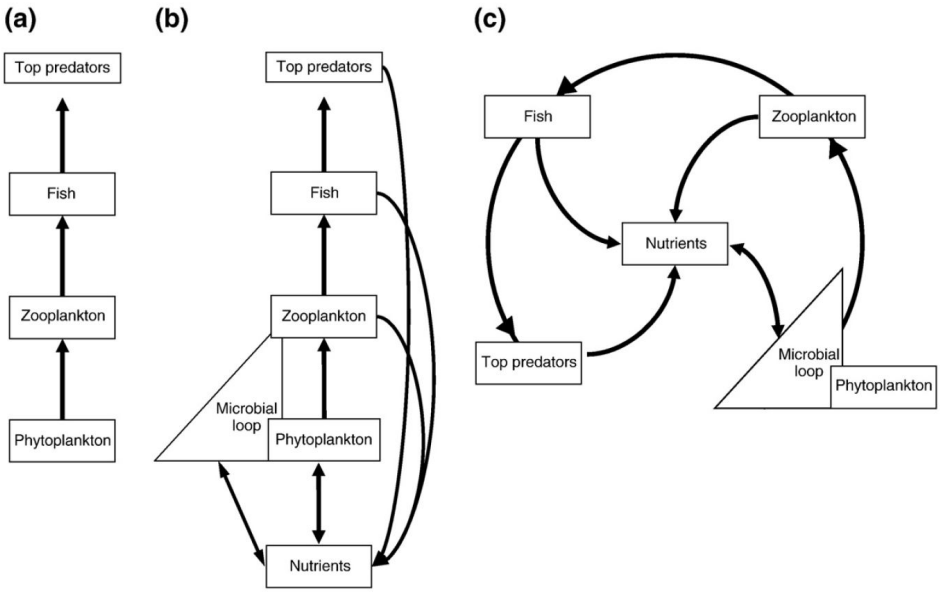

Figure 1.5: The three traditional forms of marine food web concepts. (a) Traditional linear food chain. (b) Nutrient-based feedback food chain. (c) Continues cycle food chain. Based on Molony et al. (2010).

For that reason, ecosystems are often characterised by the lifeform of its primary producers (Leeuwen et al., 2015). This lifeform is the main adaptor to prevalent environmental conditions, after which the remainder of the food chain organisation and ecosystem adepts to this structure of primary producers (Ricklefs et al., 2007). These microscopic organisms primarily use photosynthesis (and sometimes chemosynthesis) to create organic compounds in the water.

For marine ecosystems, the dominating processes that define the primary production structure, are those involving **light availability** and **nutrient availability** (Tett et al., 2007). Light availability is mainly determined by water depth, water stratification and turbidity. Nutrient availability on the other hand, is mainly determined by residual currents and stratification.

An increase in turbidity can be expected as a results of sand mining activities and increased turbulence around islands. For the flyland project however, Los et al. (2004) has demonstrated that expected impacts are likely well within the range of natural primary production variability of the North Sea. Based on these findings, turbidity will not be explored for this research project.

The most likely affected hydraulic parameters, are the water stratification and residual currents. An artificial island acts as a stirring rod within the North Sea, influencing the horizontal and vertical mixing. The vertical mixing determines the extent of water stratification, while the horizontal mixing regulates the impact on residual currents. Therefore, stratification and residual currents will be explored in more detail.

1.4.2 Research questions

The chosen model for this research project is the three dimensional Dutch Continental Shelf Model (DCSM) of the Flexible Mesh (FM) modelling suite, which is further clarified in Chapter 4 including its adjustments for this research.

This 'state of the art' North Sea model (known in short as the 3D DCSM-FM) model is capable of computing water movements in horizontal and vertical directions. The model can be used to predict characteristics such as tides and surges, but also for temperature and salinity properties.

The original model is extensively validated with measurements on the southern North Sea shelf and forms a reliable basis for case study research projects. Based on the model choice and research objective the main research question is defined:

Main research question

"What is the potential of the 3D DCSM-FM model in understanding the impact of an artificial island on the North Sea ecology?"

The main research question will be answered based on the more specific secondary questions, that will help guide the research outline. The potential of the 3D DCSM-FM model will be assessed by exploring the effects on stratification and residual currents. The secondary questions of the project are:

Secondary questions

1. Does the model reproduce the baseline water stratification and residual current patterns in the North Sea?

2. What are the effects of an artificial island on the local and far away stratification characteristic, and can we understand these effects?

3. What are the effects of an artificial island on the local and far away residual currents, and can we understand these effects?

4. Is it possible to use this 3D DCSM-FM model set-up as basis for future ecological predictions?

1.5 Research outline

To get a better understanding of the area of interest, a summary is presented of the meteorological and hydrodynamic conditions. The most important physical processes (stratification and residual currents) and their current North Sea distributions are then shortly discussed.

The impact analysis is based on several 'island cases' of a basic island design at different location. A basic design is used since the energy-hub concepts are still in a conceptual stage of development. Previously, Gerrits (2017) created a site selection model to identify the most promising locations for the construction of an energy hub-island and its surrounding wind farms from an economical perspective. The resulting net present value (NPV) contour plot is presented in Figure 1.6 with four highlighted location options.

These locations will be adopted and further investigated in this thesis, focussing on relevant hydrodynamic parameters. The alternative island locations are widespread over the North Sea each with different environmental conditions, such as depth, stratification regime and flow dynamics. This makes it possible to explore under which conditions an island has the least adverse or the most beneficial impact on ecology.

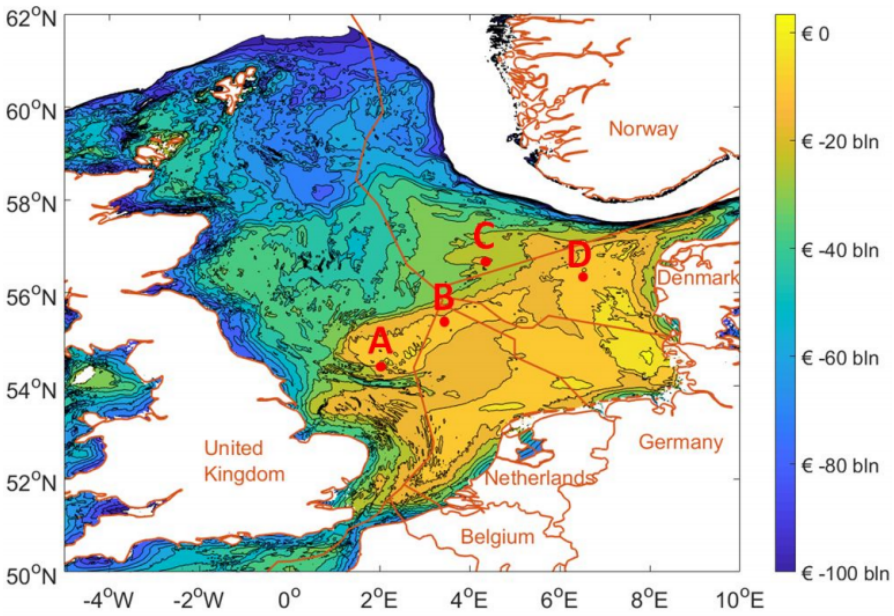

Figure 1.6: Net present value of the Hub and Spoke Concept with 30GW capacity (Gerrits, 2017).

By looking into previous research and theoretical background around the impact of (artificial) island in shallow seas, the model output can qualitatively be validated, and the impact better understood. That way the potential of the model can be assessed based on the comparison between output and expectations. The research process from start to finish is summarised in Table 1.2.

Table 1.2: Research outline.

Stage	Description
1	Environmental analysis
2	Theoretical background study
3	Adjusting the current model for island impact research
4	Qualitative validation of the baseline output
5	Evaluation of the impact on hydrodynamic parameters
6	Reflection on the model's potential as artificial island design tool

2 Environmental conditions of the North Sea

This chapter starts with an overview of the basic North Sea characteristic, as a basis for further research into hydrodynamic processes. Additionally, the prevailing North Sea stratification and residual current characteristics are considered.

2.1 General characteristics

The meteorological and oceanographic conditions are quantified as they are the major determining factors for the general North Sea flow patterns.

Topography

The North Sea is a continental shelf sea located in the north-western part of Europe, with relatively small depths and high human influence. It is enclosed by several highly populated countries and connects to the Atlantic ocean and Baltic Sea. The total extent of the North Sea covers an approximate area of 525km^2 and includes an estimated water volume of around 43,000km^3 (Los et al., 2004). The North Sea can be divided into four main sectors, these general areas are:

- Northern North Sea: Found just South of where the continental shelf quickly rises from depths around 2000m to depths of around 500m. This area is mostly dominated by oceanic flow conditions from the Atlantic Ocean.
- Southern North Sea: In this area the depths are significantly lower, reaching to a maximum of around 50m. It is much more dominated by large river inputs than the Northern North Sea and is characterised by mixed waters.
- The Skagerrak and Kattegat: This is where the North Sea connects to the Baltic sea characterised by less tidal influence than the rest of the area.
- The English Channel: Here, the North Sea is rejoined with the Atlantic Ocean. This area is usually influenced a lot by wind activity.

The Northern North Sea is mostly used for fishery and gas and oil production, while the other regions are also used for activities such as shipping, wind farming and sand mining. All these human activities are carried out while maintaining the ecological values as much as possible.

Bathymetry

The underwater equivalent to topography is called the bathymetry. It shows the distance between the seabed and the water level. Since the water levels are different in time for all location, a reference surface is used that approaches mean sea level. Figure 2.3 shows the bathymetry for the North Sea and its surrounding areas such as the Baltic Sea and Atlantic Ocean. Larger depths around the western edge of Norway are clearly visible just like the shallow areas near the Dutch coast and at the Dogger Bank. The Norwegian trench along the coast is a deviation from the general North Sea bathymetry, with depths up to 700m.

Wind conditions

On the north-west European shelf, the wind comes predominantly from the south-western direction. It is mostly responsible for the circular current pattern in the North Sea, giving it an anti-clockwise rotation within the basin. Occasional eastern winds reverse the direction of flow, while northern and southern winds now and then cause a stagnation (Sundermann and Pohlmann, 2011). The average wind speed at $10m$ altitude above the North Sea reaches values of around $9m/s$. Figure 2.1 shows how the wind speed increases over the North Sea after being slowed down by the United Kingdom.

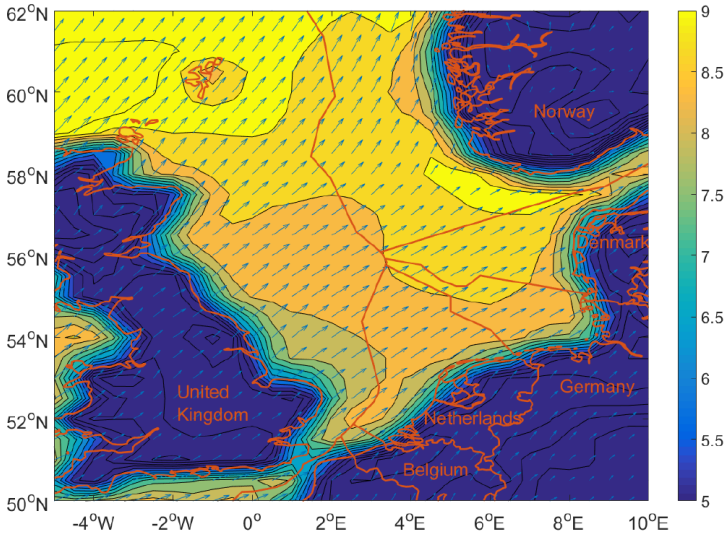

Figure 2.1: North Sea average wind speeds (m/s) for 2012-2016 at 10m altitude (Gerrits, 2017).

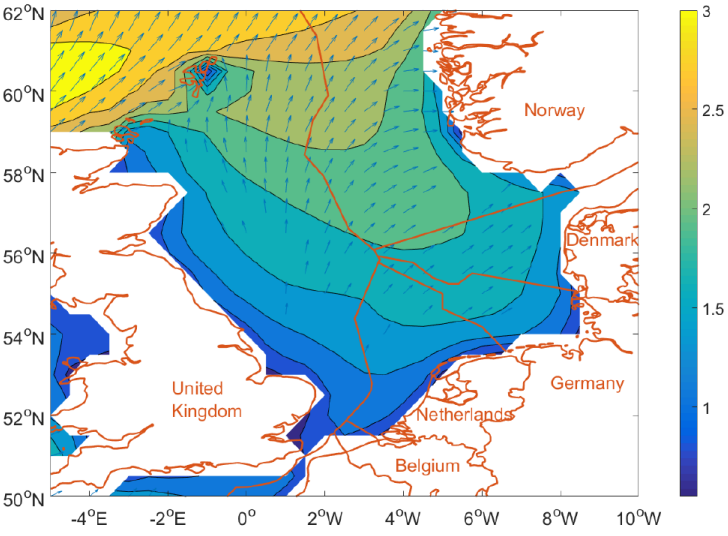

Figure 2.2: North Sea average significant wave heights (m) for 2012-2016 (Gerrits, 2017).

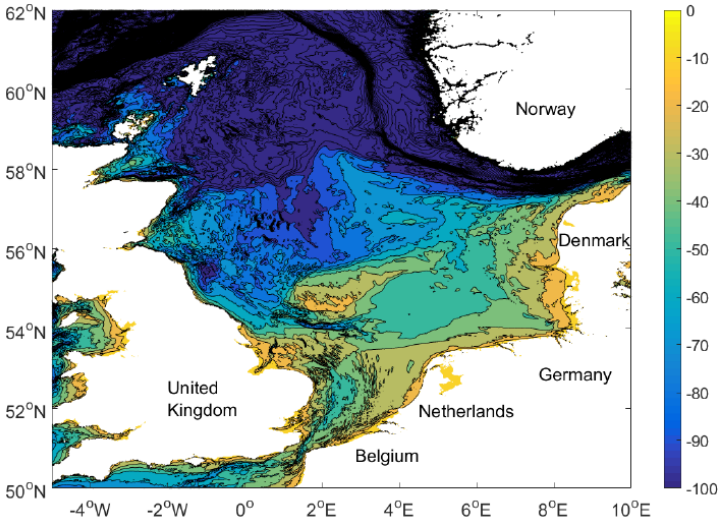

Figure 2.3: North Sea bathymetry (m) in 2016 from EMODnet (Gerrits, 2017).

Wave conditions

The North Sea usually contains both swell and wind waves. Wind waves are an direct effect of wind blowing over the water surface. The friction between the water surface and wind creates ripples, which can become large enough to be pushed forward by the wind to create wind waves. Swell waves on the other hand, are created far away by strong winds or storms and travel long distances before reaching the North Sea as long, low frequency waves compared to wind waves (Bosboom and Stive, 2015). Figure 2.2 presents the average significant wave heights and directions coinciding with the average south-western wind direction of Figure 2.1. The significant wave height represents the highest one-third of all the waves.

Surge

During high wind velocity situations, the water elevation can be increased at the coastlines. During storms, the low atmospheric pressures and high wind velocities cause water to be pushed up against the coast causing it to pile up. Other than wind speeds, the amplitude of storm surge mostly depends on the bathymetry. Figure 2.5 shows the surge levels for a northern wind with a constant velocity of 23.2m/s. Due to the decreasing depth of the North Sea toward the south, the surge effect is increased toward the coastlines (Sundermann and Pohlmann, 2011). The highest water levels in the North Sea are an effect of storm surge coinciding with large astronomical tides.

Tides

One of the dominant forcing mechanisms of the North Sea is tidal forcing. Tidal motions follow from the gravitational pull on water by planets such as the sun and the moon as well as earth's rotation. This gravitational pull is related to a planet's mass and distance from earth. Some tidal forcing is directly imposed on the North Sea water body. The biggest impact however, is caused by the tidal forcing of the Atlantic Ocean boundary (Bosboom and Stive, 2015).

The gravitational pull of the moon is two orders smaller than the gravitational pull of the sun. However, the moon contributes to about 70% of the tidal amplitudes compared to only 30% contribution by the sun. This follows from the fact that gravitational pull is not per se directly responsible for the forces that generate tides but rather the differential pull. This is the difference between the gravitational pull on the ocean waters located around the world (Bosboom and Stive, 2015).

The main tidal constituents that are imposed on the North Sea boundaries are the semi-diurnal lunar 'M2'-tide and the semi-diurnal solar 'S2'-tide with an amplitude of around 1.0m and 10.0cm respectively (Linden, 2014). More tidal constituents exist for the North Sea, for example due to the sun's declination or the moon's elliptical orbit. Yet, the contribution of these tidal constituents are much smaller than the main tidal constituents.

The bathymetry has a direct effect on the oscillations and resonance due to tidal forcing. The tidal propagation in the North Sea can be described as cyclic or an amphidromic system (Winther and Johannessen, 2006). The tidal wave enters the North Sea in the north-west after which it travels through the basin as a so-called Kelvin wave. The Kelvin wave travels in the southward direction through the west part of the northern North Sea, after which it mixes with fresh water from rivers in the southern North Sea and continuous in the eastward direction. After that it reaches the brackish water from the Baltic Sea, and leaves the North Sea through the deep Norwegian trench.

The bathymetry dominates the amphidromic character of the North Sea including the amphidromic point, at which the tidal elevations are close to zero. Kelvin waves rotate around these specific locations. During the propagation around the basin, the bottom friction at shallow areas dissipates the tidal wave and the amplitude decreases. Figure 2.4 shows the amphidromic points and the decreasing tidal range along the Kelvin wave's path.

Transport

The in and outflow of water is primarily determined by the tidal movements and bathymetry and can be divided into six main sections for the North Sea. The inflow of water into the area is mostly governed by three sections: the northern boundary, the Orkneys-sheltland section and the English channel. Simultaneously, some water enters the system from the Baltic Sea and rivers. The outflow of water primarily takes place through Baltic Sea, the Skagerrak and the eastern segment of the Norwegian trench (Winther and Johannessen, 2006).

Table 2.1: Annual in- and outflow values for main North Sea transport sections from MPIOM modelling and literature (Mathis et al., 2015).

Volume transport [$\cdot 10^6\ m^3 s^{-1}$]	Modelling mean ± standard deviation	Literature (mean)
1 Northern Boundary inflow	1.03 ± 0.09	1.67-1.71
2 Orkney-Shetland inflow	0.50 ± 0.06	0.30-0.70
3 English Channel inflow	0.15 ± 0.04	0.06-0.17
4 Baltic outflow	0.024 ± 0.003	0.014-0.016
5 Skagerrak outflow	0.54 ± 0.11	0.50-1.50
6 Norwegian outflow	1.72 ± 0.15	1.00-2.33

It is hard to measure the annual flow values for large transport transects. Literature does however contain approximations, and some ocean models predict large scale transport schemes. Based on literature and the Max Planck Institute ocean model (MPIOM) an indication of the larger annual transport sections is given in Table 2.1.

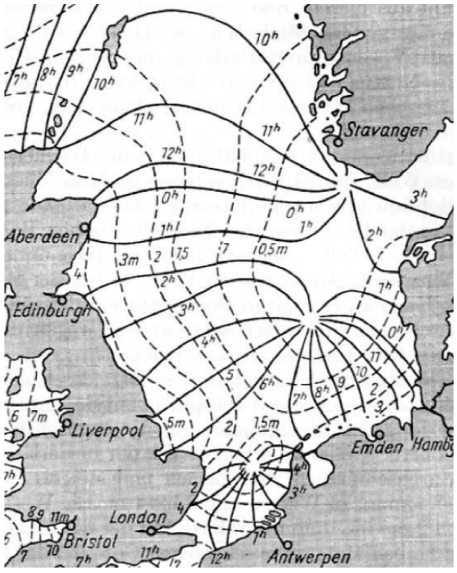

Figure 2.4: Solid co-phase lines (hours) and dashed co-range lines [m] for the semidiurnal tides (Sager, 1959).

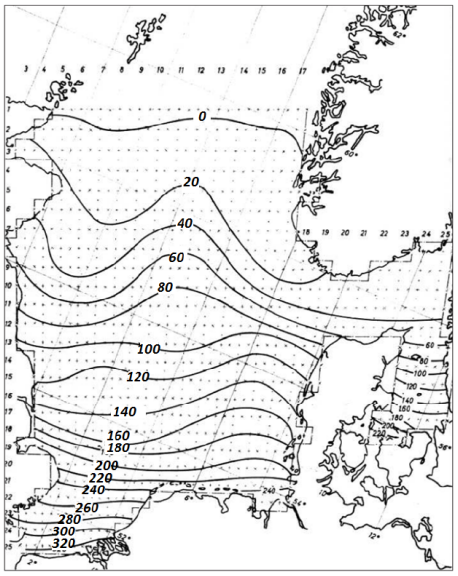

Figure 2.5: North Sea storm surge levels (cm) for a constant northerly wind of 23.2m/s (Sundermann, 1966).

2.2 Stratification

Water stratification is a phenomena in which water layers are created with different properties that form an obstacle to vertical mixing. Properties such as density, temperature or salinity can clearly show a variability over the depth profile at several locations.

Generally, the stratification is regulated by differences in water temperature and salinity and subsequently also density which occur is case of relatively a small amount of vertical mixing. The seasonal variations in atmospheric temperature dominates the North Sea stratification regimes. During the summer, the sun warms the upper water layer and the density of this warmer water becomes lower than the deeper cold waters. Because of this process, the warm water stays at

the surface. During colder periods of the year, the water cools down and wind strengths often increase, during which the stratification reduces significantly or even breaks down completely. Salinity stratification mainly takes place around river mouths where fresh water and sea water interact.

Stratification can not occur in waters that are heavily mixed. Water masses that are highly turbulent constantly get mixed and no evident density boundary layers get formed. Usually, shallow sea water gets mixed mainly by river inputs, tidal flows and wind influences. The distance from rivers, the tidal influence and the depth mainly dominate the degree of stratification for a particular location. Areas are not necessarily year-round stratified or well-mixed. Many regions are either seasonally stratified or intermittently stratified, depending on the physical environment.

The North Sea is a unique shallow sea with several inputs that define the hydrodynamic regime. The southern North Sea is strongly affected by the river inputs and it is generally a well-mixed region with large tidal flows and small depths. North Sea stratification is most prevalent in the northern regions with larger depths, smaller river influences and lower tidal amplitudes.

The exact definition of stratification is open for debate, but can defined by setting a boundary condition for the difference in surface and near-bed density conditions. Leeuwen et al. (2015) defined 'stratified' as a density difference between near-bed (one meter above the bed) density and surface (1 meter below the surface) density of more than $0.086 kg/m^3$. This is the equivalent of 0.5 degrees Celsius or 0.11PSU in waters of 10 degrees Celsius and 34.5 PSU.

Using this definition of stratification and the specific definitions for the hydrodynamic regimes of Table 2.2 the North Sea overall distribution of stratification regimes was modelled by Leeuwen et al. (2015), with an extensively validated hydrodynamic model to produce Figure 2.6. It shows the clear division of the North Sea in distinctive stratification regimes.

Table 2.2: Definitions used by Leeuwen et al. (2015) for the stratification regimes, based on maximum lengths in days of extended mixed or stratified periods.

	P(stratified) [days]	P(mixed) [days]	P(stratified) + P(mixed) [days]
Permanently stratified (PS)	> 345	< 20	
Seasonally stratified (SS)	> 120	> 90	
Intermittently stratified (IS)	< 40	[120,250]	
Permanently mixed (PM)	< 20	> 345	
Region of Freshwater Influence (ROFI)	> 3	> 3	< 120

Stratification is one of the most important large-scale physical properties of a shallow shelf sea to ecology. Distinctive separated layers over the depth profile can impair primary production by limiting the amount of nutrients that are able to get mixed up from the deep waters into the photosynthetic active upper layers. Moreover, stratification limits the vertical mixing of primary producers through the pycnocline to the deeper waters as food source for benthos.

Primary producers are able to deal with low nutrient supplies differently, depending on the ratio between their body surface and volume. For the North Sea, the main primary producer family (phytoplancton) shows a separation between thriving species based on size and mutual competition.

Many studies indicate the importance of relative primary producer contribution to differentiate marine biomes. Tett et al. (1993) shows an agreement with the results of biochemical modelling that predicts redistribution of primary producer contributions for different stratification regimes. Figure E.2 and E.3 show the distribution of phytoplankton for all different stratification regimes.

Goldman et al. (1996) also investigated the importance of thermal stratification in regions of pronounced horizontal hydrodynamic variability. A strong correlation was found between the degree of stratification and the extent of surface water nutrients and phytoplankton productivity.

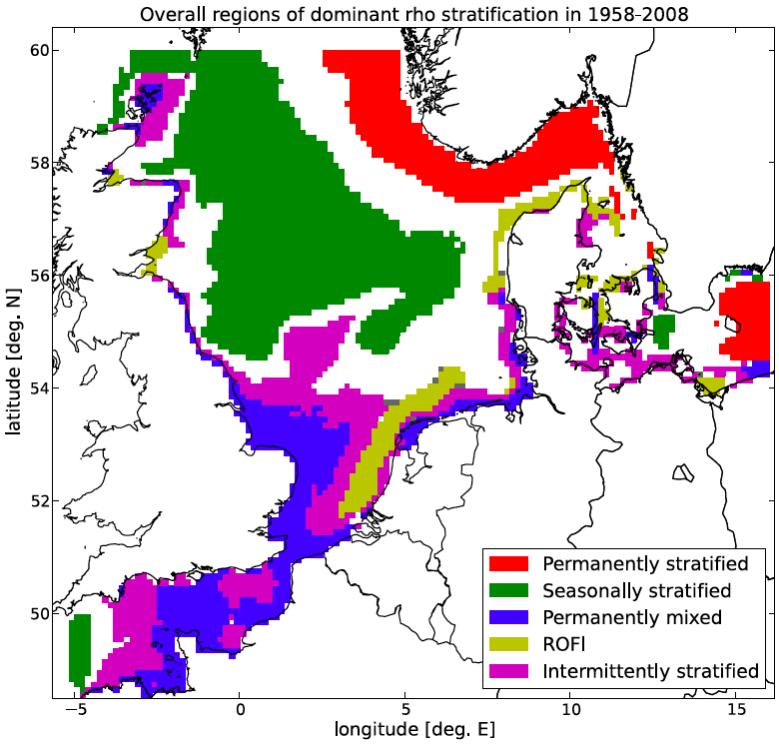

Figure 2.6: Time median results of the modelled, annual stratification regions in the North Sea (Leeuwen et al., 2015).

Likely, the implementation of an artificial island will have an effect on the physical conditions near the island and possibly also on a larger scale. Simpson et al. (1982) investigated the mixing and phytoplankton growth around an island, located in a stratified sea. A large increase in tidal mixing was found for such an island. Mainly the influence of the enhanced mixing on the phytoplankton biomass distribution was investigated and showed a clear impact. Tidal stirring on European shelf seas such as the North Sea was found to be the main driver behind vertical mixing, dominating over wind mixing.

For the Scilly Isles region in the Celtic Sea, levels of primary production and biomass were found to increase by around a factor of five, over a region of up to twenty times the island area. The effect of islands on stirring however, is dependent on the island size, shape and advection by residual flow in the area.

In order to assess the impact of artificial islands in the North Sea, it is important to identify the main changes that can occur as a results of tidal stirring. Leeuwen et al. (2015) already investigated the importance of dominant regimes on primary production dynamics, which will serve as a basis for this research project.

Whilst the dominant regimes already give a good indication of the prominent primary producers, it does not nearly tell the whole story. These regimes are based on the density differences between the top and the bottom of the water column, while the vertical stirring is much more diverse than that. The mixing process around islands is based on the top and bottom waters from the original stratified regime, that get mixed into an intermediate water layer of transitional density. This newly mixed layer of intermediate density could, but does no necessarily span over the whole water depth.

In a system of relatively low rotational influences, the water could intrude mostly into the area of the pycnocline as described in more detail by Hachey (1934), who observed the pycnocline injection in a set-up with stratification and mixing on one end of a water tank test. This would lead to an island mixing pattern similar to that of Figure 2.7. It is an schematic representation of a possible effect when rotational characteristics are low. In reality, the turbulence likely will cause a breakdown of this idealised constrained mixing layer. Nevertheless, a partially comparable

pattern could occur for the North Sea islands.

Looking at the depth profile over time will help to identify whether such patterns occur and whether a top minus bottom stratification analysis is justified. Moreover, it gives an indication of the turbulent rotations that occur for the island cases and its relative influence over viscosity.

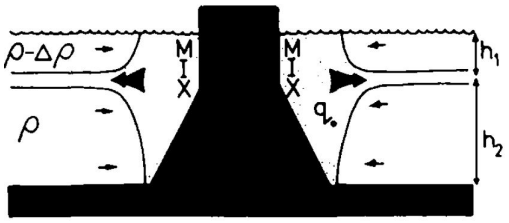

Figure 2.7: The mixing around an island, depicting the injection of mixed water along the pycnocline, rather than complete waterdepth mixing (Simpson et al., 1982).

Other than the regimes and depth profiles, the timing of extended stratification periods have also shown to be of relevance to primary productions rates. During summer, the deeper parts of the North Sea experience extended periods of stratification that hold for many months. The timing of such extended stratified periods is discussed by Ruardij et al. (1977) and mainly involves the modelling of stratification onset and breakdown timing, and its influences on primary production.

The timing of the onset especially was found to influence the phytoplankton dynamics. The timing of stratification onset around spring determines the primary producer species composition heavily, as during this time the succession of dominating phytoplankton species is determined. The composition of dominant primary producer species is rapidly determined within the first few weeks, which then influences the main composition for at least several months.

2.3 Residual currents

The influence of residual currents is slightly more straightforward. Inorganic nutrients such as nitrogen are needed for primary production to take place. The North Sea has three major sources of nutrients, the ocean, the rivers and the atmosphere. Even though only a small amount of North Sea water is supplied by the rivers, they do contribute more heavily to the total nutrient supply (especially in the near shore areas).

The residual currents in the North Sea determine the distribution of nutrients that is supplied to each area. Different parts of the shelf have diverging nutrient origin distributions, dependent on their location and residual currents. Figure E.4 shows the origin of nutrients for different North Sea areas.

If the island has a large-scale influence on the residual currents, a distribution shift can occur which will affect the primary production rates and distribution of primary producers in the specific areas. Just like stratification, the residual currents affect the nutrient availability, which is one of the main drivers behind biological activity as a whole.

Ruardij et al. (1977) investigated the effect of residual currents and advection on primary production, and concluded that local variations in lateral advection and residual currents have a relatively small impact on primary production rates, compared to that of vertical exchange rates. Only large scale differences are likely to impact primary production, as it possibly alters the origin of nutrients and its composition. Else ways, no major influences are expected.

3 Theoretical inquiry of island influences

Stratification is determined by differences in vertical water temperature and salinity, and subsequently also density which prevails in situations of low vertical mixing. Implementing an artificial island in the North Sea can be seen as the implementation of a horizontal constriction within the flow regime. Such restrictions lead to accelerations and decelerations around the object and thus changes in turbulence can be expected.

Simultaneously, the tidal waves and Earth's rotation coincide to change the tidal characteristics and residual currents around an artificial island. This chapter briefly describes the theoretical background of an island's impact on both parameters, while Chapter B gives extra insight on the processes that determine the general stratification and residual current patterns in the North Sea.

3.1 Turbulence

The main feature of turbulent motion is that the velocity and pressure present irregular fluctuations (Schierik, 2016). Statistically distinct average values can be distinguished, however it is still an irregular motion. A way of expressing the distinct average and irregularity of fluid velocities is through Equation 3.1:

$$x = \overline{x} + x' \qquad y = \overline{y} + y' \qquad z = \overline{z} + z' \tag{3.1}$$

This equation consists of term with an over-line which represent the averaged values and $'$ represents the fluctuations for every direction. A way of expressing the turbulence is through the parameter k which is known as the total kinetic energy in a turbulent flow.

$$k = \frac{1}{2}(\overline{x'^2} + \overline{y'^2} + \overline{z'^2}) \tag{3.2}$$

Such turbulent kinetic energy is dependent on accelerations and decelerations within the fluid. In the ideal (uniform flow) case, no turbulence is present. In practice however, flow in never uniform and decelerations and accelerations occur constantly, in all directions. The amount of turbulent kinetic energy is therefore dependent on the magnitude of velocity gradients, and the resistance to such deformations.

A fluids resistance to accelerations and decelerations can be described in the form of viscosity. This parameter is dependent on the type of fluid and is used to define the degree of turbidity in many different flow situations. The dimensionless quantity known as the Reynolds number (Re) describes this degree of turbulence for free-stream flow (Battjes, 2002):

$$R_f = \frac{U \cdot h}{\nu} \tag{3.3}$$

with:
U = mean free stream velocity
h = water depth
ν = kinematic viscosity

It stresses the relationship between molecular viscosity and flow velocities. Turbulence is induced by velocity differences that overshadow the viscosity's ability to prevent turbulent eddies. The Reynolds number can be used in many different occasions to indicate the turbulent regime.

3.2 Mixing around islands

Recently, some attention has gone to the mixing effects of islands in a stratified shallow sea. In such locations, the tidal flow is dominant, causing the distribution of stratification to be dominated by the tidal amplitude $\overline{u}$ and the water depth h. Simpson et al. (1982) investigated

the occurrence of stratification in shallow seas and concluded it to be mostly dependent on the parameter $h/\overline{u}^3$. This suggests that the presence of an island can cause a (partial) breakdown of stratification patterns around the island due to both the decreased water depths and the increase of velocity magnitudes along the flanks.

The implementation of an island in coastal regions can cause large-scale eddies due to 'flow separation'-like effects around the detached body. Flow separation is known as the transition from wall-flow to free-flow (Schierik, 2016) causing both boundary layer turbulence and velocity differences turbulence. The flow separation mainly determines the flow pattern around detached bodies. However, since flow separation is very much dependent on the local surface roughness and the Re-number, it is very hard to predict such flow pattern. The flow around detached bodies is completely three-dimensional and differs for all types of objects.

In order to grasp the context of tidal stirring effects around a North Sea island, the flow disturbance of idealize islands is first discussed. First for a steady current which has been extensively investigated, but also for the more complicated case of oscillating flow circumstances.

3.2.1 Steady current

As previously mentioned, the flow around cylinders for a steady non-rotating current has been extensively examined in laboratory experiments. Many of the properties of rotatory, oscillating flow around an artificial island can be identified by studying the reference case of steady non-rotatory flow of a homogeneous liquid past a cylinder.

For such circumstances, the existence of a cylinder forms an area of increased flow velocities around the sides of the horizontal constriction with areas of flow stagnation near the cylinder at the central flow lines. This can be seen in Figure 3.1 (a). For this idealised case, the flow velocity can increase up to a factor of two along the flanks.

Yet, in practice this idealised flow almost never exists. It does not attune to the symmetrical streamlines around the cylinder. In practice the form of the streamlines is more 'chaotic' behind the cylinder with wakes that change shape and size depending mostly on the Reynolds numbers of the flow. Figure 3.1 shows examples of turbulent flow behind a circular cylinder for different values of Re with and without the presences of a rotating system.

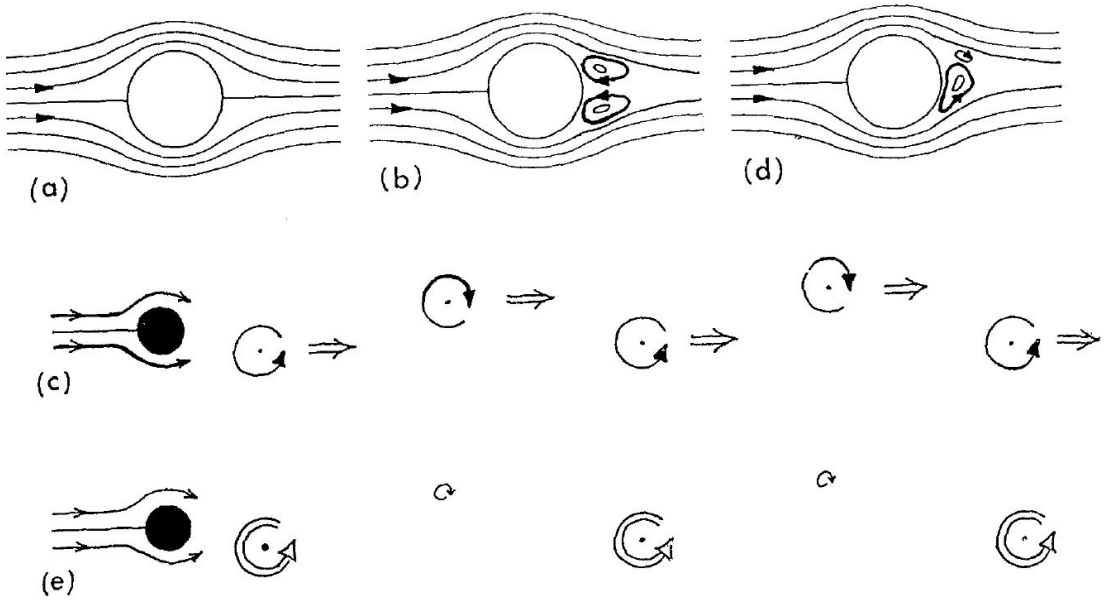

Figure 3.1: Flow past a cylinder for 5 cases. (a) $Re \sim 1$ without rotation: fully attached flow. (b) $1 < Re < 70$ without rotating: a steady region of separation. (c) $70 < Re < 2500$ without rotation: shedding of vortices. (d) $Re \sim 50$ with rotation: asymmetric steady region of separation. (e) $Re \sim 500$ with rotation: asymmetric shedding of vortices. Adapted from (Simpson and Tett, 1992).

The Reynolds number for flow around a cylinder is dictated by the radius rather than the water depth for free stream flow as prevailing length scale:

$$Re_c = \frac{2 \cdot R \cdot U}{\nu} \tag{3.4}$$

with:
R = radius of the cylinder

For very low values of Re, the viscous effects dominate and the flow represents upstream-downstream symmetry. For more realistic Re numbers up to 70, a separation region is created behind the cylinder and wakes are formed. At even larger Re numbers, the separation effects start to dominate and organised wakes arise in the form of a vortex street.

3.2.2 Oscillatory flow

In the case of oscillatory flow conditions, the disturbance of flow around a cylinder is further complicated. The free stream velocity is replaced by an oscillating velocity signal. The alternating currents with an amplitude $\overline{u}0$ generated by the tidal flow engender a varying Reynolds number. Such reciprocating tidal current is described by the adjusted Strouhal number for cylinders:

$$St' = \frac{2 \cdot \omega \cdot R}{\overline{u}} \tag{3.5}$$

with:
ω' = tidal flow frequency
$\overline{u}$ = tidal current amplitude

The Strouhal number emphasises the relation between the flow velocity amplitude and the characteristic length scale and describes the mechanics of oscillating flow. Generally, large Strouhal numbers indicate a dominance of viscosity over fluid flow. Only for Strouhal numbers much smaller than 1.0, do extended wake regions occur (Simpson and Tett, 1992). In such case, the cylinder is small enough for the tidal excursion to dominate over the scale of the island.

Relations have been developed between the Stouhal number and the Reynolds number for several objects such as the circular cylinder (Fey et al., 1998). These relations however are dependent on several experimental factors. For examples, observations of small islands in shallow water (thus with relatively low values of St') in oceanic circumstances indicate the importance of bottom friction. This seems to be responsible for a much lower 'effective' Reynolds number than initially expected. Denniss and Middleton (1994) describe this effect as the extraction of energy from the flow as a result of vertical viscous transfer of momentum to the seabed.

Generally, the range of tidal currents present in the shelf seas such as the North Sea, are too small for significantly low Strouhal numbers. Only for very small features ($<<$ 1km), can vortex streets be expected. Otherwise, the tidal cycles are too short to allow any significant development of effective Reynolds numbers.

3.2.3 Modelling studies

Since the flow around detached bodies is completely three-dimensional, predictions based on the steady current base case are hard to make. For that reason, 2D numerical models of oscillating flow (including coriolis effects) were made by Pingree and Maddock (1979) in order to investigate the effect of a conical island on the flow patterns.

A far-field rectilinear oscillatory flow of 0.5 ms^{-1} was modelled and its effects on a conical island with a radius of 4.5 km. With this model, the effects of the islands on the distribution of the stratification parameter $h/\overline{u}^3$ were investigated while also looking into the residual currents. Figure 3.2 visualises the model output for the $h/\overline{u}^3$ parameter.

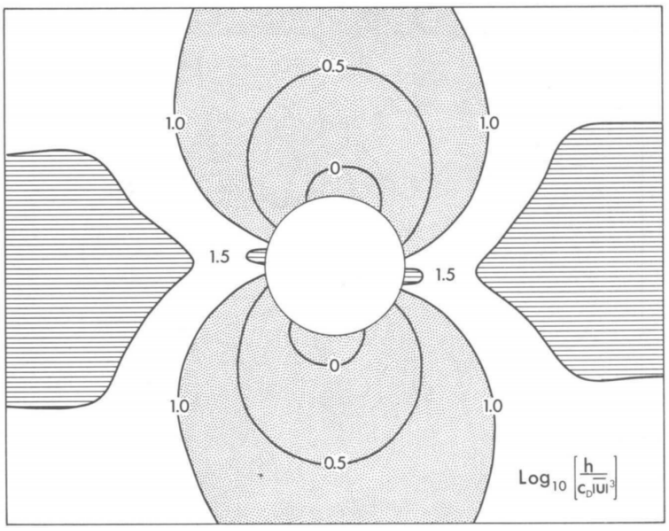

Figure 3.2: The stratification parameter showing stratified (horizontal shading), frontal and well-mixed regions (stippled) around an island (Pingree and Maddock, 1979).

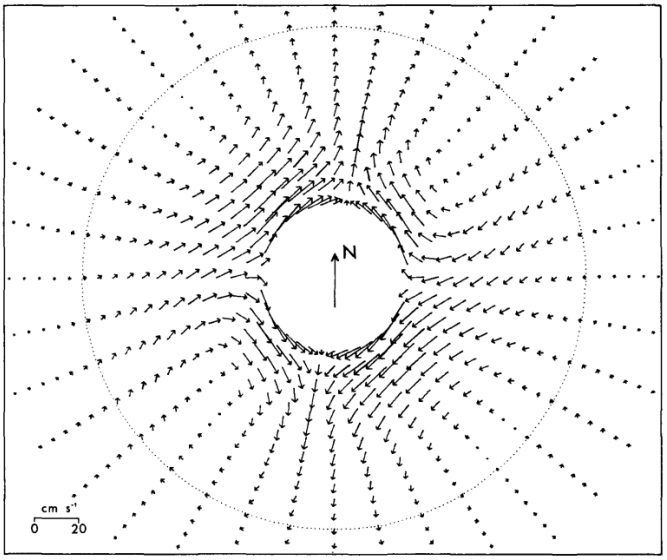

Figure 3.3: Residual flows impact on the northern hemisphere based on hourly changing (oscillatory) flows without the presence of forced far-field residual flows (Pingree and Maddock, 1979).

The stratification parameter distribution indicates areas of de-stratification along the 'sides' of the island, where the tidal amplitude is increased and stagnation areas along the axis of flow. A slight clockwise deformation from the axis of flow is seen however compared to the fully attached flow pattern of Figure 3.1a, which can be explained by Figure 3.3.

Figure 3.3 shows the computed residual flow as a result of the rectilinear east-west directed oscillatory far-field tidal flow. The island's influence on the tidal flow introduces four residual eddie-like structures which blend to create offshore directed flows at the island 'flanks', with a slightly clockwise rotated element due to the Coriolis forces.

Similar residual current characteristic are expected for the artificial islands on the North Sea shelf. The difference however, is the presence of a far-field residual current which was not present in the 2D modelling research. The North Sea islands are placed within an amphidromic system with its own residual flow pattern (Figure E.1) and will likely show an adjusted impact pattern.

The modelled $h/\overline{u}^3$ distribution is a good first indication for impact on stratification, however yet again, it does not include the influences of an already present far-field residual flow. Moreover, the results of Figure 3.2 do not include any actual turbulence or three-dimensional effects and thus do not tell the full story on vertical mixing, it is merely an indication of the possible effect on free flow turbulence around an island.

3.3 General North Sea mixing

Since there are no long time-scale density measurements available for the North Sea area, modulations were made using the $h/\overline{u}^3$ parameter to predict the likeliness of stratification. Since no blunt horizontal constrictions exist in the North Sea (such as natural islands), it is a good first impression of the spatial distribution.

Schloen et al. (2017) used an unstructured-grid ocean model called SCHISM coupled with wind waves to identify this $h/\overline{u}^3$ distribution for the southern North Sea, as is shown in Figure 3.4. These spatial patterns can be compared to the modelled stratification map of Figure 2.6 to see the correlation between the free flow stratification parameter $h/\overline{u}^3$ and the actual stratification of the North Sea.

In order to identify the importance of wind waves, Schloen et al. (2017) compared the model results between two computations: one with the influence of wind waves and one without wind waves. The impact of including wind waves in the model on the $h/\overline{u}^3$ parameter is shown in Figure 3.5.

Figure 3.5 highlights that the effect of wind waves in the North Sea on overall mixing is almost negligible. It does however, identify the relatively higher importance of wind waves along the coastal areas. Since the concepts of an artificial hub-island are located outside this area, it can be safely assumed that for this research project, wind waves will be of small significance compared to tidal mixing.

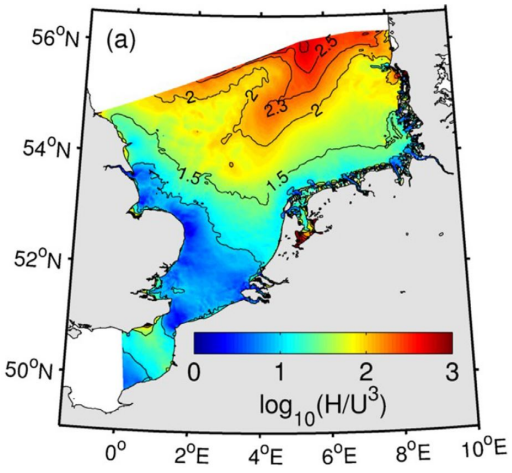

Figure 3.4: The stratification parameter for the southern North Sea. Low values indicate higher probability of turbulent mixing, whereas higher values indicate more stratified areas (Schloen et al., 2017).

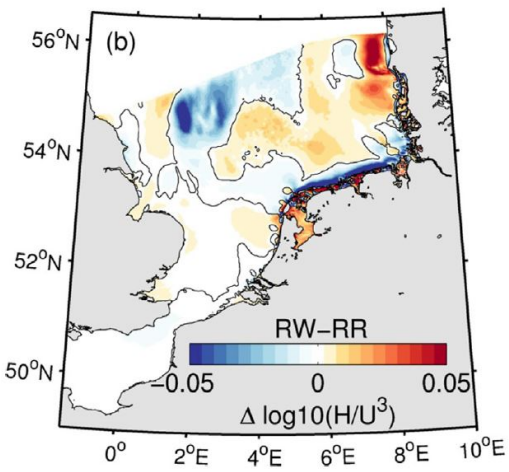

Figure 3.5: The difference in the stratification parameter, between a model simulation with the influences of wind waves (RW) and a simulation without wind waves (Schloen et al., 2017).

4 Three dimensional DCSM-FM model

The physical processes that govern the North Sea hydrodynamics are complex. Numerical modelling allows identification of the relative effect of an artificial hub facility. These models are schematisations of the actual hydrodynamics and can be calibrated and validated to improve its performance and make it sufficiently accurate to perform case study projects.

4.1 Modelling Suite

The normative modelling suite for large scale hydrodynamics is the Delft3D modelling environment, containing numerical models for hydrodynamics, but also for suspended particle matter (SPM) transport, water quality, morphology and ecology. Delft3D is an integrated software suite developed by Deltares capable of simulating two-dimensional and three-dimensional hydrodynamics of estuarine environments, coastal areas and rivers.

This module works with either curvilinear or rectangular grids. Implementations of irregular connections are not possible and grid refinements can only be realised by domain decomposition increasing the total computational effort and time. The Delft3D-Flow module can be found at the heart of the Delft3D modelling environment. This module computes the homogeneous shallow water equations using a finite-volume method for the hydrodynamics.

Recently, a successor of the Delft3D suite was developed that is capable of handling the same curvilinear or rectangular grids, but now with the addition of triangles, hexagons, pentagons and quads as grid-cell shapes. This successor is called Delft3D-Flexible Mesh (FM) with the D-Flow FM module that represents the successor of the Delft3D-Flow module. With the ability to utilise multiple grid forms, the Flexible Mesh environment provides great flexibility for setting up a model with varying grid resolutions, and for modifying existing model grids.

The new unstructured grids are used to solve the shallow water equations with the finite-volume method similar to its structured predecessor. The ability of unstructured grids to locally refine computational grids is very useful for case-studies and the performance is comparable to that of Delft3D-Flow and other shallow water equation solvers, which are known as efficient modules as demonstrated by Kernkamp et al. (2010). Since additional accuracy might be required to judge local impacts at the area of interest, the Delft3D-FM environment is ideal for case studies on the hydrodynamic effects of an artificial island in the North Sea.

4.2 Model set-up

For North Sea simulations, the well known ZUNO (Zuidelijke Noordzee) model grid is often used and can be seen as the standard for recent southern North Sea numerical modelling studies. It is reviewed by international specialist making it a reliable model as concluded by Kaaij et al. (2017). Los et al. (2004) even used it for the ecological impact of an artificial island. The problem with the ZUNO-model for this research project however, is the northern boundary which is located rather close to the Dogger bank. The ZUNO model is generally used to assess Dutch near shore processes and could possible show instability issues during the implementation of artificial islands near the northern boundary.

Since a larger modelling domain is required, the Dutch Continental Shelf Model (DCSM) is a great option. This model covers a much larger area than the ZUNO model. Moreover, the newest 'state of the art' North Sea model known as the 3D DCSM-FM model is a three dimensional model also capable of modelling vertical variations such as stratification. Three versions of 3D-DCSM have been tested and validated recently. All do a great and similar job at predicting tides, surges and water levels even surpassing the ZUNO performance. Section C.1.2 describes the original model set-up in more detail. For even more details and southern North Sea validation, consult Zijl and Veenstra (2018).

4.3 Adjustments

During this research project, some non-converging modelling outputs were found for the deeper northern parts of the North Sea shelf. After some additional exploration, instabilities were discovered at the southern model boundary. In order to produce reliable case study results, instabilities may not be present near the area of interest, as it will become unclear whether the model's output is an actual impact of the implemented islands, or simply a numerical instability.

The elaboration on this boundary instability and its corresponding solution methods that were analysed are found in Section C.2. After several adjustment tests, an extra boundary condition of zero advection was implemented, as well as an adjusted form of lateral temperature and salinity forcing along all boundaries. With these adjustment, the instabilities were resolved while also improving the overall performance of the model's prediction capabilities in the previously validated area.

After the model adjustments, temperature, salinity and density spin-up test were carried out to determine the required spin-up time for this research project. Further explanation can be found in Section C.3, boiling down to a two year spin-up requirement rather than the original one year spin-up for water level and surge research objectives.

The potential of the 3D DCSM-FM model will be tested on the basis of one baseline scenario run, and five island cases. The base run includes no islands and is simply used as a reference case for the impact analysis, as well as to judge the current performance of the model for stratification representation and residual current patterns. The base run and the five island cases each employ an adjusted model grid (see Section C.4) with refinements around the area of the islands, and an interpolated bathymetry.

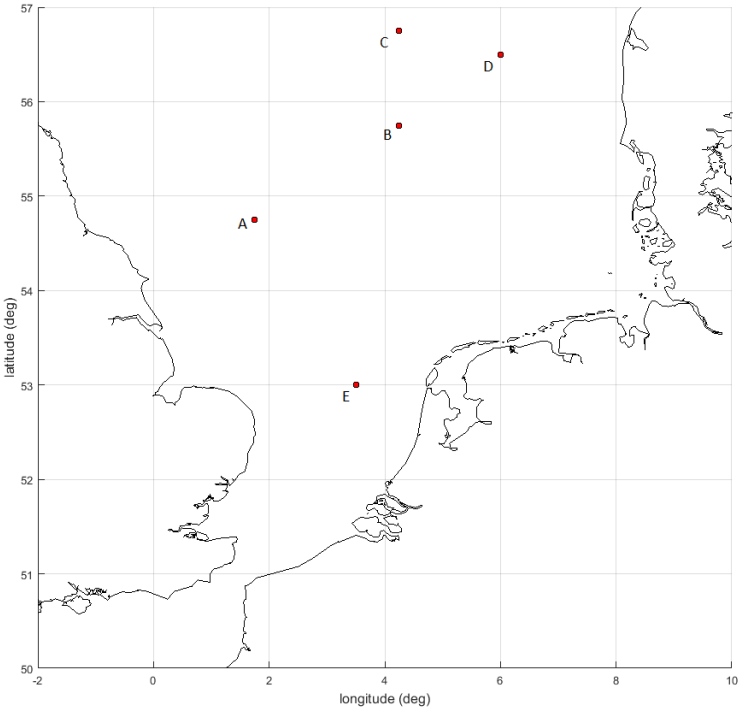

Figure 4.1: The locations of each modelled island case within the North Sea.

Table 4.1 sets forth the island locations and the corresponding depths and depth averaged velocity amplitudes. Two of the island locations are based on the proposed concept by TenneT for a hub island on the Dogger Bank. One island is implemented on the western side of the Dogger Bank (location A) while the other is placed on the eastern side (location B), together comprising both of the Dogger Bank's stratification regimes (being seasonally and intermittently stratified), with location B falling just outside the Natura2000 protected area.

Table 4.1: Basic properties of each island location.

Location	Latitude [deg]	Longitude [deg]	Depth [m]	Average velocity amplitude [m s^{-1}]
A	1.75	54.75	19	0.27
B	4.25	55.75	32	0.21
C	4.25	56.75	45	0.18
D	6.00	56.50	30	0.16
E	3.50	53.00	25	0.75

Two more locations are based on the recommendations of Gerrits (2017), and implemented near the Danish coast and to the north of location B on a relatively shallow area, comprising two different physical environments. Finally, one closer to shore location (E) is investigated based on the current plans for a hub-island system around Ijmuiden Ver. All islands are implemented as a 6 km^2 cylinder in the middle of the refinements, for simplicities sake. This island size is based on the presented concept by TenneT (2017) and the island investigation by Gerrits (2017).

The grid refinement with a factor eight let to a large increase in computational burden, as the modelling time of one calendar year increased from around 29 hours to more than 80 hours using the deltares h6 linux cluster. Even though this is a considerable increase in computation time, it is deemed necessary to correctly compute the hydraulic processes around the artificial islands. The qualitative validation of Section 4.4 is based on the last year from a three year base case computation.

4.4 Qualitative validation

As a basis the model was first used without any island implementations, just with the adjusted grid refinements and the corresponding interpolated bathymetry. This way, the stratification regime representation of the five locations can be compared with the expectations from Chapter 2. The same will be done for the velocity regime and the resulting residual current.

4.4.1 Stratification

Based on Figure 2.6, differentiating regimes are to be expected at each investigation location. As presented by Leeuwen et al. (2015), location A is expected to be intermittently mixed, while location B and C are seasonally stratified and location D is undefined (a mixture of regimes). Location E is expected to be permanently mixed.

The 3D DCSM-FM model calculates densities for each cell and allows users to select temperature and salinity as output variables. This way the influence of both parameters on the final density stratification can be analysed. Figure 4.2 shows the density depth profile over time for the entire calendar year of 2016. It is made up of output data with a time-step of ten minutes, at twenty depth layers. As far as regime representation goes, all locations seem to represent the correct form of annual stratification. Location B is clearly stratified during the summer season, with more prominent stratification during July and August, before becoming slightly better mixed in the following months. Location C is even heavier stratified with its larger water depth, showing larger density stratification from June all the way into October.

Location E is well-mixed during the entire year, with no evident density stratification during the entire year of 2016. It does show relatively low density values for the water column during the colder winter and autumn months. This is an effect of the fresh water inputs of the nearby rivers, since it is located much closer to the shore. Figure D.2 clearly shows the fresh water influence. Location D shows a more diverse stratification regime, as it stratified during June and July, but unlike location B a permanently mixed period exists from halfway down August all the way until half October.

Since sea water temperatures are dominated by exchanges with the atmosphere rather than by river inputs and transport, all locations show similar periods of high increased water temperatures. Dependent on the depth and vertical mixing at each locations, either thermal stratification develops or the entire water column is heated up during the summer months. Salinity is far more location dependent, which is evident from Figure D.2, where the fresh water influences are well represented. More information on the development of stratification is found in Section B.2.

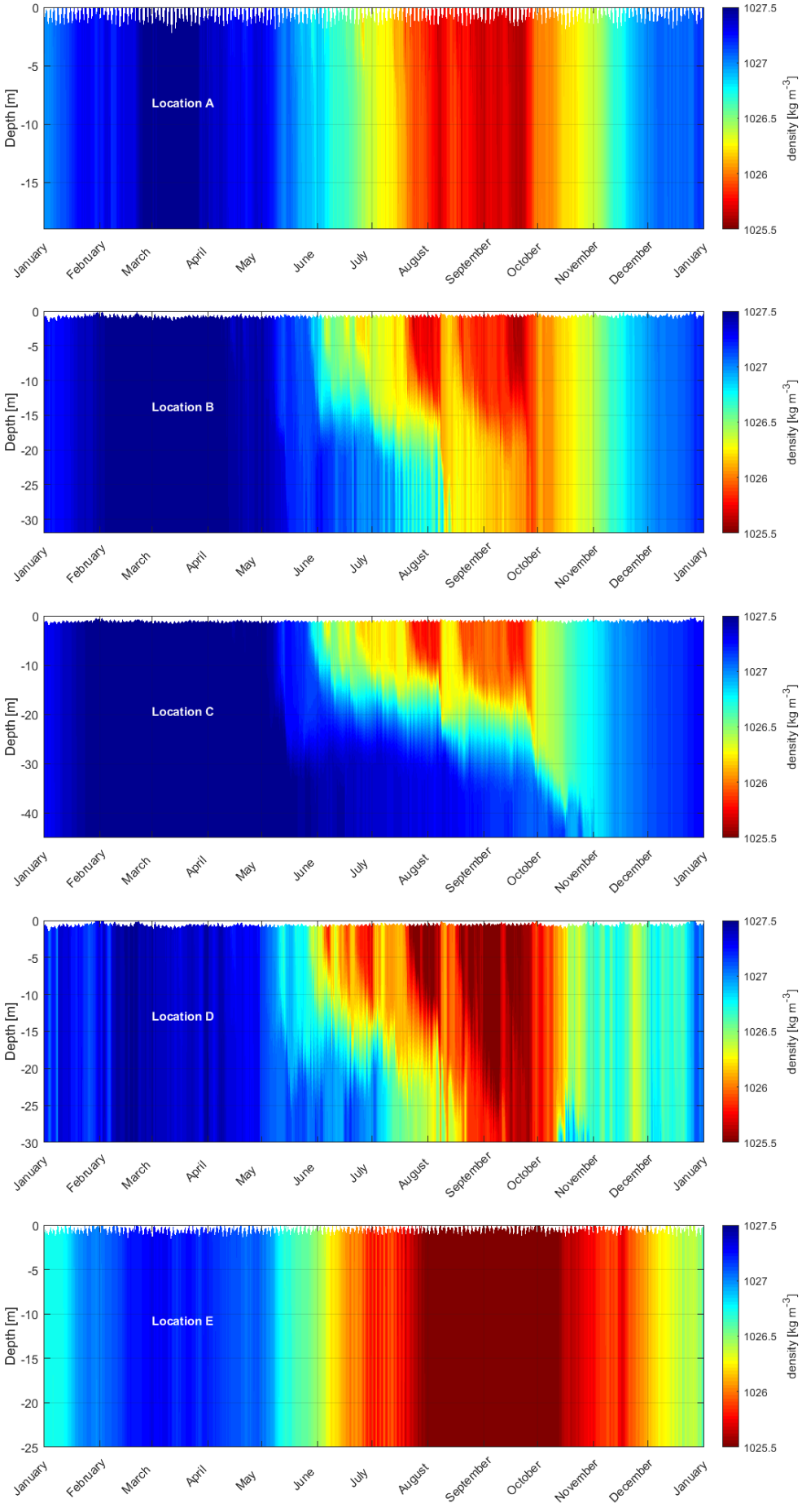

Figure 4.2: The density distribution over depth, at each location for one calendar year (2016).

Locations A and E are somewhat harder to judge looking at Figure 4.2. An intermittently stratified result is expected for location A, but is hard to distinguish. Figure 4.3a however, clearly identifies intermittent periods of density stratification and break ups of extended well-mixed periods. The expected permanently mixed regime of location E (Figure 4.3b) however, does seem to show some unexpected fluctuations of stratification that cross the $0.086 kg/m^3$ threshold of stratification. The reason for this unexpected feature is further investigated in Section 4.5. For now, only location E indicates a slight mismatch with Figure 2.6.

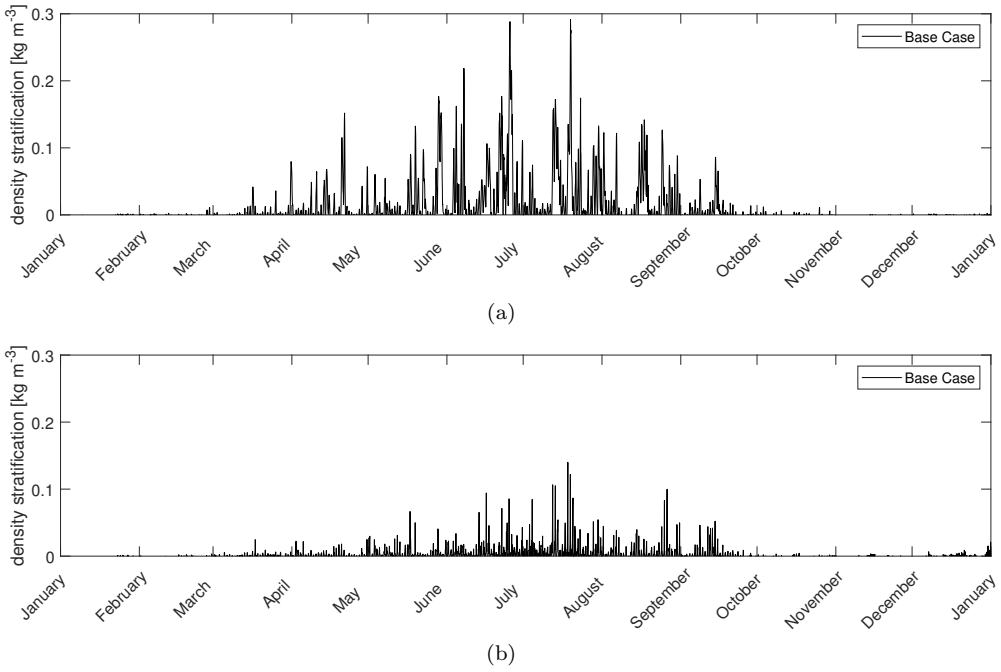

Figure 4.3: (a) The density difference between the water surface and bottom layer for location A. (b) The density difference for location E.

4.4.2 Residual currents

For the impact analysis, it is import to analyse the main direction of the tidal current at the research locations. These help to define the main regions of interest around the island, being parallel and perpendicular to the main tidal flow directions as discussed in Section 2.3.

Flow however, is not perfectly rectilinear for most locations in the North Sea, and is much more rotary. A great tool for analysing the main tidal directions and residual currents is the flow velocity ellipse. This ellipse averages the current velocities of several tidal cycles in order to get a tidal averaged velocity pattern (Harvey et al., 1977).

In order to create a flow velocity ellipse, the duration of one tidal cycle is defined by the lunar day or tidal day. This tidal day is defined by the rotation of the earth and the time it takes to complete 360 degrees around it axis, and the rotation of the moon around the earth. A tidal day is defined as 24 hours and 50 minutes. During this period the semi-diurnal tidal pattern will be completed after which it will iterate.

The current velocities in the North Sea are obviously not completely defined by the tidal cycles but, for example, also by the wind influences. However, the North Sea is a tide dominated system and the tidal day services merely as a reference period. Figures 4.4a to 4.4e show the velocity ellipses for each investigation location, including all modelling processes such as wind strength, atmospheric pressures and freshwater influences.

From the velocity ellipses, the main rectilinear directions can be identified as they mainly represent the tidal character of the location. These directions are defined by the largest fluctuations in velocity magnitude. Table 4.2 presents the chosen primary tidal directions for each location.

Location B has the least rotary velocity character of all the locations. All other locations are far more rotary, especially locations C and D. The flow ellipse magnitudes of locations A, B, C and D are relatively comparable, while location E shows larger magnitudes as it located closer to the shore where the influence of the kelvin wave is much greater.

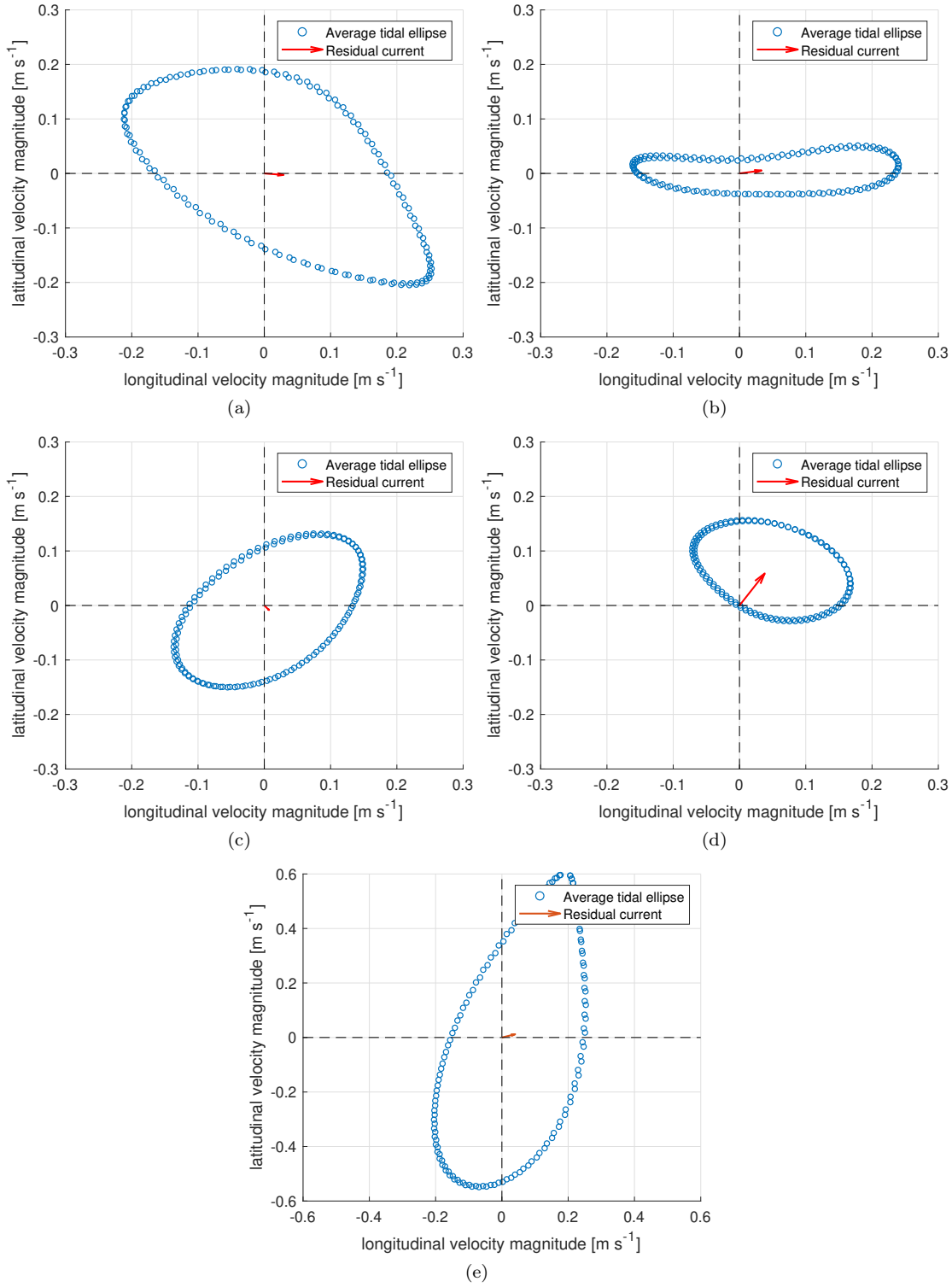

Figure 4.4: Annually averaged current ellipses for each island location. The dots are the data points (every ten minutes) for the average lunar day cycle. The red arrow represents the average residual velocity vector. Notice the different scales for location E.

Table 4.2: Main flow (and observation) directions for each location.

Location	Main recti-linear direction	Residual current direction
A	North-west ⟷ south-east	East
B	East ⟷ west	East
C	North-east ⟷ south-west	South-east
D	North-west ⟷ south-east	North-east
E	North ⟷ south	East

The main areas of interest are those parallel to the main recti-linear flow direction and perpendicular to that. The observation points for the island impact analysis are based on the directions of Table 4.2, and comprise four cross-sections with an observation point at 500, 1000, 2500, 5000, 7500, 10000, 12500 and 15000 metres away from the island boundary. More explanation on the observation points is found in Section C.4.2

Moreover, the velocity ellipses are used to define the residual current at each location. The displacement of the ellipse's centre from zero represents the yearly averaged residual current. This is also plotted in Figures 4.4a to 4.4e as indication of direction and magnitude compared to the lunar day averaged velocity magnitudes.

Since Figures 4.4a till 4.4e do not have the same scales, just the residual currents are shown on the same scale in Figure 4.5 for comparison convenience. These are the yearly averaged velocity magnitudes of one grid cell at the corresponding location.

Locations A, B and E show a similar eastward direction with comparable magnitudes of around 0.04 m/s. Location C has a much lower residual current in the south-eastern direction and Location D experiences the greatest residual flow in the north-eastern direction. All the directions of the 3D DCSM-FM model output seem to match the expectations, comparing to the results found by Linden (2014) and Sundermann and Pohlmann (2011) as can been seen in Figure E.1 and B.2.

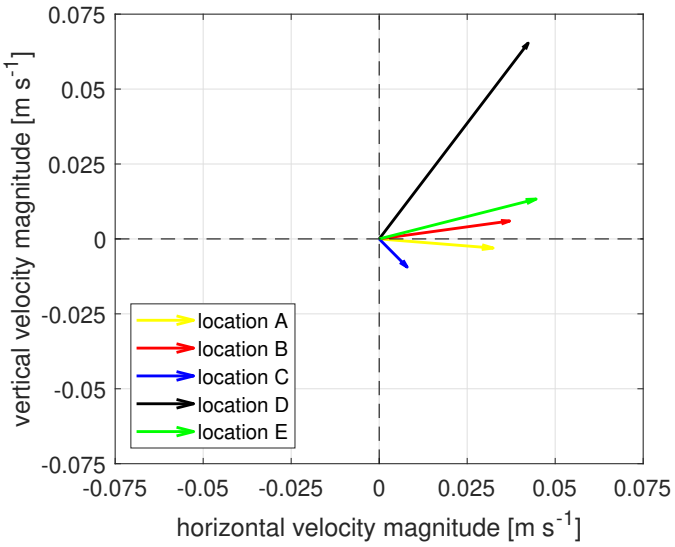

Figure 4.5: The residual current magnitudes and directions of all research locations.

To further identify the residual currents produced by the 3D DCSM-FM model, an extra yearly averaged output is presented in Figure 4.6. This shows the depth-averaged annual residual current magnitudes based on a Fourier analysis of Flexible Mesh. The computed magnitudes show a comparable pattern to that of the dominant tidal influence of Figure B.2, and gives extra trust in the output of the model.

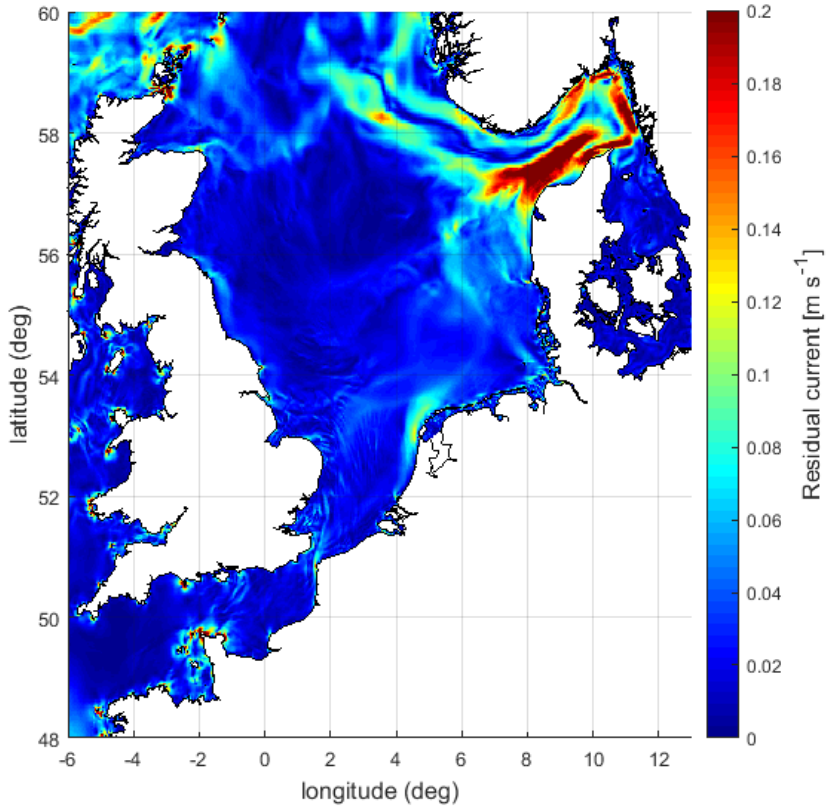

Figure 4.6: Annual mean, baseline depth-averaged magnitude of the residual flow velocity in 2016.

Flexible Mesh computes the residual currents separated into the x-component and y-component, which helps to identify the directions of the main residual currents. The individual maps for longitudinal and latitudinal residual currents are found in Appendix D.

4.5 Quantification of chaotic behaviour

As explained in Section C.3, some chaotic behaviour remains present after the spin-up period of two years, either numeric or physical. No further investigation will done into the cause of this chaotic behaviour. However, during the case-studies it is import to quantify the (location dependent) chaotic behaviour in order to separate it from the actual impact analysis.

The chaotic behaviour or differences with measurements are often expressed in the form of a root-mean-squared-deviation (RMSD) to quantify its existence. The RMSD of salinity and temperature help to separate both influences on density and find the most sensitive parameter. Table 4.3 shows the density RMSD and the corresponding salinity and temperature percentages, which clearly indicate that the chaotic behaviour is salinity dominated in every location. These percentages are based on the assumption that 0.086kg/m^3 is equivalent to 0.5°C or 34.5PSU. Even though this is an approximation, it does highlight the main contributions of chaotic behaviour.

Table 4.3: The surface density RMSD after extensive spin-up time (five years) between similar runs with slightly altered initial conditions.

Location	RMSD of density $[kg\ m^{-3}]$	% due to salinity	% due to temperature
A	0.0089	82.0	18.0
B	0.0079	82.3	17.7
C	0.0109	81.7	18.3
D	0.0260	81.9	18.1
E	0.0595	82.0	18.0

To visualise the location dependency expectations that follow from Table 4.3, a map was made of two almost identical base runs that had slightly different initial conditions. After several years of spin-up, only the chaotic behaviour of surface density remains, which is plotted in Figure 4.7.

It confirms that the near-shore locations show a more chaotic character than relatively further offshore locations. To separate this chaotic behaviour from the island's impact, Figure 4.8 shows the 2016 chaotic behaviour for each research location. The relative influences of temperature and salinity are included to highlight the differences in at every location. In this research project, no further assessment will be done of the chaotic behaviour and its source, as this could be a research project on its own.

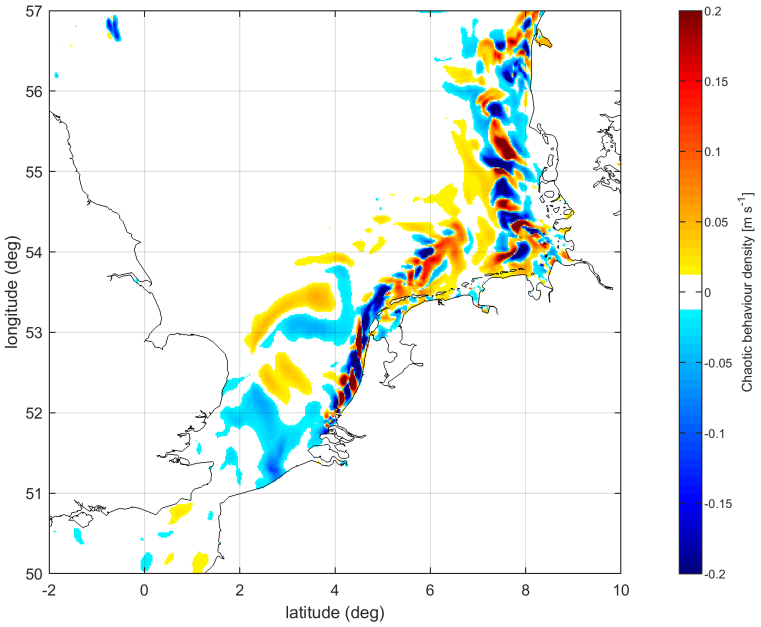

Figure 4.7: North Sea map showing a snapshot of the difference between two identical model computations (except for the initial conditions) in surface density. This gives an indication of the spatial distribution of chaotic behaviour.

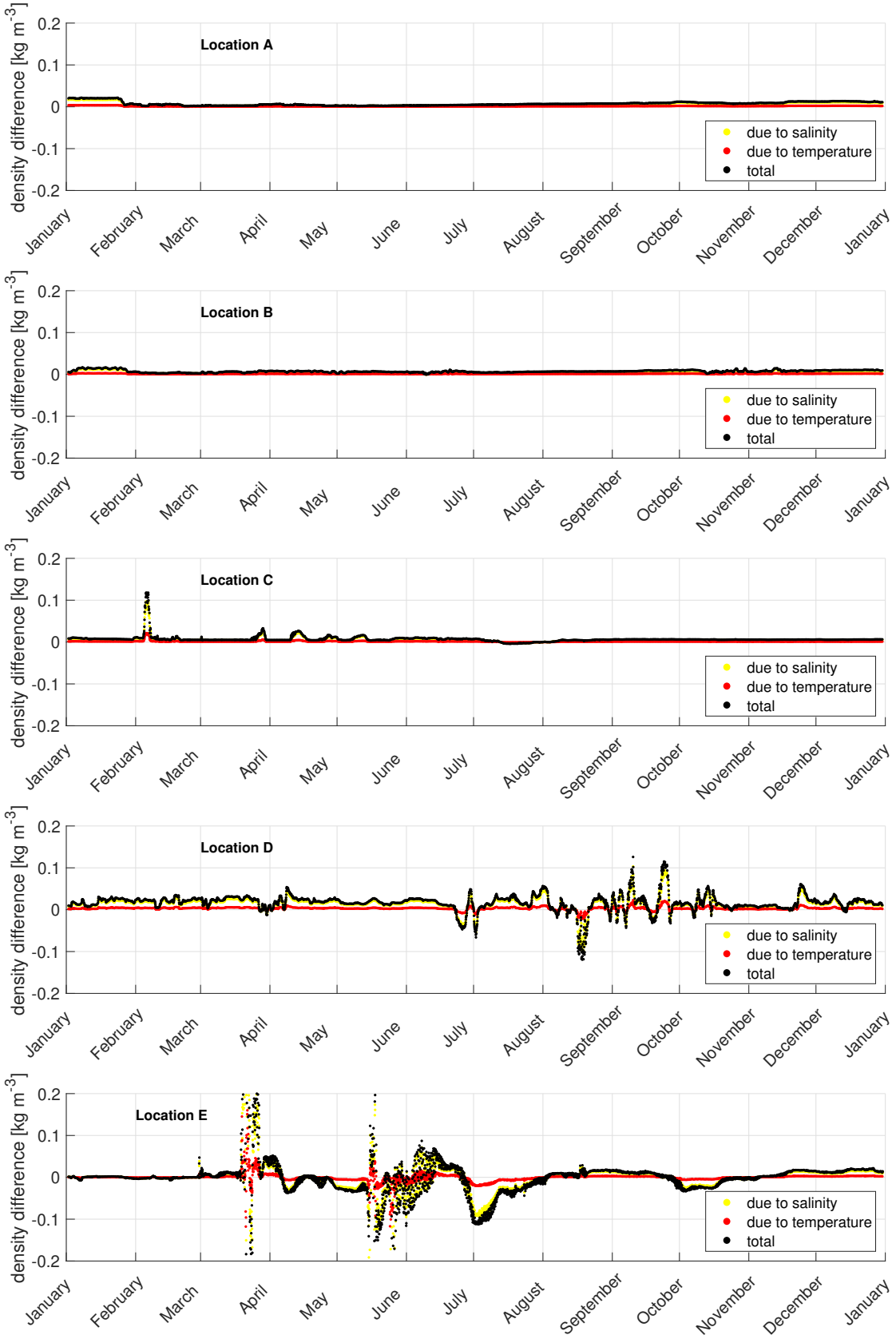

Figure 4.8: Chaotic behaviour of surface density for all locations in 2016, including the relative influence of salinity and temperature.

5 Computed island impacts

This chapter describes the differences in the hydraulic parameters; stratification and residual currents. The island implementation is described in Section C.4, and is equal for every island. The results follow from the comparison between the base run with grid refinements only, and the five other runs each including one island case. This chapter limits itself to the presentation of the computed model impacts and short descriptions of them, while Chapter 6 discusses the output's actual purport.

All impact assessments are done for the computation of the calendar year 2016. During this research, the required boundary condition data and lateral forcing values are available for the years 2012 up to and including 2016. The most recent available year was used for the baseline investigation, and the same will be done for all the impact analyses. Every calendar year has somewhat different conditions, yet only relative effects will be analysed to quantify the island's influences.

5.1 Stratification

As defined earlier in Section 2.2 there are two main stratification interests that are interesting to explore. The regime changes, and the timing changes. Moreover, the main impacted directions and distances will be described in order to determine the footprint of each island. The residual currents are discussed separately in Section 5.2.

5.1.1 Regimes

In Chapter 4, density plots over the depth and time were used as a form of regime interpretation to look at the different density layers, and their distribution over the year and depth. Figure 5.1 represents the same visualisations for the island cases, 500 metres away from the island's bank.

The observation point at each island is chosen in the dominant direction of impact, to showcase the maximum possible mixing phenomena. These locations coincide with the direction of the far-field residual currents and is further disclosed in Section 5.1.4. The beginning of the month is indicated for each month with a tick along the axis.

The islands have a mixing effect that breaks down the distinct density layer separations during the year. As expected, this mixing is most evident for location B, C and D. Even thought the islands do not mix the water over the entire water depth for a full calendar year at any location, it is clearly redistributing density over the depth for the full year. This increases the exchange between the previously separated water depths, and is expected to have a significant effect on the nutrient mixing that was previously limited in the vertical direction. Depending on original nutrient availability distributions, this could have a significant effect on the primary production dynamics of the water column.

Figure 5.1 shows near-island effects in each predominantly affected direction. This mixing effect however, is present in each direction and for longer distances than 500m. Section 5.1.4 demonstrates this directional distribution in more detail. For some islands (but not all), the mixing influences of the island reach for more than 20km.

In order to deduce the changes in regimes in more detail, the density difference threshold between water surface and bottom is used again. This way location A and E are also included in the analysis, which show density differences of much smaller quantities and thus are hard to discern from the density distribution figures.

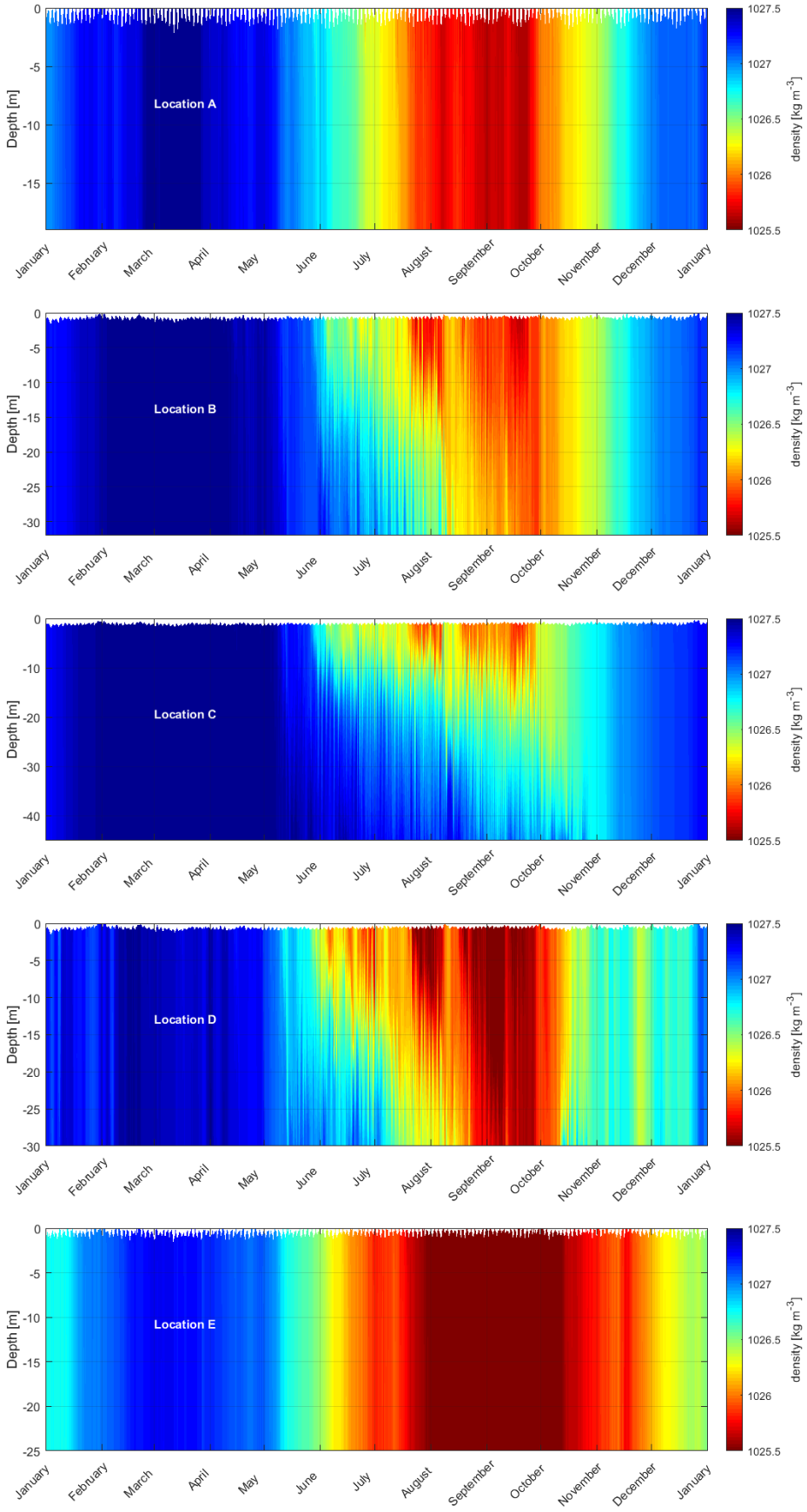

Figure 5.1: The density distribution over the depth, at each location for one calendar year (2016) including the implementation of each artificial island.

The definition by Leeuwen et al. (2015) is based on the density difference threshold between surface and bottom of 0.086 kg/m^3. The extended continuous periods of stratified and mixed days are given in Table 5.1 for all the locations with and without the presence of an Island. For the base case, the defined stratification regimes of location A, B and C match the predictions of Figure 2.6.

Location E does however not match the expectations. Location E possibly differs as a result of the chaotic behaviour, as occasional outliers in density values cause a break in the extended period of mixed waters. This theory is fostered by the fact that the computed period of extended stratification equals zero, which also emphasises the fact that only short bursts of stratification are computed. Nevertheless, the most likely cause of this mismatch with the predictions of Leeuwen et al. (2015) is the fact that it is a comparison between two different models and not with actual measurements. The difference in time step for example, affects the results as the 3D DCSM-FM model computes outputs every ten minutes, compared to the daily time-step used to create Figure 2.6. As no full days of stratification commence, the area at location E is assumed to be permanently mixed and will remain permanently mixed with the presence of the island.

The seasonally stratified regime for location D can be explained by the fact that only one year is analysed for this research project. Location D is listed as undefined as it shifts between intermittently stratified and seasonally stratified, depending on the year and the corresponding conditions. For the 2016 baseline computation a seasonally stratified regime is deemed correct and will not be investigated further.

For all islands, the mixing impact of the island is clearly visible as every single extended stratified period is reduced in length (except for location E, which never had a full day of continuous stratification to begin with). Moreover, an increase in extended mixed periods is identified for location A and E, indicating the breaking down of occasional short stratified periods.

Table 5.1: The longest consecutive periods of stratified and mixed water columns [days] within a year for the base case and each island case.

	Base case			Island cases		
	P(mixed)	P(stratified)	Regime	P(mixed)	P(stratified)	Regime
A	242	5	IS	290	0	IS
B	187	94	SS	186	29	IS
C	127	204	SS	126	165	SS
D	143	139	SS	132	95	SS
E	282	0	Undefined	306	0	Undefined

5.1.2 Timing

It is important to know whether the presence of an island will imply changes to the timing of stratified periods. The timing of onset and breakdown was found to have a significant effect on the phytoplankton dynamics of the full stratified period. The timing of these periods is analysed with the help of Figure 5.2 and 5.3 for locations C and D. The other islands are disregarded as they either have no periods of extensive stratification in their near proximity, or because the regime has changed from seasonally stratified to intermittently stratified which is the case for island B.

Islands C and D cause an overall decrease in stratification during the entire stratified season. With 0.086 kg/m^3 as threshold for stratification regimes, the same threshold will be used here to identify the timing difference. The striped line indicates this threshold in the figures. For location C, the extensive stratification period starts on the 8th of May for the base case, and ends on the 29th of October. The island's de-stratifying effect causes a delay in the onset of the stratification period by around sixteen days, and breaks the stratification down earlier by around eight days. Island D seems to have a slightly lower effect on the stratification, as the timing effect of the build-up and break-down only comprise around one and three days respectively.

The threshold used to define stratified periods defines the timing differences near the island, and to which distances the timing is affected. For this threshold, significant timing differences are to be expected up to around 2.5km away from the islands. The results can differ slightly for adjusted threshold values, yet no changes are made in this research project in order to remain consistent. The most important result to take away from this analysis, is the fact that timing differences are definitely to be expected near the islands, indicating an important possibility of changes to the local primary production dynamics.

Up to about 2km away, the changes in onset timing can be in the order of around ten to fifteen days. Ruardij et al. (1977) described that differences of this scale in onset alone, can affect the phytoplankton dynamics for several months.

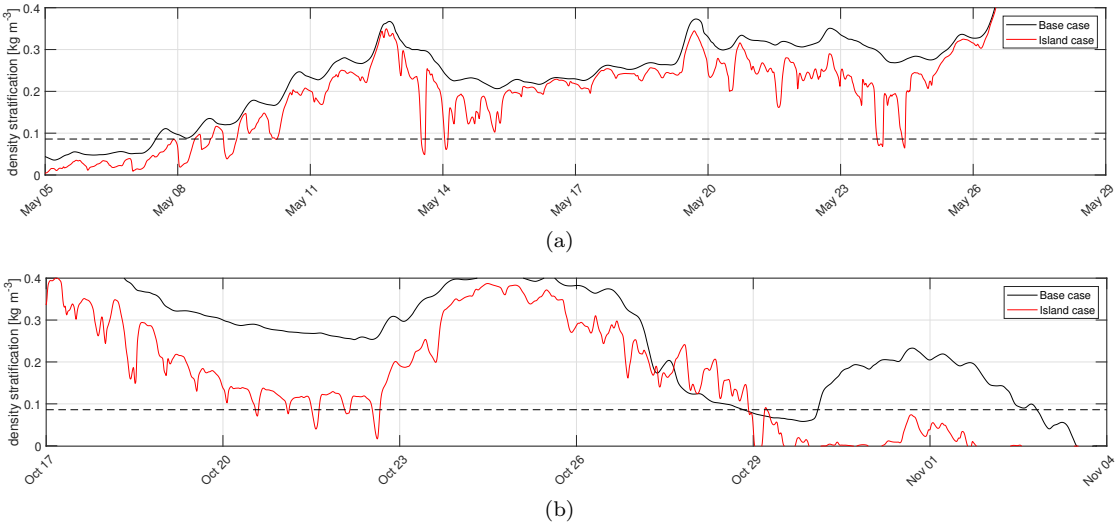

Figure 5.2: Density stratification for the base case and island C case at 500 metres to the north-west. (a) The commence of the extended stratified period. (b) The conclusion of the extended stratified period.

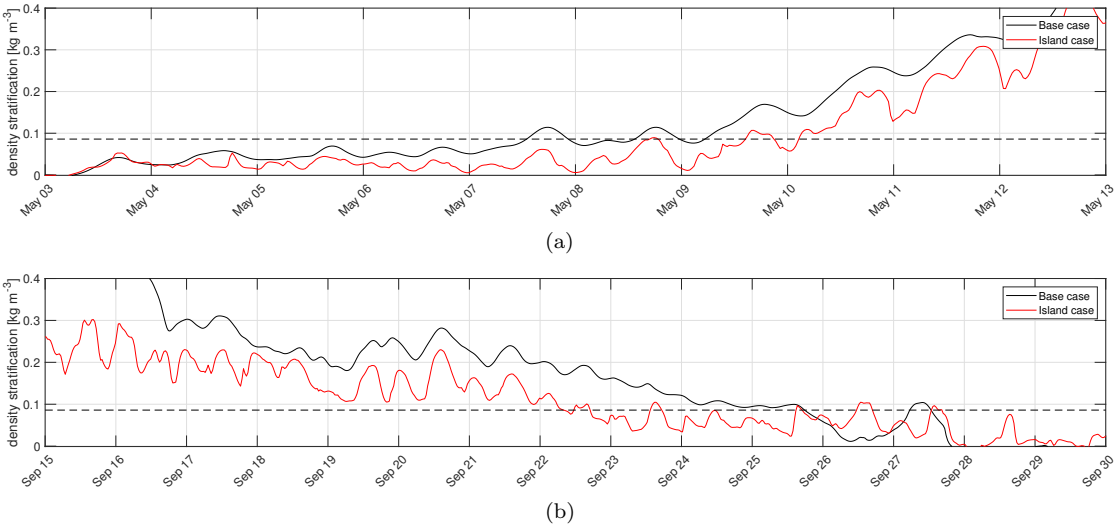

Figure 5.3: Density stratification for the base case and island D case at 500 metres to the north-east. (a) The commence of the extended stratified period. (b) The conclusion of the extended stratified period.

5.1.3 Depth profiles

Depth profiles are an important characteristic of stratification. It elaborates on the vertical mixing, more so than the traditional form that subtracts the bottom density from the surface density. Mixing could be concentrated around the pycnocline rather than affecting the entire water-column, as discussed in Section 2.2. To visualise this impact over the water depth, the difference in density is computed over time for each depth layer. That way, Figure 5.4 shows the density differences over time and depth. Essentially, it is the difference between Figure 4.2 and Figure 5.1 for each location.

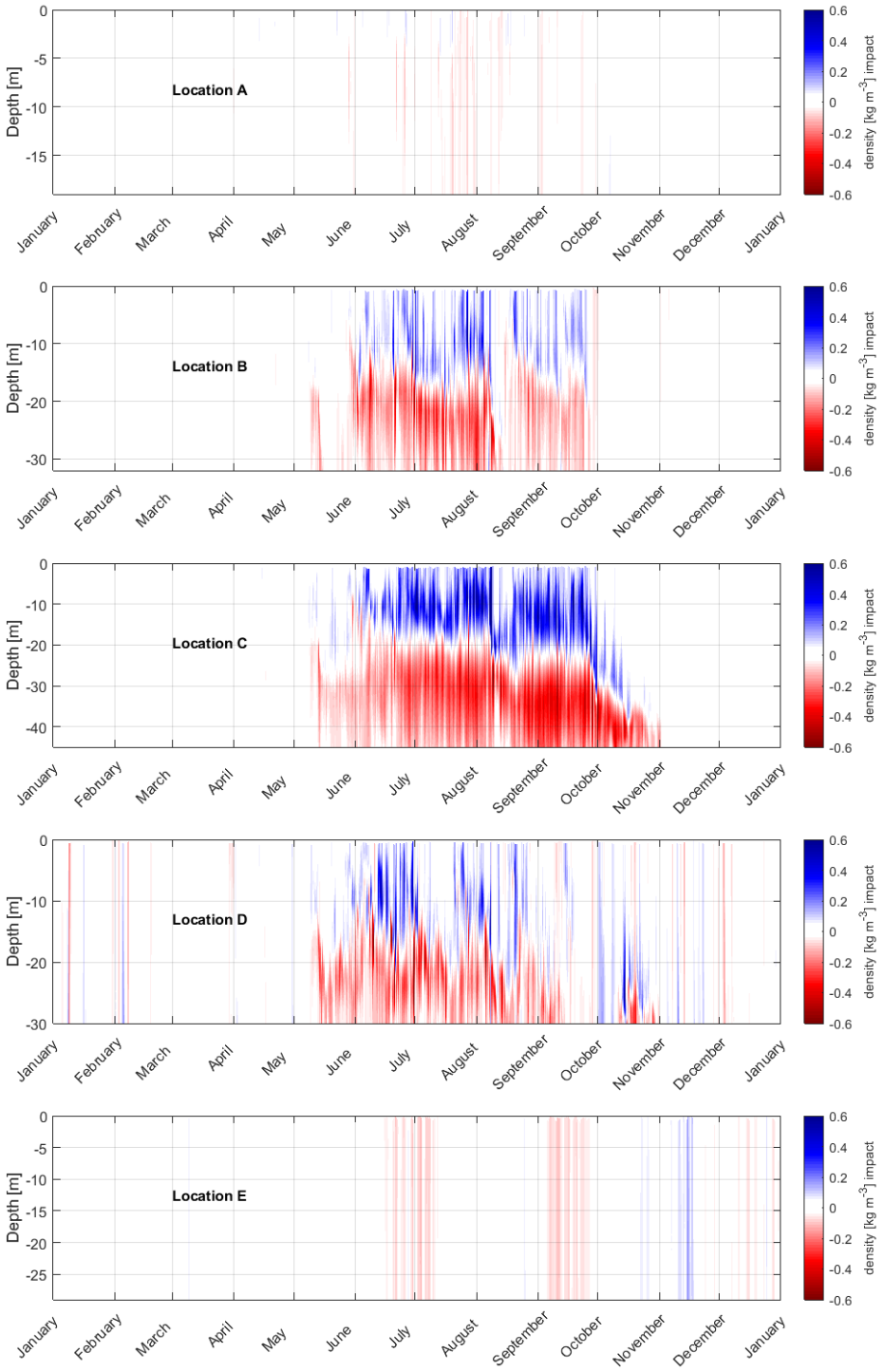

Figure 5.4: Density impacts over the depth, at each location for one calendar year (2016) as a result of the artificial islands.

Not much impact on the density profile is seen for locations A and E, as they are already relatively well mixed. Some minor impact is seen over the entire water column for Location E which is likely the visualisation of chaotic behaviour which is most prevalent for this island case, or small changes in salinity distributions. Moreover, some small changes are seen at Location A, which are likely the mixing of the already short periods of stratification.

Locations B and C show clear mixing influences around what seems to be the original location of the pycnoclines, with an almost constant mixing at location C and a slightly more throbbing character for location B. Island D also shows some impact, but has a more precarious character than the other islands. Additionally just like location E, some occasional density differences are seen throughout the year, as location D is also under slightly more influence of salinity and chaotic behaviour.

5.1.4 Distance and directions

When debating on the location of an artificial island and it's impacts, it is important to know the footprint of such decision. The impact on stratification decreases over distance from the island, while also being different in all directions. Figure 5.5a until 5.5c show the averaged amount of density stratification impact for all observation points around each island with an extended stratified period, in the four main directions. The impact is averaged over the months June until (and including) October, during which all three of these locations show significant stratification. The percentages indicated how much the stratification reduced over that period of time. Notice how there are no average increases in stratification around any of the islands in any direction. This does not mean that occasional enhanced stratification is ruled out, it just means that on average, de-stratification seems to occur in all directions.

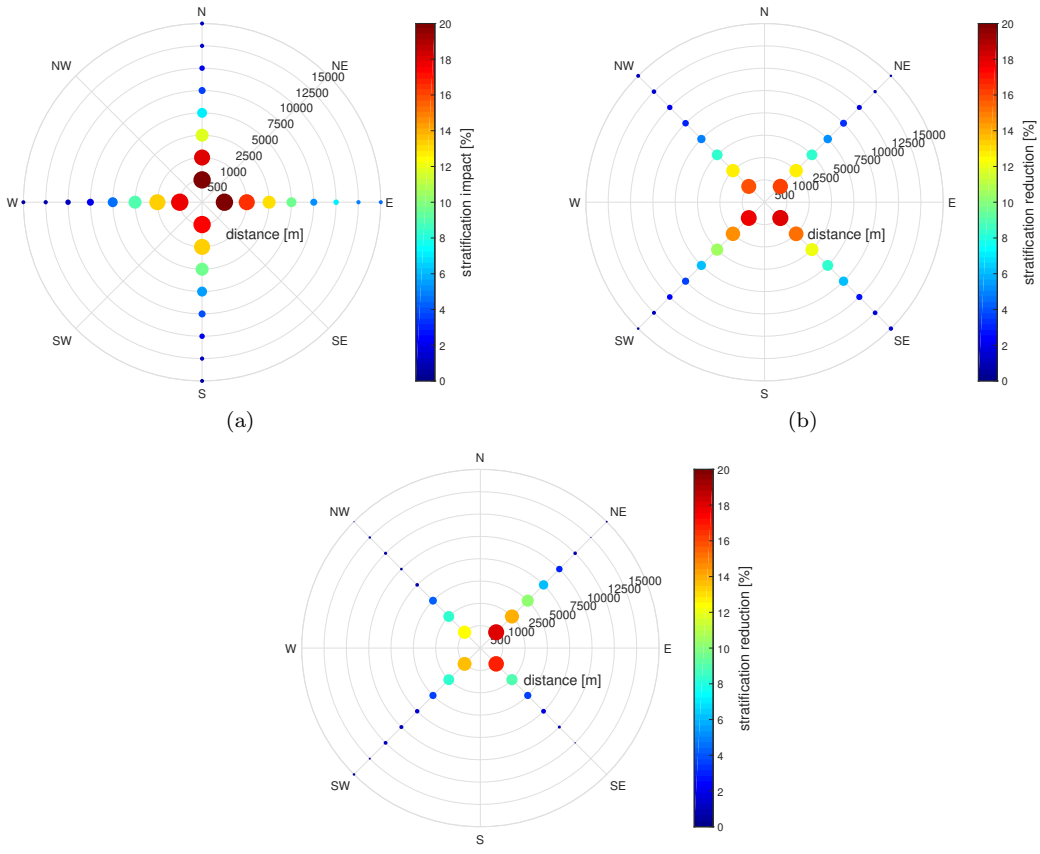

(a) (b) (c)

Figure 5.5: Polar plots of location B, D and D respectively, showing the decrease in stratification (averaged over June until October 2016) compared to the baseline run. Based on the difference between surface and near-bed density.

Figures 5.6a to 5.6c visualise the same data as Figures 5.5a until 5.5c, yet in an one dimensional manner. Even though this makes the distinction between different observation cross-sections less congenital, it does highlight one of the most evident returning characteristics. For every location, the predominant direction of impact is equal to the far-field residual flow depicted in Figure 4.5. This is most evident for Location D, where the residual current is significant larger than for the other locations. Still, for relatively low far field residual currents the correlation remains conspicuous.

Additionally, Figure 5.6 re-emphasises the fact that on average, none of the directions around any of the islands show an area of enhanced stratification. Near the island, each orientation seems to experience similar de-stratification influences, after which the dominance in the direction of the far-field residual current commences.

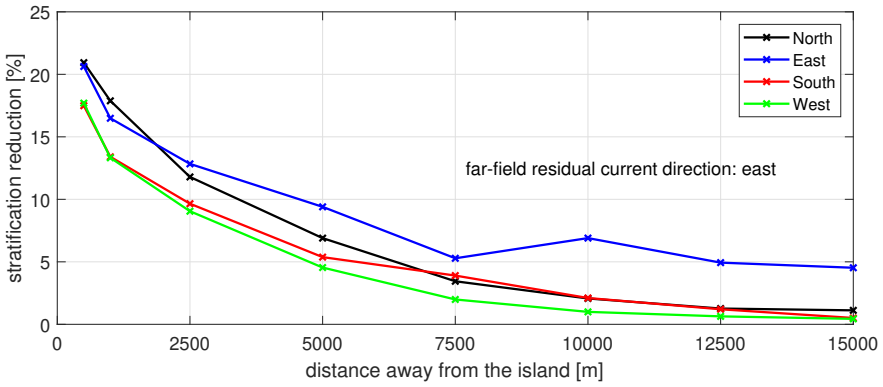

(a)

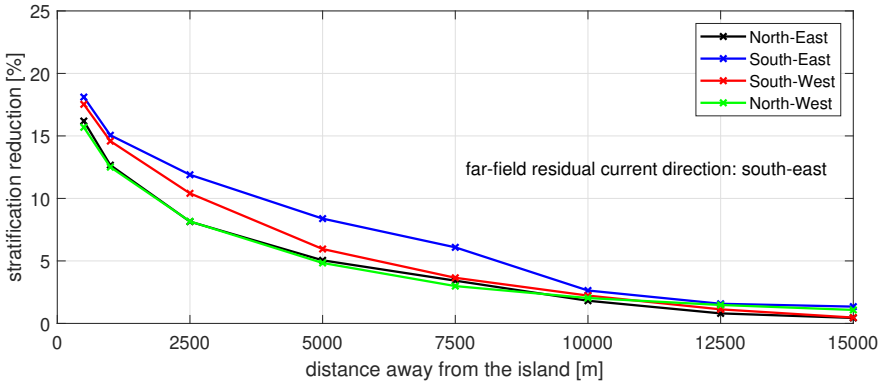

(b)

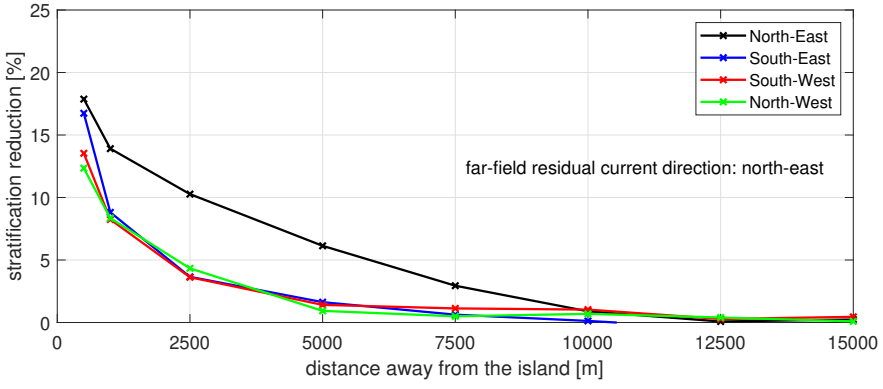

(c)

Figure 5.6: Line plots of location B, C and D respectively, showing the decrease in stratification (averaged over June until October 2016) compared to the original base run. Based on the difference between surface and near-bed density.

Interestingly enough, the model shows that it is indeed true that the $h/\overline{u}^3$ stratification parameter can not be used as trustworthy indication of increased and decreased stratification areas around constrictions with flow separation and turbulent eddies. The turbulent eddies play a large role in the vertical mixing profile, and the residual flow clearly affects the distribution too. Figure 5.5 shows that for every location, the impact is dominant in the direction of the far-field residual flow direction. Simultaneously, Figure 5.7 highlights the areas of increased and decreased velocity amplitude and their mismatch with areas of de-stratification.

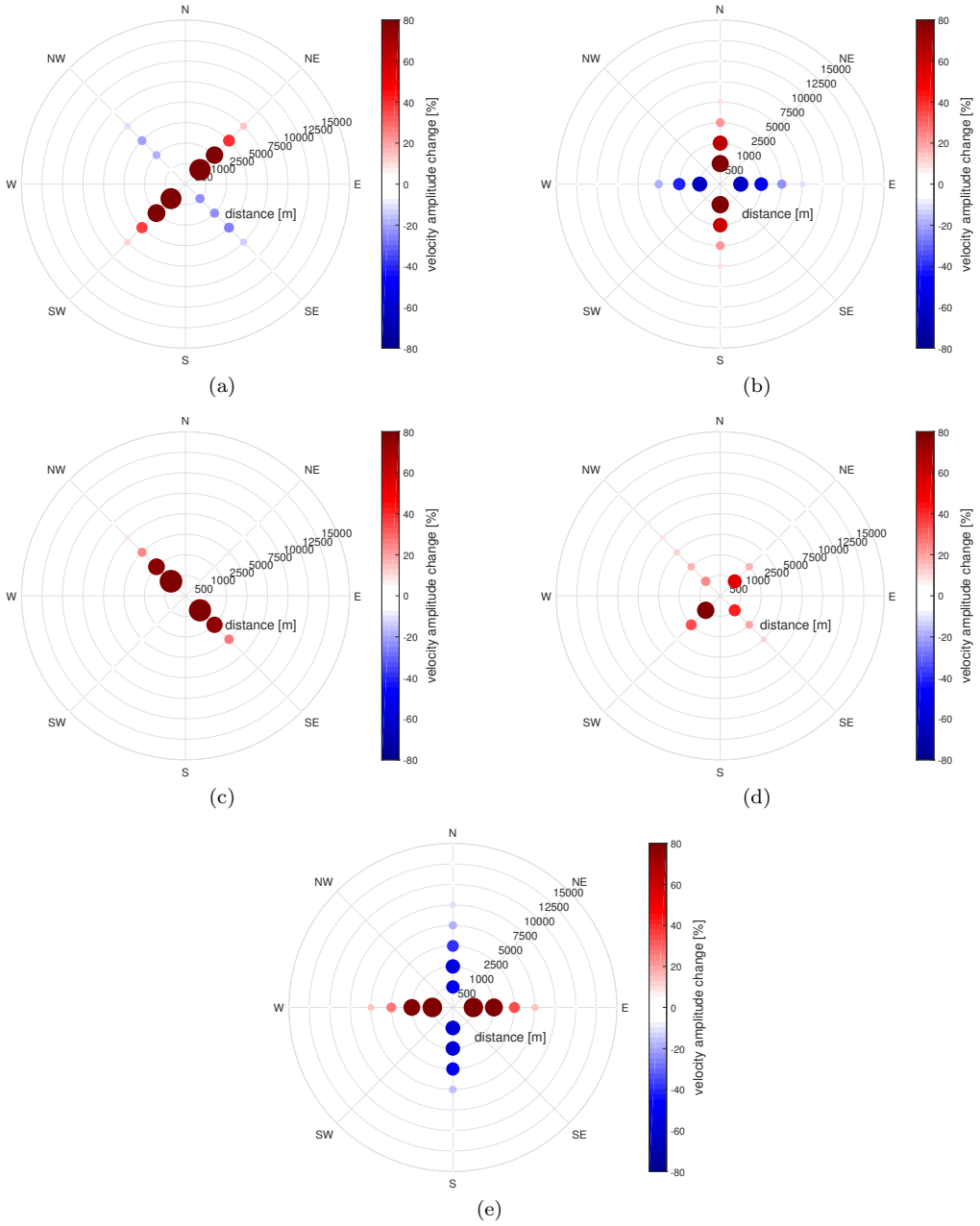

Figure 5.7: Polar plots of each island location, showing the decrease and increase in depth averaged velocity magnitude amplitude (averaged over June until October 2016) compared to the original base run.

Observation cross-sections do however not tell the full story. The distribution over the horizontal is truly two-dimensional and can not be fully represented by simple cross-sections. Maps help to visualise the spacial distribution of stratification impacts around the islands. Figure 5.8 shows a snapshot of the stratification impact around island B. It highlights the need of map calculations over observation points, and the fact that occasional increased stratification can occur.

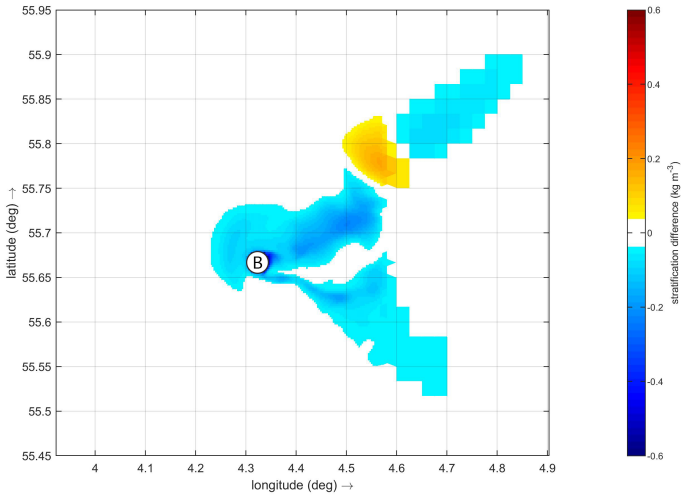

Figure 5.8: Impact snapshot of stratification around artificial island B (negative values indicate de-stratification).

5.2 Residual currents

Since yearly residual currents are a time-averaged parameter, an annually averaged output map can be computed to visualise the impact of each island. This is done through the use a Fourier analysis in Flexible Mesh. It computes the depth-averaged residual flow velocity in x, and y-direction over the full 2016 calendar year. These can be post-processed to compute the resulting residual current magnitude impact around the artificial islands, as presented in Figure 5.10 for the local impacts. Figure 5.9 highlights the fact that the residual current impact remains local within a distance of around 10km, which is the case for every location.

Unfortunately, the Flexible Mesh Fourier analysis is still a beta function, meaning that it is not completely supported yet. Because of this, no indication can be given of vertical residual currents or layer separated results. These options will become available in the future.

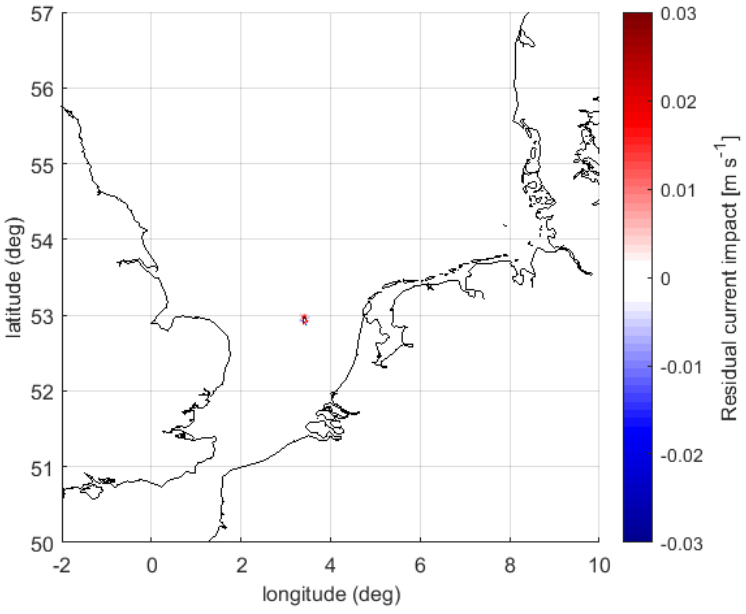

Figure 5.9: Large scale effects of island E on the residual currents of the North Sea shelf. Positive values indicate an increase in magnitude by the island.

Figure 5.10 shows the residual current impact patterns as a result of each artificial island. The far-field residual current magnitudes and directions are different for each location, as are the characteristics of the oscillatory flow velocity magnitudes. This causes each pattern of residual current impact to be different from one another. The resulting patterns will be further discussed in Chapter 6.

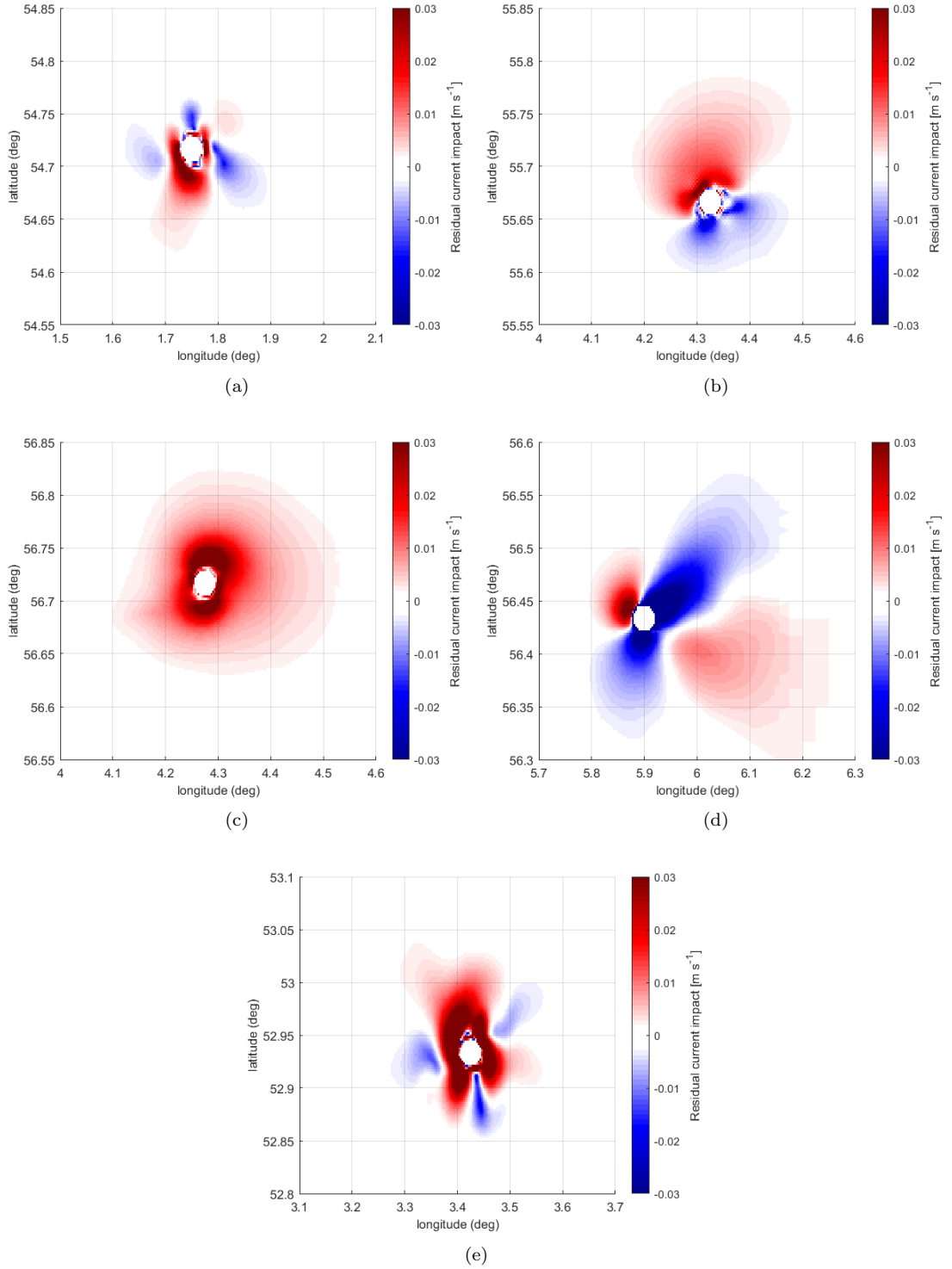

Figure 5.10: Annual depth averaged residual current impact at all locations. Positive values indicate an increase in magnitude by the island.

5.3 Summary

The impact of the artificial island on stratification and residual currents differ for every location. The original baseline characteristics determine the pattern and type of impact for both parameters. An artificial island is capable of altering the stratification regimes or onset timing up to a distance of around 2.5km, with density mixing effects up to 20km. The residual current impacts also remain local, up to a distance of around 10km. All general impacts for each island location can be found in Tables 5.2 and 5.3.

Table 5.2: Baseline stratification characteristics and impact for each artificial island case.

	Baseline			Island Impact	
Location	Depth	Velocity amp.	Regime	Type of impact	Predominant direction
A	19	0.27	IS	*Little impact*	*N.A.*
B	32	0.21	SS	Regime change	East
C	45	0.18	SS	Timing change	South-east
D	30	0.16	SS	Timing change	North-east
E	25	0.75	Undefined	*Little impact*	*N.A.*

Table 5.3: Baseline residual current characteristics and impact for each artificial island case.

	Baseline			Island Impact
Location	Depth	Residual flow magnitude	Far-field direction	Type of impact
A	19	0.032	East	Local
B	32	0.038	East	Local
C	45	0.012	South-east	Local
D	30	0.076	North-east	Local
E	25	0.047	East	Local

6 Discussion

Before the main research questions are discoursed and conclusions are drawn, this research as a whole will be reflected on. This helps to put the research results into perspective and strengthens the conclusions. First, the chosen methodology will be discussed after which the modelling results will follow. To finalise, the usage of the 3D DCSM-FM model as island design tool will be discussed.

6.1 Reflection on methodology

In the world of hydrodynamic modelling, there are many options when it comes to the choice of simulation module, modelling domain and case study implementation into the domain. This section discusses the chosen modelling set-up and both its benefits and downsides.

6.1.1 Flexible mesh module

One of the main reasons for the choice of D-Flow Flexible Mesh as modelling suite is the ability to use unstructured grids. Flexible Mesh is great for the use of local refinements, which can relatively easily be implemented in the modelling grid. Other modelling suites require nesting for more detailed numerical simulations, which can be a very time consuming process. More over, the coarsening of the grid in locations where spacial scales allow it greatly reduces the computational time compared to the structured grids of for example Delft3D-FLOW. During model validation, the DFLOW-FM version of the 3D DCSM was found to even outclass its Delf3D-FLOW predecessor (Zijl and Veenstra, 2018).

6.1.2 Modelling set-up

The biggest advantage of the 3D DCSM-FM model over the creation of a new modelling domain for this investigation purpose is the fact that it has been validated for many locations, forming a great base for an impact analysis knowing that the current set-up decently represents actual measured conditions. It makes the results of the impact analysis on the North Sea much more trustworthy.

With this advantage comes one of the disadvantages, being the extended modelling domain. The domain covers an area much larger than the expected area of impact, leading to larger computational burdens than possibly necessary. It is a deliberation between reliability and computational effort, since it unlikely that a newly build model grid will produce output of similar quality with the time reserved for this research project.

The implementation of the island could be improved for more detailed case studies. Currently, the grid refinement is carried out by refining an area of ten by ten original grid cells with a factor of eight. This is done by three casulli-type refinements of factor two, resulting in a more detailed grid area as explained in Section C.4. This set-up does a satisfactory job for the initial exploration of island impacts, but could be improved by using triangles around the island to better approach the circular form of the island.

Moreover, the refinement requires new definitions of the depth values at each node. For this research, it is done through interpolating the depth values at the locations of the original grid nodes. A more detailed bathymetry can be defined through the presence of additional nodes, by using more detailed samples within the refinement.

Since it is not possible to define the area of output for map files, only the whole model domain can be selected as map output. For smaller modelling domains this is not much of a problem, but for this modelling set-up the map output files are simply too large to do long time scale analyses. Currently, an output time step of 4 days leads to a map file size of around 30 gigabytes for a run of one year. For the observation points, the output time step of t minutes is used. Using this for map files would lead to around 17.3 terabytes of data, which was not available for this research project. Moreover, the post-processing of such files would greatly increase the required time or computing power. Consequently, this research is based mostly on observation points rather than map outputs.

Since the modelling domain is relatively large, parallellisation of the computations is almost a must. Using the high-performance, distributed-memory computing cluster of Deltares to split the model in twenty partitions helps to keep the computational time reasonable. The downside however, are the twenty partitioned map outputs which take about four hours to be merged after the computation has finished (in case of a 30 GB output). Moreover, during busy periods the cluster can be flooded with many request of modelling colleagues, which leads to large (and more importantly uncontrollable) waiting times.

6.1.3 Output reliability

As described in Chapter 4, the 3D DCSM-FM does show some chaotic behaviour for the density after the spin-up time has completed. This chaotic behaviour of density values is mostly dependent on the salinity rather than temperature, meaning that areas with higher fluctuations in salinity are more prone to these inconsistencies. This means that areas near the shore, where freshwater influences are significant, show the most chaotic behaviour.

Figure 6.1 shows the chaotic behaviour for three different observation points away from the Dutch coast of Terschelling. At 4 kilometres, 50 kilometres and 175 kilometres away from the coast. It indicates the decrease in chaotic behaviour away from fresh water influences of river inputs, as the chaotic behaviour decreases with distance from the coast. Figure 4.7 presents a visualisation of the model's chaotic behaviour distribution.

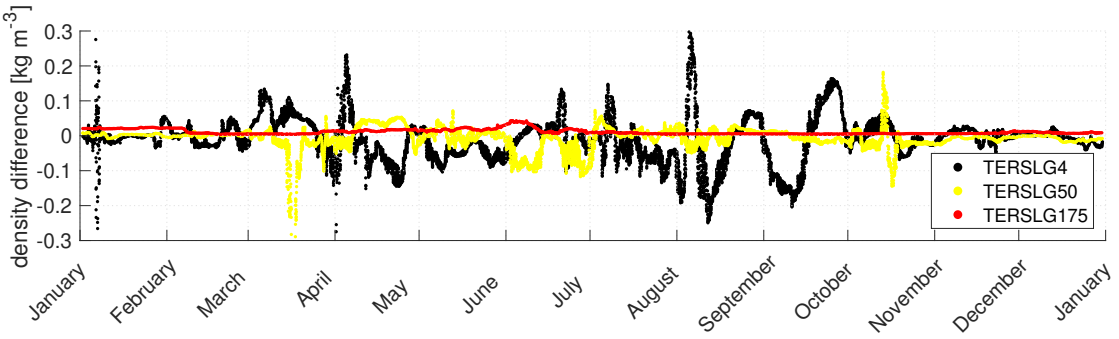

Figure 6.1: Choatic behaviour of stations at three different distances from the Dutch coast for the year 2016.

For case studies, it is mostly important that the model does not produce any instabilities (which it does not), and that it produces realistic predictions. That way case studies can be carried out as long as the chaotic behaviour for each case is quantified.

As long as the impact of the modelled artificial island is larger than the chaotic behaviour, it is possible to look into its influences. As soon as the output analyses shows impacts of the same order as the chaotic behaviour, it becomes uncertain if the changes are caused by the artificial island or by such chaotic behaviour.

For this particular research project, density changes due to the islands (see Figure 4.1 for the exact locations) are found to be in the order of around ten times larger than the chaotic behaviour at location B, while location A and C barely show any chaotic behaviour at all. This confirms the computed impact is reliable. The near-shore location E shows more chaotic behaviour, but since the area is already well-mixed no stratification changes are found anyway. Finally, Location D is a somewhat harder to judge location, where the computed impact is slightly less dominant over the chaotic behaviour. The impact is still clearly larger than the chaotic behaviour, so qualitative analyses can still be carried out.

6.2 Island impact analysis

In this section, the modelling output presented in Chapter 5 will be discussed. Discussions are presented regarding the found forms of impact, and the important processes around the artificial island cases.

6.2.1 Stratification

For stratification, there are multiple ways to interpret the impact. More so than residual fluxes which are more straightforward. The stratification impact output will be discussed on the basis of its regime, onset timing, depth profile and spatial influences.

6.2.1.1 Regimes

Stratification regimes play a big role in the North Sea primary production rates and distribution of phytoplankton dynamics. Different types of primary producers thrive under different types of regimes. Using the model, shifts in regimes can be identified. Table 6.1 shows that near the islands, regime changes can happen. Especially island B shifts from a clearly seasonally stratified (SS) regime to an intermittently stratified (IS) regime, as the original extended periods of stratification are broken up by the island's mixing. Some of the stratified period at location C is broken up, however due to its much larger water depth and somewhat smaller velocity amplitude, the regime remains seasonally stratified. The impact remains restricted to timing differences rather than regime changes for locations C and D.

Table 6.1: The longest consecutive periods of stratified and mixed water columns [days] within a year for the base case and each island case. The corresponding stratification regimes are included.

	Base case			Island cases		
	P(mixed)	P(stratified)	Regime	P(mixed)	P(stratified)	Regime
A	242	5	IS	290	0	IS
B	187	94	SS	186	29	IS
C	127	204	SS	126	165	SS
D	143	139	SS	132	95	SS
E	282	0	Undefined	306	0	Undefined

The regimes are dependent on the consecutive days a water column is stratified or completely mixed. The 3D-DCSM model does a fine job at predicting such periods of continuous stratified and mixed condition, based on the comparison with other modelling studies such as the one from Leeuwen et al. (2015).

Not all regimes perfectly match with other modelling studies. The generic expectations of stratified and mixed periods align, while some minor differences are found. It is important to realise that this is a comparison between two modelling studies with different modules and settings, so minor differences are to be expected.

Moreover, for locations with high fresh water influences chaotic behaviour can alter the results slightly. Whereas the chaotic behaviour is not very problematic for long time-scale trends such as residual currents, it does intervene when looking at extended periods of stratification, since short burst of chaotic behaviour can break up periods of continuous stratified or mixed conditions. Post processing the model's output to daily averages overcomes most of this problem, as it filters the occasional short periods of stratification. Whether this is a reasonable post-process adjustment to be made remains open for debate, as it possibly filters out actual (non chaotic) short periods of mixing and stratification.

The most important effect to take away from Table 6.1, is the fact that for seasonally stratified areas, an artificial island is most certainly able to alter the dominant stratification regime depending on the surrounding characteristics such as water depth and velocity magnitude. For location B, the regime is altered for distances up around 2.5km. At the observation point 2.5km away, the stratification remains just above the breakdown threshold, meaning that extra observation points are required to identify the exact extent to which stratification regimes get altered.

6.2.1.2 Timing

Timing of stratification is most important for locations with extended periods of stratification like locations B, C and D. The island causes a regime change at location B, where the extended periods of stratification are broken up into multiple smaller periods of stratification. Location C however, preserves a period of seasonal stratification of 165 days. Since onset timing likely affects the primary production as explained in Section 5.1.2, it is interesting to see that the model predicts a sixteen day postponement of extended stratification in Figure 6.2a while it shows an eight day earlier breakdown in Figure 6.2b.

The fact that stratification onset is delayed and breakdown expedited, can be explained by the fact that in general, the density stratification is lower as a whole around each island. The model does not predict however, any expedition or delay of the full stratification period. Some delay of the full period is indicated by the difference in build-up postponement and breakdown expedition, yet this seems mostly coincidental as it is dependent on the used threshold for stratification (0.086 kg/m^3 in this case). This is endorsed by the fact that the build-up postponement and breakdown expedition are nearly equal at 2500 metres from the island, where the de-stratification effects are slightly smaller (see Figures D.5a and D.5b). Based on this modelling research, no 'full-period' timing difference are expected, only build-up postponements and breakdown expeditions due to generally reduced stratification values.

Mostly onset postponements or delays of stratification periods have a significant effect on the local primary production. The phytoplankton dynamics of the whole stratified period are determined during the first few days of stratification and its timing. Consequently, artificial islands will likely affect the primary production and ecology on a local scale through influences on onset timing at locations where the dominant regime remains unchanged.

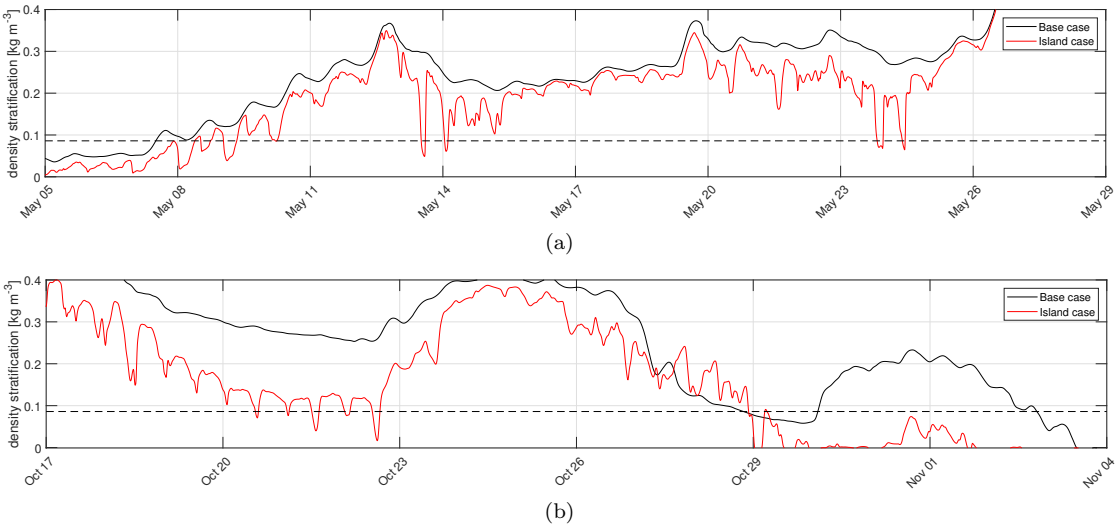

Figure 6.2: Density stratification for the base case and island C case at 500 metres to the East. (a) The commence of the extended stratified period. (b) The conclusion of the extended stratified period.

6.2.1.3 Depth profile

In theory, the impact on stratification is not as straightforward as the difference between surface density and near-bed density. The vertical mixing profile is truly three dimensional, making the 3D DCSM FM model a great tool for diving deeper into the de-stratification around islands.

With twenty depth layers a more detailed profile of the impact over the depth was created which shows that the impact on density values is more concentrated around the pycnocline than that it is distributed over the full depth-profile. This can be explained by the theory that water is imported from the island surface back into to water depth of the pycnocline. This causes an

increased mixing at that area, while the deeper areas are not mixed as much.

This is especially evident for locations B and C, where the water just under the original pycnocline (at a depth of around 20 meters and 30 meters respectively) experiences a strong decrease in density, and the water just above the pycnocline (at a depth of around 10 meters and 20 meters respectively) shows a strong increase in density.

This stresses the three dimensionality at hand, and the fact that it is likely true that water is re-injected around the pycnocline by the presence of the island, as described in more detail in Section 2.2. The analysis of stratification based on the difference between surface and near-bed density remains valid however, as during most of the year the mixing extents all the way to the bed (be it in a slightly reduced manner).

The relative mixing impact seems to be inversely related to the original $h/\overline{u}^3$ parameter of the North Sea. The effects of the island on turbulent density mixing are the largest at locations where the mixing was originally the least forthcoming. The mixing effect of the island is largest at the locations with the highest original stratification parameter in Figure 3.4.

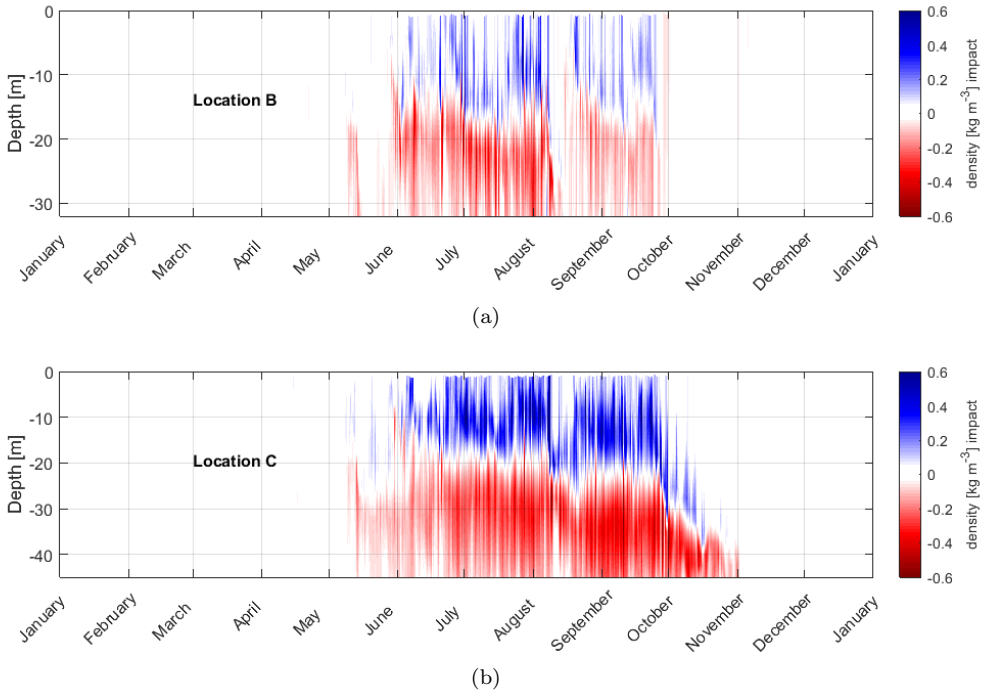

Figure 6.3: Density impacts over the depth, at location B (a) and location C (b) for one calendar year (2016) as a result of the artificial island.

6.2.1.4 Distances and direction

When it comes to the distances over which the stratification is affected, islands B and C show similar results. Both islands show an average density de-stratification of at least 10% up to a distance of 2500 metres during the period between the beginning of June and October.

Figure 6.4a shows the spatial distribution of stratification differences around island B, which clearly indicates the distances over which de-stratification is most prominent. Stratification is mostly affected up to a distance of around four to six times the island's radius. This does however differ depending on the direction of observation.

The model clearly predicts an increased de-stratification effect in the direction of the residual current. The far field average advection in eastern direction causes a higher amount of de-stratification in the that direction, showing a stratification reduction of almost 10% even at a distance of 10 kilometres. At 15km away from the island (being around ten times the island's

radius) an average de-stratification of around 5% is found.

It is important to realise that these values are large time scale averages, meaning that it helps to identify main directional tendencies, yet it does not represent the actual instantaneous impacts at different points in time. Those are better represented by Figure 6.3a.

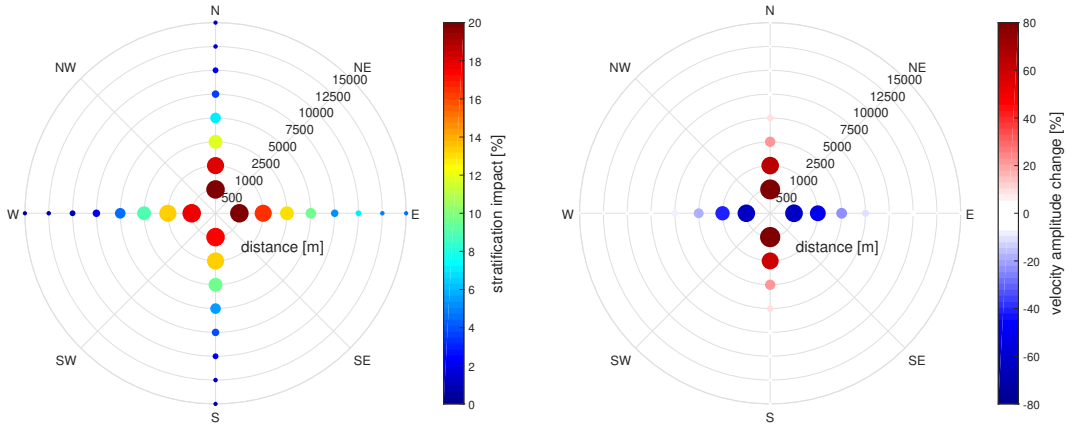

(a) (b)

Figure 6.4: Polar plot at location B, showing the decrease in stratification (a) and changes in velocity amplitude (b) averaged over June until October 2016 compared to the base run

Figure 6.4b shows the changes in amplitude of the velocity magnitude around the island. For location B, which shows the least curricular tidal direction characteristics of all investigated areas, it nicely follows the spatial pattern as predicted by Pingree and Maddock (1979). Increased velocity amplitudes along the 'flanks' of the island, with a decreased amplitude near the island on the axis parallel to the main flow direction.

While it is a common habit to link North Sea vertical mixing (and thus stratification) to the depth and velocity magnitude amplitude, it is not recommended for the area around an artificial island. In such locations, vertical mixing 'behind' the horizontal constriction can be just as large, while the velocity magnitude amplitude is strongly decreased. This can be explained by the presence of turbulent eddies and wakes as discussed in Chapter 3.

$h/\overline{u}^3$ is a good parameter for tidal mixing in shallow shelf seas without obstacles, and seems to be a good indication for the relative impact of islands on the density distribution (Section 6.2.1.3). The use of $h/\overline{u}^3$ mainly focusses on tidal amplitude and depth which are most important for free flow turbulent mixing without the presence of an island. As an indication for most affected areas around an island however, the parameter misses out on turbulent wakes and flow separation, and becomes less effective.

As discussed in Section 6.1.2, it is not possible to have map outputs for every ten minute time step due to the available storage capacity for this research project. A small amount of maps were made however to give a better indication of the spatial extent to which the island affects stratification, showing that the islands can have instantaneous impact profiles of up to around 30 times the island's radius. Moreover, the snapshots show that occasionally, stratification is increased in a small area. This emphasises the added values of map output analyses.

6.2.2 Residual currents

As opposed to the stratification analysis, the residual current exploration is more straightforward. Firstly, since the annual residual currents are by definition a time averaged quantity. Secondly, because the Fourier analysis used to create residual current outputs in Flexible Mesh is still a beta-functionality, meaning it is not fully supported yet.

Flexible Mesh currently only supports a Fourier analysis of velocity vectors separated into x and y direction, and averaged over the depth. Vertical residual currents or layer separated horizontal

residual currents are not available. These will be added in the future and form a interesting source of extra information once available.

The impact on depth averaged residual current magnitudes that is produced with the help of the Fourier analyses, shows that the magnitude is influenced in a region of order 20 times the island's area. This is in line with predictions by Pingree and Maddock (1979). The patterns of decreased and increase magnitude also match with the predictions of residual flow that is forced by tidal motion from Figure 3.3. Combining these tidal forced residual flows with the existing far-field residual current, explains the produced impact patterns of location B. This location originally has a (nearly) rectilinear flow field in east-west direction with an eastward residual flow.

The possibility that residual flow is influenced on a larger scale was not confirmed, but rather denied by the model. It does not predict any far field changes in residual currents outside the near-island area of about 10km. Thus, it is not likely that the island will have any significant effect on the horizontal distribution of nutrient by influencing residual currents. The horizontal distribution of nutrients in the North Sea remains mostly unchanged and is unlikely to affect the primary production.

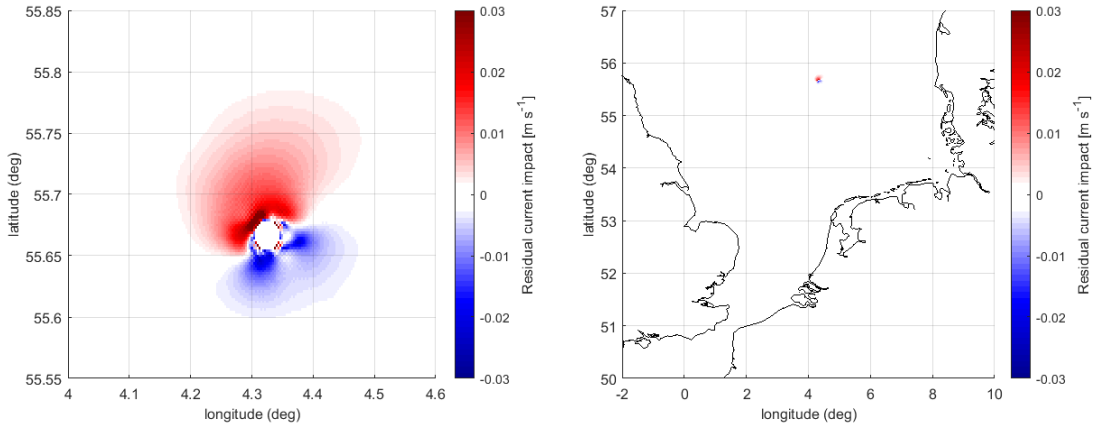

(a) (b)

Figure 6.5: Annual residual current impact at location B, showing the near island impact (a) and the far away influences (b). Positive values indicate an increase in magnitude.

6.3 3D DCSM-FM model as an island design tool

Over the last years, the modelling of ecological quality has developed in order to assess coastal and shallow waters. Especially for the North Sea, generic modelling instruments have been developed that help to investigate the southern North Sea ecological quality and the potential effects of for example new coastal infrastructures. The BLOOM/GEM (Generic Ecological Model) is able to decently predict primary production and phytoplankton species composition of any water system. It has been regularly applied to southern North Sea, through the well known coarse ZUNO grid. It supports 1D, 2D and 3D model grids and can be used in various complexity forms (Blauw et al., 2009).

Through stratification and residual current analyses, it is found that the 3D DCSM-FM model can be used to assess the impact of an artificial island on the most important hydrodynamic characteristics to ecology. The main impediment that currently stops the next step of GEM modelling as a design tool, is the fact that it requires the hydrodynamic output of the DFLOW-FM module over the whole grid, which would come in the form of map outputs. As previously explained, these are currently to large for this research project's available storage capacity.

If the storage capacity obstacle can be overcome, GEM modelling can be used to investigate the actual ecological impact of an artificial island within the North Sea.

7 Conclusions and recommendations

In this chapter, the final conclusions of this research project are presented followed by the recommendations for further research. The conclusions are based on the baseline and impact characteristics, of which an overview is found in Tables 7.1 and 7.2.

7.1 Conclusions

An artificial island as hub facility for offshore wind farms is a much discussed concept that is being explored for many locations distributed over the North Sea, such as the Dogger Bank and IJmuiden ver. There are some technical uncertainties, but the major impediment is the effect it could have on nearby and faraway ecology. The construction of an artificial island is a permanent solution to the current expenses of offshore wind energy. Once constructed, the hydrodynamic environment is altered with all its possible effects on the local and far-field ecology.

It is important to investigate the potential of hydrodynamic modelling as a form of impact analysis, and to use it for a first exploration of expected influences. By using the state-of-the-art hydrodynamic Three Dimensional Dutch Continental Shelf Flexible Mesh Model (3D DCSM-FM) to predict influences on the most important hydrodynamic parameters to ecological health, the potential of the model as design tool for artificial islands is tested and a first indication of potential impact is presented. For this research, the impact on stratification and residual currents is explored, through five island location cases. The main research question for this report reads:

"What is the potential of the 3D DCSM-FM model in understanding the impact of an artificial island on the North Sea ecology?"

The 3D DCSM-FM model can be used as an island design tool for artificial islands in the North Sea. This research has shown that the model produces realistic North Sea stratification and residual current patterns, and that ecological changes are to be expected in the area around the island. Since the implementation area significantly alters the expected ecological impact, tools such as the 3D DCSM-FM model can help to identify the best suitable locations for an offshore energy hub island in the North Sea. This conclusion is based on the answers to the secondary research questions.

1. Does the model reproduce the baseline water stratification and residual current patterns in the North Sea?

The model produces realistic baseline water stratification patterns. The results are in accordance with the stratification parameter $h/\overline{u}^3$ by Schloen et al. (2017) for free flow within the North Sea, and closely match the predicted regimes of Leeuwen et al. (2015) at each case study location. Moreover, the stratification is validated for one measurement location in the North Sea by Zijl and Veenstra (2018). Simultaneously, the computed residual current patterns of the model follow expert expectations, are in accordance with the previous modelling studies and produces realistic velocity values.

2. What are the effects of an artificial island on the local and far away stratification characteristic, and can we understand these effects?

The artificial island acts as a stirring rod within the North Sea. Horizontal and vertical mixing are a result of the island's presence at every case study location because of the North Sea's tidal character. The widely used $h/\overline{u}^3$ stratification parameter for free surface flow predicts both stagnation areas with increased stratification and areas with a decrease in stratification around the 'flanks'. This research however, confirms the hypothesis that flow separation turbulence around the island is mostly dominant over the original free flow turbulence, causing an average increase in vertical mixing all around the island without areas of increased average stratification. These mixing effects can reach as far as 20km away from the islands.

Even though increased mixing is found around each island, this research shows that the island's location is paramount to the type of stratification impact. The absolute density differences can clearly be linked to the original $h/\overline{u}^3$ values in its area, as the absolute density difference of the islands is highest at the locations with the highest original stratification parameter. More important than the absolute density difference however, are changes in stratification regimes and timing. The stirring of the islands can cause a change in stratification regime depending on its location, for distances up to 2.5km from the island. Locations close to the transition zone between two dominant stratification regimes, are most likely to experience a regime change to a less stratified regime as an effect of the artificial island. For the locations where the island's surroundings remain in its original regime, timing changes of several days still occur for the onset as well as the breakdown.

3. What are the effects of an artificial island on the local and far away residual currents, and can we understand these effects?

The effects of an artificial island on the residual currents remain local with a footprint of around 10km. The large scale residual currents remain unchanged as they are determined by the tide and large scale North Sea topography. The presence of an artificial island of this scale does not alter the amphidromic system, regardless of its location. The smaller scale residual current effects are in line with previous research for locations with recti-linear flow, which gives trust in the results of the model's output at locations with more complicated flow patterns.

4. Is it possible to use this 3D DCSM-FM model set-up as basis for future ecological predictions?

The near-field impact of an artificial island on residual currents is unlikely to affect the primary production dynamics of the North Sea. The stratification characteristics however, are significantly changed for several island cases and emphasises the importance of investigating the ecological impact of artificial islands. The 3D DCSM-FM model allows for relatively easy island implementations, and can be used as a basis for further Generic Ecological Modelling.

7.2 Recommendations

The conclusions of this chapter are completely based on the output of modelled baseline and island cases. In this section, some recommendation are presented to improve the current model and the corresponding research method. Research possibilities are never ending, so some suggestions are given for further research. Finally, some advice is given on the applicability of this research's output.

7.2.1 Methodology

Based on the experience with the current model set-up and Flexible Mesh, the following suggestions are made in order to improve the model outputs of this research project.

- *Implement an island slope.* Currently, the islands are put into the model in the form of a vertical cylinder. Even though this comprises the most important hydrodynamic effect, adding the slope of the islands appends the effect of reduced water depth along the banks. This does however require an even more refined grid and will certainly increase the computational burden.
- *Enlarge the refinement area around islands.* The major influences of the islands currently fortune within the refined area (of 10 original grid cells), however some effects are found slightly outside this refinement, meaning this spatial extent is less detailed than the rest of the output.
- *Use more detailed bathymetry samples at the refinement locations.* For this research project, the original bathymetry was interpolated to the newly created nodes within the refinement. To capture the local depth profile in more detail, a higher resolution of samples would increase the new bathymetry's precision.

7.2.2 Future research

This research was set up as a first step towards the impact analysis of artificial island in the North Sea. Additional research will help to evolve the prediction capabilities of potential ecological changes when designing an hub island in the North Sea.

- *Broaden to a morphodynamic model.* The main link that is currently missing between this hydrodynamic impact analysis and actual ecological predictions is the morphodynamic modelling. This will allow Generic Ecological Models (GEM) to predict light penetration, completing the most important parameters for ecology. With this addition, the results of this extended DFlow-FM module can be used as offline input for primary production predictions by GEM models.
- *Investigate the chaotic behaviour in more detail.* Although the chaotic behaviour of density was briefly explored for this research project, it is interesting to determine the source of this behaviour and whether it is a physical or numerical property. The comparison between more refined and courser versions of the 3D-DCSM FM could help identify such characteristics for further impact research.
- *Add the influence of waves.* Even though the North Sea is a tide dominated system, the addition of waves to the model opens up extra analytical possibilities around islands. The nature enhancing opportunities along the banks for instance (such as investigated by Frolke (2018)), largely profit from a three-dimensional wave analyses around the artificial islands. Moreover, it increases the amount of processes that are taken into account for all research types and makes the model a more complete package.
- *Add the surrounding wind parks.* This research is solely focussed on the artificial hub island's impact. To judge the impact of the proposed system as a whole, an increased refinement makes way for the addition of wind parks surrounding the island.

7.2.3 Applicability

This research shows that the implementation of artificial islands on the North Sea shelf has the potential to change the primary production dynamics and the ecosystem as a whole through changes in stratification properties. In order to improve the applicability of these finding, the following recommendations are given for further research.

- *Apply further location research.* This research confirms that stratification impacts are location dependent. Further research could identify the areas in which an island causes regime changes, and in which areas the impact is limited to timing differences. Defining the transitions zones between regime and timing impact, can be a useful guideline to the final location choice.
- *Apply GEM modelling.* By using the 3D DCSM-FM as hydrodynamic basis for GEM modelling, the impact on ecosystem health can be examined which helps to identify ecological advantages and drawbacks of stratification changes.
- *Further hub-island design research.* This research project is based on the most basic form of the hub-island concept, a vertical cylinder as horizontal constriction for different case study locations. It would be interesting to do further research on the effect of design parameters such as island slope, size and shape.

Table 7.1: Baseline stratification characteristics and impact for each artificial island case.

	Baseline			Island Impact	
Location	Depth	Velocity amp.	Regime	Type of impact	Predominant direction
A	19	0.27	IS	*Little impact*	*N.A.*
B	32	0.21	SS	Regime change	East
C	45	0.18	SS	Timing change	South-east
D	30	0.16	SS	Timing change	North-east
E	25	0.75	Undefined	*Little impact*	*N.A.*

Table 7.2: Baseline residual current characteristics and impact for each artificial island case.

	Baseline			Island Impact
Location	Depth	Residual flow magnitude	Farfield direction	Type of impact
A	19	0.032	East	Local
B	32	0.038	East	Local
C	45	0.012	South-east	Local
D	30	0.076	North-east	Local
E	25	0.047	East	Local

8 Bibliography

Battjes, J. A.
2002. *Vloeistofmechanica CT2100.* Delft University of Technology.

Berrisford, P., D. P. Dee, P. Poli, R. Brugge, K. Fielding, M. Fuentes, P. W. Kallberg, S. Kobayashi, S. Uppala, and A. Simmons
2011. *The ERA-Interim archive Version 2.0.* Reading: ECMWF.

Blauw, A. N., H. J. F. Los, B. M., and P. L. A. Erftemeijer
2009. *GEM: a generic ecological model for estuaries and coastal waters.* Hydrobiologia.

Bosboom, J. and M. J. F. Stive
2015. *Coastal Dynamics I, lecture notes CIE4305.* Delft: Delft Academic Press.

Boveri, A. B.
2012. *Focus on offshore renewables special issue.* Zurich: ABB.

Cronin, K. and M. Blaas
2015. *Maasvlakte 2 and fine sediment fluxes towards the Wadden Sea.* Delft: Deltares.

Dam, M.
2016. *Aanwijzings besluit Natura 2000-gebied Doggersbank.* Den Haag: Directie Natuur en Biodiversiteit.

Delbelke, J. and P. Vis
2016. *EU Climate Policy Explained.* European Union.

Deltares
2018. *Delft3D Flexible Mesh Suite user manual.* Delft: Deltares.

Denniss, T. and J. H. Middleton
1994. *Effects of viscosity and bottom friction on recirculating flows.* Journal of Geophysical Research: Oceans.

European Environment Agency
2017. *Trends and projections in Europe 2017.* Luxembourg: Publications Office of the European Union.

Fey, U., M. Konig, and H. Eckelmann
1998. *A new Strouhal Reynolds number relationship for the circular cylinder in the range 47 $< Re < 2 * 10^5$.* Physics of Fluids volume 10.

Foyn, L. and M. Hagebo
1998. *Nutrients and hydrography in the North Sea autumn 1998.* Bergen: Institute of Marine Research.

Frolke, G.
2018. *Nature enhancing opportunities for an artificial North Sea island.* Delft: Delft University of Technology.

Gerrits, S. B. J.
2017. *Feasibility Study of the Hub and Spoke Concept in the North Sea.* Delft: Delft University of Technology.

Gill, A. E.
1982. *Atmosphere-Ocean dynamics.* International Geophysics Series vol. 30.

Goldman, C. R., J. J. Elser, and R. C. Richards
1996. *Hydrobiologia.* Kluwer Academic Publishers.

Hachey, H. B.
1934. *Movements resulting from the mixing of stratified waters.* Journal of the Biological Board of Canada.

Harvey, R. R., J. C. Larsen, and R. Montaner
1977. *Electric field recording of tidal currents in the Strait of Magellan.* Journal of Geophysical research.

IPCC
2013. *Summary for Policymakers: Climate Change 2013, the Physical Science Basis.* Cambridge: Cambridge University Press.

Jongbloed, R. H., J. T. Wal, and H. J. Lindeboom
2014. *Identifying space for offshore wind energy in the North Sea.* Energy Policy.

Kaaij, T., T. Kessel, T. Troost, P. Herman, L. Duren, and N. Villars
2017. *Modelondersteuning MER winning suppletie- en ophoogzand Noordzee.* Delft: Deltares.

Kernkamp, H. W. J., A. Dam, G. S. Stelling, and E. D. Goede
2010. *Efficient scheme for the shallow water equations on unstructured grids with application to the Continental Shelf.* Delft: Ocean Dynamics.

Lane, A.
1989. *he heat balance of the North Sea.* Proudman Oceanography Rep. 8.

Leeuwen, S., P. Tett, D. Mills, and J. Molen
2015. *Stratified and nonstratified areas in the North Sea: Long-term variability and biological and policy implications.* Journal of Geophysical Research: Oceans.

Linden, R.
2014. *A modelling study on the residual circulation in the North Sea, with the focus on water fluxes through the Strait of Dover.* Delft: Delft University of Technology.

Locarnini, R. A., A. V. Mishonov, J. I. Antonov, T. P. Boyer, H. E. Garcia, O. K. Baranova, M. M. Zweng, C. R. Paver, J. R. Reagan, D. R. Johnson, M. Hamilton, and D. Seidov
2013. *World Ocean Atlas 2013, Volume 1: Temperature.* Silver Spring: NOAA Atlas NESDIS.

Los, F. J., S. Tatman, and A. W. Minns
2004. *A Future airport in the North Sea? An integrated modelling approach for marine ecology.* Delft: Deltares.

Los, F. J., T. A. Troost, and J. K. L. Beek
2014. *Finding the optimal reduction to meet all targetsApplying Linear Programming with a nutrient tracer model of the North Sea.* Journal of Marine Systems 131.

Mathis, M., A. Elizalde, U. Mikolajewicz, and T. Pohlmann
2015. *Variability patterns of the general circulation and sea water temperature in the North Sea.* Hamburg: Progress in Oceanography.

Meijden, M. A. M. M.
2016. *Future North Sea Infrastructure based on Dogger Bank modular island.* Arnhem: TenneT TSO BV.

Molony, C. L., M. A. John, K. L. Denman, D. M. Karl, F. W. Koster, S. Sundby, and R. P. Wilson
2010. *Weaving marine food webs from end to end under global change.* Journal of Marine Systems 84.

O'Connor, M. I., J. F. Bruno, S. D. Gaines, B. S. Helpern, S. E. Lester, B. P. Kinlan, and J. M. Weiss
2007. *Temperature control of larval dispersal and the implications for marine ecology, evolution, and conservation.* Carolina: Curriculum in Ecology.

Ormerod, S. J. and K. R. Wade
1990. *The role of acidity in the ecology of Welsh lakes and streams.* Dordrecht: Monographiae Biologicae.

Pecuchet, L., G. Reygondeau, W. Cheung, P. Licandro, D. Denderen, M. Payne, and M. Lindegren
2018. *Spatial distribution of life-history traits and their response to environmental gradients across multiple marine taxa.* Ecosphere 9.

Pingree, R. D. and L. Maddock
1979. *Tidal flow around an island with a regularly sloping bottom topography.* Marine Biological Association of the United Kingdom.

Queste, B. Y., L. Fernand, T. D. Jickells, and K. J. Heywood
2012. *Spatial extent and historical context of North Sea oxygen depletion in August 2010.* Dordrecht: Springer Netherlands.

Ricklefs, R. E., J. Losos, and T. M. Townsend
2007. *Evolutionary diversification of clades of squamate reptiles.* Journal of evolutionary biology.

Rijkswaterstaat and Deltares
2017. *Beschrijving Modelschematisatie DCSMv6, DCSMv6-ZUNOv4 en 5e-generatie WAQUA.* RWS-WVL and Deltares.

Ruardij, P., H. Haren, and H. Ridderinkhof
1977. *The impact of thermal stratification on phytoplankton and nutrient dynamics in shelf seas: a model study.* Journal of Sea Research.

Sager, G.
1959. *Gezeiten und Schiffahrt.* Leipzig: University of Leipzig.

Schierik, G. J.
2016. *Introduction to Bed, bank and shore protection.* Delft Academic Press.

Schloen, J., E. V. Stanev, and S. Grashorn
2017. *Wave-current interactions in the southern North Sea: The impact on salinity.* University of Oldenburg.

Simpson, J. H. and P. B. Tett
1992. *Island stirring effects on phytoplankton growth.* Springer-Verlag Berlin.

Simpson, J. H., P. B. Tett, M. L. Argote-Espinoza, A. Edwards, K. J. Jones, and G. Savidge
1982. *Mixing and phytoplankton growth around an island in a stratified sea.* Continental Shelf Research.

Solan, M. and N. Whiteley
2016. *Stressors in the Marine Environment: Physiological and ecological responses; societal implication.* Oxford: Oxford Scolarship Online.

Sundermann, J.
1966. *Ein Vergleich zwischen der analytischen und der numerischen Berechnung winderzeugter Stromungen und Wasserstande in einem Modellmeer mit Anwendungen auf die Nordsee.* Hamburg: University of Hamburg.

Sundermann, J. and T. Pohlmann
2011. *A brief analysis of North Sea physics.* Warschau: Polish Academy of Sciences.

TenneT
2017. *North Sea Wind Power Hub.* Arnhem: TenneT.

Tett, P., R. Gowen, D. Mills, T. Fernandes, L. Gilpin, M. Huxham, K. Kennington, P. Read, M. Service, M. Wilkinson, and S. Malcolm
2007. *Defining and detecting undesirable disturbance in the context of marine eutrophication.* Marine pollution bulletin.

Tett, P. B., R. Joint, D. A. Purdie, M. Baars, S. Oosterhuis, G. Daneri, F. Hannah, D. K. Mills, D. Plummer, A. J. Pomroy, A. W. Walne, and H. J. Witte
1993. *Biological consequences of tidal stirring gradients in the North Sea.* The Royal Society.

United Nations
2015. *Paris Agreement.* UNFCCC.

Wilson, B.W.
1960. *Note on surface wind stress over water at low and high wind speeds.* Geophysical Research Letters.

WindEurope
2018. *Wind in power 2017.* Brussels: Wind Europe.

Winther, N. G. and J. A. Johannessen
2006. *North Sea circulation: Atlantic inflow and its destination.* Hoboken: Journal of Geophysical research, Vol. 111.

Zijl, F. and V. Veenstra
2018. *Setup and validation of 3D DCSM-FM.* Delft: Deltares.

A Ecological framework

In order to fully grasp the inner workings of population dynamics, the relevant processes need to be understood. The conditions that determine ecological welfare are complex and form a hard to understand web. Favourable ecological conditions are difficult to determine as ecological welfare is dependent on the interaction between many processes.

In order to understand the hierarchy and biological interactions of an environment, food webs can be used to clarify the general ecosystem structure. The interactions between species and their environment, and between and within species determine the marine food web dynamics (Molony et al., 2010). Forcing factors affect the marine food web on different levels and in different ways.

It is impossible to isolate the effects of an artificial island completely to one specie. However, by taking a look at the marine food web the generic levels within an ecosystem can be determined including the likely affected food web levels. The influence of the hydrodynamic environment highly varies, based on an organism's ability to adapt to physical conditions and its receptivity to the chemical environment.

With the help of an environmental forcing hierarchy, Molony et al. (2010) was able to visualise the trophic pyramid and the main levels within the foodchain that are affected by oceanic variables. Doing so, the two distinctive types of environmental variables were separated into: Those that (directly) influence individuals and those that influence populations.

The variables that affect on an individual level mainly determine the processes of production and mortality of one particular specie. Some specific environmental variables such as temperature, have a direct effect on all trophic levels. Meanwhile, other variables such as light availability have a direct effect on lower trophic levels and only affect the higher levels indirectly via bottom-up influences such as the increase or decrease of lower level prey availability.

The oceanic processes that influence populations rather than individuals, do not necessarily affect the mortality of a specific specie, but more so show a consequence for the distribution and abundance of marine organisms (Molony et al., 2010). These processes such as advection and vertical mixing can be modelled well with the use of hydrodynamic flow models.

Unfortunately, the extent to which the two forms of variables impact the environmental welfare requires great understanding of the ecosystem at hand to unravel the complexity of all its interactions. Typically, it is not possible to consider all the issues at hand at the same time or by using a standardised food web model for different environment assessments.

For the analysis of an ecosystem and possible impact of an intervention, a so-called 'end-to-end food web' can be used to incorporate all the influences of chemistry and ocean dynamics into a web of interactions between all levels of the system from primary producers all the way up to the top predators. These webs become infinitely more complex with the increase of organisms within a considered ecosystem. Figure A.1 shows the end-to-end food web framework for research. It consists of eight major thematic areas with keywords illustrating processes, approaches and issues. It emphasises the complexity of environment prediction research.

Even though an analysis of impact on an ecosystem prefers a general scope including all interactions within a food web, this is generally impossible and very time consuming. Therefore, a food web needs to be both unravelled and reconstructed in order to identify the appropriate amount of research detail. The correct amount of simplification and generalisation can be determined by keeping in mind the available amount of research time and the main objectives.

Figure A.1 includes the main themes of an end-to-end ecological research project, including the interactions between the ocean physics and the feedback loops of primary producers, consumers and the decomposers of a marine system. The ocean processes affecting individuals and populations change the behaviour of one or more of the major thematic areas of the food web framework.

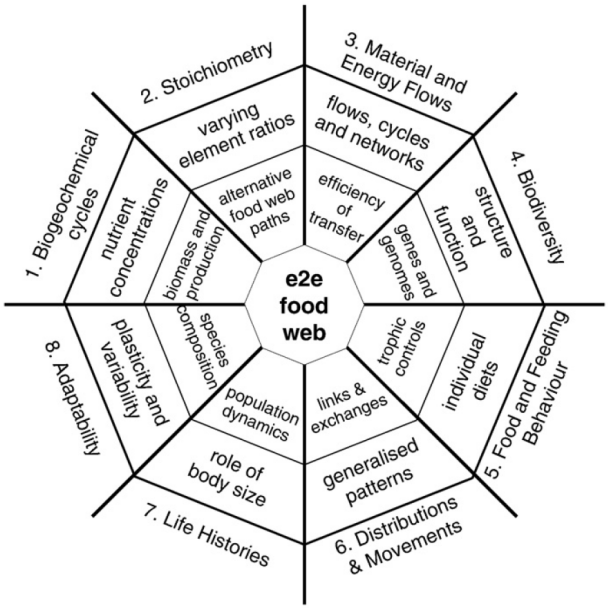

Figure A.1: Framework for end-to-end food web research. Eight major thematic areas are shown, with threads spanning small to large time and space scales and dealing with issues across different levels of organisation (Molony et al., 2010)

Sine this is an exploratory research project, the ecological scope of the project must be clearly defined in order to capture the most important effects. Not all processes and interactions can be included and therefore the most important parameters must be selected that allow the assessment of the 3D-modelling potency as island design tool.

A.1 Hydrodynamic parameters

In order to define the scope of this research, an overview is needed of the hydrodynamic parameters that either influence marine species on a individual or population level. With the overview, the most influential parameters can be selected for investigation. The most important hydrodynamic parameters that affect ecological welfare can be subdivided into two main categories: Physical parameters and water quality parameters. There are seven physical and four water quality parameters respectively, which will be briefly described hereunder to get a general overview.

A.1.1 Physical parameters

- Currents
  For many organisms, both the maximum and the average current velocity are important. If the current exceeds a specie's specific maximum, it could mean that the organisms are washed due to large advection forces or turbulence. On the other hand, a good average current is required in many cases too. For species a sufficient average current is required for the supplying of food and nutrients

- Waves
  Just like currents, wave action creates force on the bed and causes turbulent flow. However, as opposed to the currents, wave action does not supply any form of food. This means that for waves there is no optimal average wave strength, but rather a maximum wave strength that species must be able to withstand.

- Depth
  The maximum wave strength obviously is much related to the depth. For large water depths, the effect of wave action decreases compared to shallower areas. Moreover, the depth is important for the amount of light penetration to the bottom, the temperature and the type of predators. Different species have different preferences for the range of depths they live in.

- Stratification
  Light penetration is not only depended on the depth, but also the grade of stratification. Stratification is the forming of water layers with different properties (such as density, salinity or temperature) that act as mixing boundaries. The stratification is also an important nutrient availability parameter determining the amount of vertical mixing.

- Soil movement
  The bathymetry of the North Sea slowly changes all the time. Sediment is picked up and dropped in different locations. Sand waves occur that travel along the sea floor. Large soil movements or sand waves can be of influence to North Sea ecology when they cover the species living on the bottom of the Sea. These species will not survive being covered by soil for long.

- Salinity
  Like most of the ecological parameters, the tolerance to salinity levels are different for many species. Meaning, that changes in salinity shift the distribution of species that can survive in the new habitat. The behaviour and reproduction capabilities get limited, reducing the fitness for survival (Solan and Whiteley, 2016).

- Temperature
  For many aquatic species, the metabolic rate varies with the water temperature, since temperature affects the rate of most biochemical processes. This means that the temperature heavily regulates the development rate and survival of organisms that live in the North Sea (O'Connor et al., 2007).

A.1.2 Water quality parameters

- Turbidity
  The Turbidity is another parameter which heavily affects the light penetration through the water, as it represent the measure of cloudiness. High sludge concentrations can limit the light penetration which becomes an issue if it occurs for too long. High peaks of turbidity are not an issue, long-term increases of average turbidity levels is much more relevant to ecology. Moreover, the turbidity influences water clarity which determines visibility.

- Acidity
  The acidity and the corresponding chemistry is important to water ecology in many ways (Ormerod and Wade, 1990). Waters with too high or low pH values are not suitable for many organisms to live in. Most aquatic organisms prefer a pH level between 6.5 and 9.0 with some exceptions. Considerable changes in acidity lead to direct effects on the aquatic ecology.

- Nutrient supply
  The nutrients supplied by rivers and the Atlantic Ocean to the North Sea are important to the survival of organisms. Large rivers deliver a lot of nutrients such as nitrate and phosphate to the North Sea as shown by Foyn and Hagebo (1998), while the salinity of the North Sea is still mostly dominated by the Atlantic Ocean.

- Oxygenation
  Organisms need oxygen to breath, and thus to live. The amount of oxygen in the North Sea water is not constant and is differently distributed over the area. In August 2010 for example, the southern (well-mixed) North Sea showed oxygen saturation levels up to 90%. The more stratified regions however, generally showed lower oxygen levels between 75% and 80% as investigated by Queste et al. (2012). A redistribution of oxygen can change the North Sea ecology.

It is important that these parameters all interact with each other on different levels. The (denbsity) stratification for example, is affected by both the temperature and salinity. This list is mainly used as a way of separating dominant hydrodynamic conditions for ecology.

B Technical analysis

This chapter gives an overview of the most relevant North Sea mechanisms that determine the residual currents patterns, and the density stratification.

B.1 North Sea residual currents

It is important to digest the separate mechanisms that currently dominate the residual currents of the North Sea. The role of different mechanisms on the North Sea residual currents will be explained by referring to the famous Navier-Stokes equations. The equations describe the second law of Newton ($F = m \cdot a$) for a volume of fluid. The Navier-Stokes equations can be written in many different forms and are given here for an incompressible fluid. The set of equations consists of a continuity equation that describes the conservation of mass, and a momentum equation for each direction.

$$\frac{\partial u}{\partial x} + \frac{\partial v}{\partial y} + \frac{\partial w}{\partial z} = 0 \tag{B.1}$$

$$\left(\frac{\partial u}{\partial t} + u\frac{\partial u}{\partial x} + v\frac{\partial u}{\partial y} + w\frac{\partial u}{\partial z} - fv\right) = -\frac{1}{\rho}\frac{\partial p}{\partial x} + \nu\left(\frac{\partial^2 u}{\partial x^2} + \frac{\partial^2 u}{\partial y^2} + \frac{\partial^2 u}{\partial z^2}\right) + F_x \tag{B.2}$$

$$\left(\frac{\partial v}{\partial t} + u\frac{\partial v}{\partial x} + v\frac{\partial v}{\partial y} + w\frac{\partial v}{\partial z} + fu\right) = -\frac{1}{\rho}\frac{\partial p}{\partial y} + \nu\left(\frac{\partial^2 v}{\partial x^2} + \frac{\partial^2 v}{\partial y^2} + \frac{\partial^2 v}{\partial z^2}\right) + F_y \tag{B.3}$$

$$\left(\frac{\partial w}{\partial t} + u\frac{\partial w}{\partial x} + v\frac{\partial w}{\partial y} + w\frac{\partial w}{\partial z}\right) = -\frac{1}{\rho}\frac{\partial p}{\partial z} + \nu\left(\frac{\partial^2 w}{\partial x^2} + \frac{\partial^2 w}{\partial y^2} + \frac{\partial^2 w}{\partial z^2}\right) - g + F_z \tag{B.4}$$

with:

u, v, w = The directional components of the currents
x, y, z = The spatial coordinates
t = The time
f = The Coriolis parameter
ρ = The water density
p = The pressure
ν = The kinetic viscosity
F = The external forcing acting of the fluid
g = Gravitational constant

These equations basically describe the interaction between pressure, density and the velocity of a moving fluid in three dimensions, including the effects of viscosity. Analytically these equations are currently too hard to solve, however with some simplifications and approximations they can be solved and used to predict hydraulic regimes numerically. These equations combined with several assumptions lead to a set of equations known as the shallow water equations (SWE), which are used in most sophisticated hydrodynamic modelling suites.

B.1.1 Coriolis

Newton's equations of motions (and thus also the Navier-Stokes equations) are valid as long as it is placed in a x,y,z-reference frame that does not accelerate. Since the North Sea is located on the rotating earth, the reference frame is also rotating as depicted by Figure B.1. In order to compensate for the rotation of the earth, a Coriolis force must be introduced for tidal motion to make the equations valid for large water bodies. This is done through the Coriolis parameter of Equation B.5.

$$f = 2\omega_e sin(\phi) \tag{B.5}$$

with:
f = The Coriolis parameter
ω_e = The earth's angular velocity
ϕ = The latitude

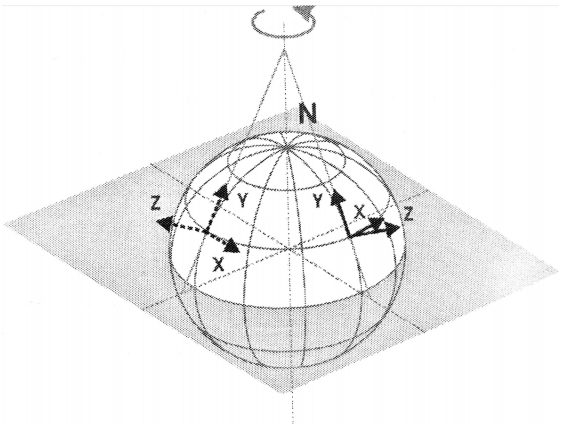

Figure B.1: Rotation of an x,y,z-reference frame on the earth's surface (Bosboom and Stive, 2015).

The necessity of introducing the Coriolis deflection depends on its effect relative to inertia. In order to access this necessity, the Rossby number can be used which indicates the significance of the Coriolis deflection as Equation B.6. For Rossby numbers lower than or equal to 1.0, the Coriolis deflection is considered to be of importance. Using the typical orders of magnitude of the North Sea, the Rossby number ranges anywhere from 0.1 to 0.001 as found by Linden (2014). Coriolis is therefore of importance to the residual current of the North Sea.

$$R = \frac{V}{|f| \cdot L} \tag{B.6}$$

with:

R = The Rossby number
V = The typical order of magnitude of flow velocities
f = The Coriolis number
L = The length scale of motion

B.1.2 Topography

In absence of river discharges or different 'nontidal' forcing mechanisms like wind, the averaged discharge in shallow coastal water should be zero as describe by Bosboom and Stive (2015). However, large vertical or horizontal circulations and residual currents often exist. Structures or irregular coastlines are more often than not present in coastal areas, which always introduce residual currents.

The contraction of streamlines around structures or irregular coastlines lead to changes in the flow field and cause tidal residual currents. Hence, the bathymetry is of large importance to created tidal residual currents. The bathymetry determines the boundaries through which currents cannot take place. The directional component of the current must be zero in case of a topographic boundary in that direction.

The bathymetry especially influences the eigen-oscillation and resonance of the tidal forcing as briefly mentioned in Section 2.1. The propagation of the tide is directly affected by the shape of the shallow sea. It creates an amphidromic system as presented in Figure 2.4.

An amphidromic system is generated by the Coriolis deflection of the tidal movement into the land masses which block the tidal wave creating rotary movements in the North Sea. For the northern hemisphere, this rotation is directed anti-clockwise. The tidal wave that is generated moving along the land boundaries, is known as the resulting Kelvin wave. Residual currents are mostly determined by this amphidromic system.

B.1.3 Role of the Tide

The North Sea itself is not large enough for a direct effect of the tidal potential as is the case for larger water bodies. It is however, significantly influenced by the astronomical tides. These co-oscillations follow from the autonomous tidal waves created in the Atlantic, entering the North Sea at its boundaries. Together with the geometry of the North Sea basin, the tide creates eigen-periods, resonance and a semi-durnal, amphidromic system (Sundermann and Pohlmann, 2011).

The shallow southern region of the North Sea causes energy dissipation and causes non-linear effects on the tidal waves. Because of all these effects, the tidal signal is highly non-harmonic and different in many North Sea regions. The tidal movements in the North Sea are the dominant forcing mechanism for residual currents. Averaging the tidal flow of the North Sea, results in the most significant residual current pattern without the influence of wind or density forcing. Figure B.2 presents the residual currents of the M2-tide, which represents the main tidal residual current pattern within the North Sea.

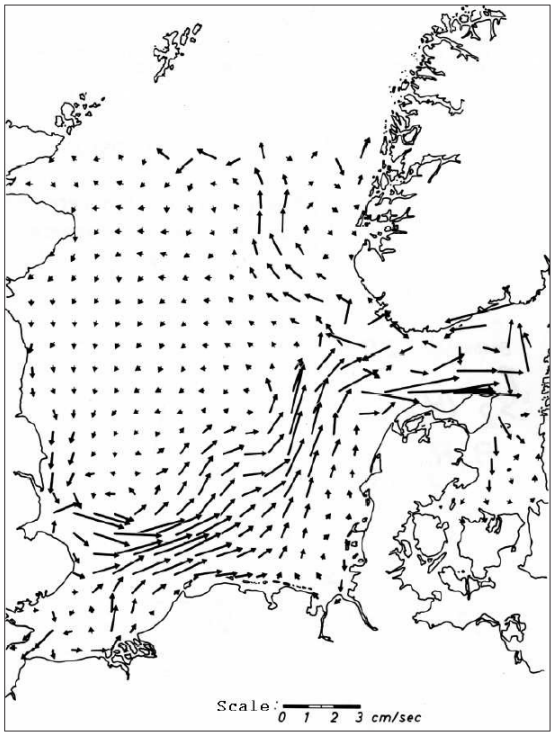

Figure B.2: Residual currents of the M2-tide (Sundermann and Pohlmann, 2011).

B.1.4 Role of the atmosphere

The general circulation created by the tides and topography is significantly influenced by the atmosphere. The atmosphere implies a vertical momentum flux with an extra circulation as a result. Wind alters the general circulation depending on its main direction. Figure B.3 shows four basic states of circulation patterns due to wind influence. The North Sea experiences mostly westerly winds which lead to a strengthening of the tidal residual current pattern. Occasionally, changes in wind direction cause opposing current influences, or smaller scale circulation patterns within the North Sea.

The atmosphere also controls the heat budget of North Sea through heatfluxes, and the vertical

mixing that is wind strength dependent. More on the heat transport is found in Section B.2.1 for the basic principles of stratification within the North Sea.

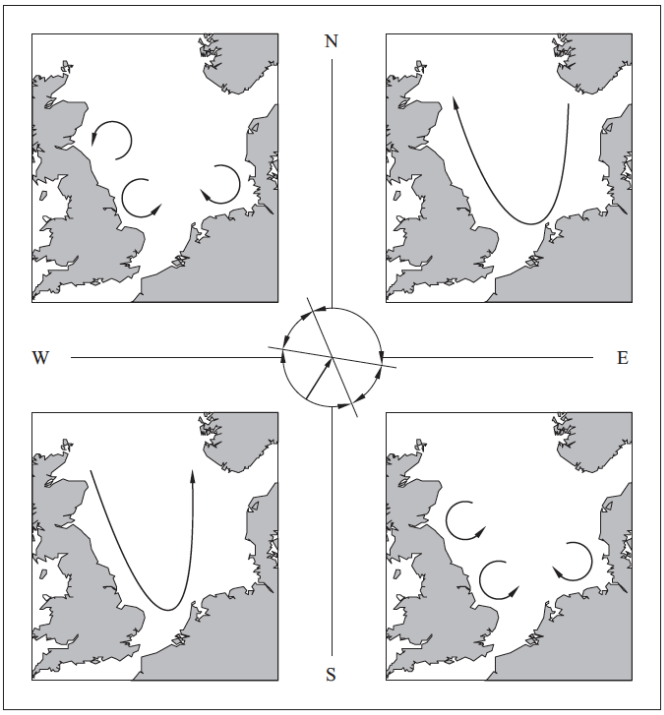

Figure B.3: Wind-driven circulation in the North Sea with four basic states, corresponding to the prevailing wind patterns (Sundermann and Pohlmann, 2011).

B.1.5 Role of the freshwater inputs

The North Sea water budget and its salinity is controlled by four major in and outflows. It is dominated by the exchange with the Atlantic Ocean, the Baltic Sea, the many river influences, and the exchange with the atmosphere through evaporation and precipitation. Salinity differences occur as a result of flow interaction between all these influences and their respective original salinity input. The combination of temperature and salinity differences causes a density structure with separated water masses. These differences in water masses also slightly influence the general residual current pattern, with a cyclonic current pattern.

B.2 Stratification

The phenomenon of stratification is caused by alterations in density over the water column. The density stratification of the North Sea is dominated by the thermal processes and influenced further by the salinity changes. The northern areas of the North Sea become stratified during the summer as wind influences are relatively small, and heating by the sun is most consistent. During early autumn, the thermal heating reduces and wind strength increase, which breaks down the thermal stratification. In the ROFI area, density stratification occasionally occurs as a result of fresh water inputs that interact with relatively salty sea water.

B.2.1 Heat transport

The main heat exchange mechanisms that determine the heat distribution within the North Sea, are visualised in Figure B.4. All the mechanisms between the earth, sun and atmosphere which are included in the model are given below. Most of this section is a summary of the heat transport by Deltares (2018), which goes in more detail on model mechanisms.

Qsc = Radiation for clear sky condition
Qco = Heat loss due to convection
Qsr = Reflected solar radiation
Qs = Solar (short wave) radiation

Qsn = Net incident solar (short wave) radiation
Qa = Atmospheric (long wave) radiation
Qan = Net incident atmospheric (long wave) radiation
Qar = Reflected atmospheric radiation
Qbr = Back radiation (long wave) radiation
Qbv = Heat loss due to (latent) evaporation

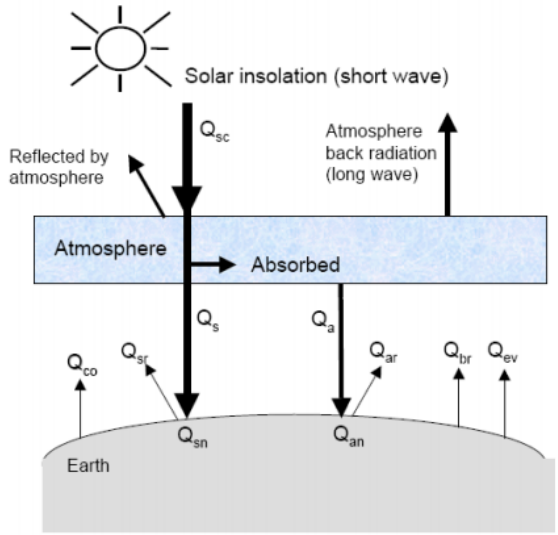

Figure B.4: Overview of the heat exchange mechanisms at the surface (Deltares, 2018).

Electromagnetic waves that reach the earth are a form of heat radiation emitted by the sun. Their wave lengths are relatively small (about 0.15 m to 5.0 m). The atmosphere in between the sun and earth changes the radiation through scattering, reflection and absorption. These mechanisms depend on the air density, cloudiness and particles within the air. On the other hand, heat is emitted back toward the sky again, in the form of long waves (around 4m to 50m), as neither the earth or atmosphere collects a net increase in heat.

A composite heat flux model is used in the model to represent these mechanisms, and determine the amount of heat that is exchanged between the top water layers and the atmosphere. This way, the thermal stratification of the North Sea is predicted. The heat transport is further determined by the movement of water as concentrations within the Navier-Stokes equations.

B.2.2 Salinity

Just like temperature transport, salinity transport is handled as a concentration determined by the water movements as predicted with the Navier-Stokes equations. The water movements determine the distributions of fresh and saline water in the North Sea and over the water column. If large salinity differences are created between the higher and lower water layers, density stratification is present. Together with the thermal stratification, salinity influences determine the final density stratification.

C Model disquisition

C.1 Simulation model

The normative modelling suite for large scale hydrodynamics is the Delft3D modelling environment, containing numerical models for hydrodynamics, but also for suspended particle matter (SPM) transport, water quality, morphology and ecology. Delft3D is an integrated software suite developed by Deltares which is used for the simulation of two-dimensional and three-dimensional hydrodynamics of estuarine environments, coastal area and rivers.

This model works with either curvilinear or rectangular grids. Implementations of irregular connections are not possible and grid refinements can only be realised by domain decomposition increasing the total computational effort and time.

The Delft3D-Flow module can be found at the heart of the Delft3D modelling environment. This module solves the two-dimensional (depth-averaged) or three-dimensional non-linear shallow water equations. These are derived from the three dimensional Navier-Stokes equations for incompressible flow (Equations B.1 until B.4). A few assumptions are made to derive the shallow water equations, which can all be found in the Delft3D-Flow manual Deltares (2018).

Using these shallow water equations, flow predictions can be made to identify the water systems at hand. The first step in modelling activities is the flow itself, which is determined by several system characteristics as explained in Chapter B. This flow module then provides the hydrodynamic basis for countless problem analyses such as the implementation of artificial islands.

C.1.1 Delft3D Flexible Mesh

Recently, a successor of the Delft3D suite was developed that is capable of handling the same curvilinear or rectangular grids, but now with the addition of triangles, hexagons, pentagons and quads. This successor is called Delft3D-Flexible Mesh (FM) with the D-Flow module that represents the successor of the Delft3D-Flow module.

With the ability to utilise multiple grid forms, the Flexible mesh environment provides great flexibility for setting up a model with varying grid resolutions, and for modifying existing models.

The new unstructured grids are used to solve the shallow water equations with the finite-volume method similar to its structured predecessor. The ability of unstructured grids to locally refine computational grids is very useful for case-studies and the performance is comparable to that of Delft3D-Flow and other shallow water equation solvers which are known as efficient modules as demonstrated by Kernkamp et al. (2010).

Since additions accuracy is required to judge local impacts at the area of interest, the Delft3D-FM environment is ideal for case studies on the hydrodynamic effects of an artificial island in the North Sea.

C.1.2 Model set-up

For North Sea simulations, the well known ZUNO (Zuidelijke Noordzee) model grid is often used and can be seen as the standard for recent North Sea numerical modelling studies. It is reviewed by international specialist making it a reliable model as concluded by Kaaij et al. (2017). The ZUNO Delft3D model has been validated and used for many large projects, Los et al. (2004) even used it for the ecological impact assessment of an artificial island due to SPM:

- The Flyland project (airport in the North Sea) (Los et al., 2004).
- The Maasvlakte 2 project (port of Rotterdam expansion) (Cronin and Blaas, 2015).
- The Dutch coast sand mining research (Kaaij et al., 2017).

The problem with the ZUNO-model for this research however, is the northern boundary which is located rather close to the Dogger bank. The ZUNO model is generally used to assess Dutch near shore processes and could show instability issues when implementing an artificial island close to the northern boundary.

Since a larger modelling domain is required, the Dutch Continental Shelf Model (DCSM) is a great option. This model covers a much larger area than the ZUNO model. Moreover, the newest 'state of the art' North Sea model known as the 3D DCSM-FM model is a three dimensional model also capable of modelling vertical variations such as stratification. Since it is made in the successor of Delft3D-FLOW called Delft3D-Flexible Mesh it also allows for easy grid adjustments which simplifies the process of implementing artificial islands.

Three version of 3D-DCSM have been tested and validated recently. All do a great and similar job at predicting tides, surges and water levels even surpassing the ZUNO performance (Zijl and Veenstra, 2018). When it comes to stratification research, Table C.1 shows the performance of the three versions of the model. Since,the *1nm*-version performs best for stratification and has a smaller computational burden than the *0.5nm*-version, it is chosen for this research project.

Table C.1: Quality of the representation of temperature stratification in the 3D DCSM-FM model, in terms of bias, standard deviation (std) and Root-Mean-Square Error RMSE (Zijl and Veenstra, 2018).

	bias (°C)	std (°C)	RMSE (°C)
3D DCSM-FM (org)	0.32	1.01	1.06
3D DCSM-FM (1nm)	0.16	1.36	1.37
3D DCSM-FM (0.5nm)	0.76	1.49	1.67

The DCSMv6 model area lies between 64°N to 43°N and 15°W to 13°E. This domain covers the entire Northwest European Continental Shelf (NWECS), with all the boundaries located within deep water where non-linearities are negligable. The downside of this large domain is the computational burden. The DCSMv6 combination with ZUNO-DD contains around 1.100.000 active computational cells (Rijkswaterstaat and Deltares, 2017).

C.1.2.1 Grid

A conversion of the DCSMv6 model was made from the Delft3D suite to the Delft3D-FM suite. Using the new modelling suite, grid optimization was used to improve computational efficiency while maintaining good accuracy. The grid was coarsened where local spatial scales allow it, while maintaining the fine resolution in the shallow areas to correctly model non-linear interactions. This highly reduces the computational burden making the DCSM-FM model much more suitable for a thesis research project such as this one. Figure C.1 show the computational model network of the DCSM-FM domain with coarsening of the three different nets and grid cell sizes.

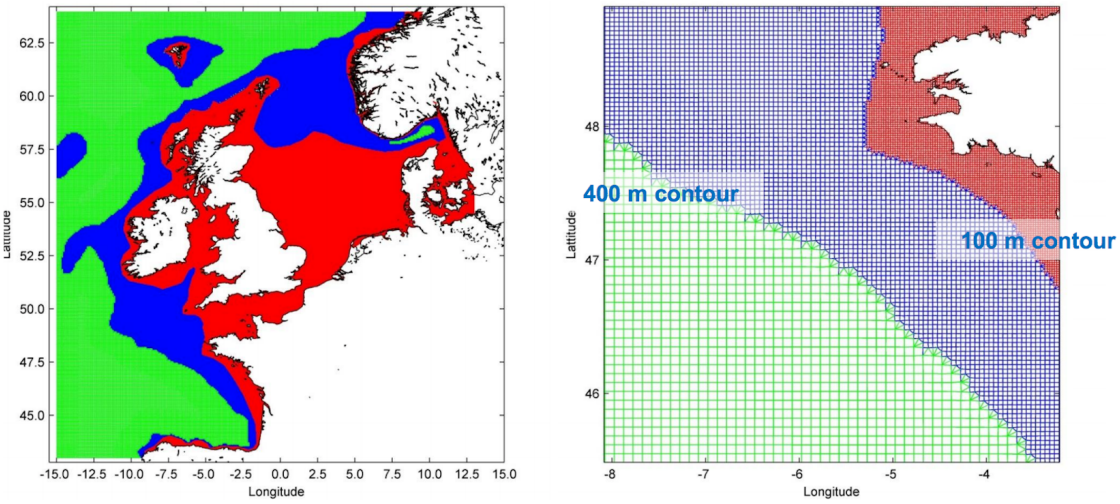

Figure C.1: DCSMv6-FM computational net, with the detailed transition from the fine to coarse grid (green is around 4nm; blue is around 2nm; red is around 1nm (Zijl and Veenstra, 2018)).

In order to investigate the effects of an artificial island on stratification, a depth averaged model will not suffice. This means a three dimensional model is needed. The 3D DCSM-FM model is, as the name suggests, a three-dimensional model based on the 2D DCSM-FM model, with the inclusion of a vertical schematisation of sigma-layers. The depth is divided into 20 layers with an uniform distribution of 5% of the water depth. Depth layers are an important characteristic for this research and its goals, and the three dimensional model has shown to outperform its two dimensional predecessor.

In this thesis only the 3D DCSM-FM model is used to do the numerical computations and to obtain results, none of the older models are used. Flexible Mesh is a modelling suite that is still under construction. Any of the issues or obstacles encountered during this research will help serve as feedback to the programmers, improving the new 'state-of-art' modelling suite.

C.1.2.2 Bathymetry

The bathymetry of the model is derived from the European Marine Observation and Data Network known as EMODnet, by adjusting the delivered data relative to Lowest Astronomical Tide (LAT) into data relative to Mean Sea Level (MSL). Some local Dutch water Baseline bathymetry is also available, and is implemented into the bathymetry where possible, after conversion from Normaal Amsterdams Peil (NAP) to MSL. Figure C.2 shows the resulting bathymetry used in the 3D DCSM-FM model.

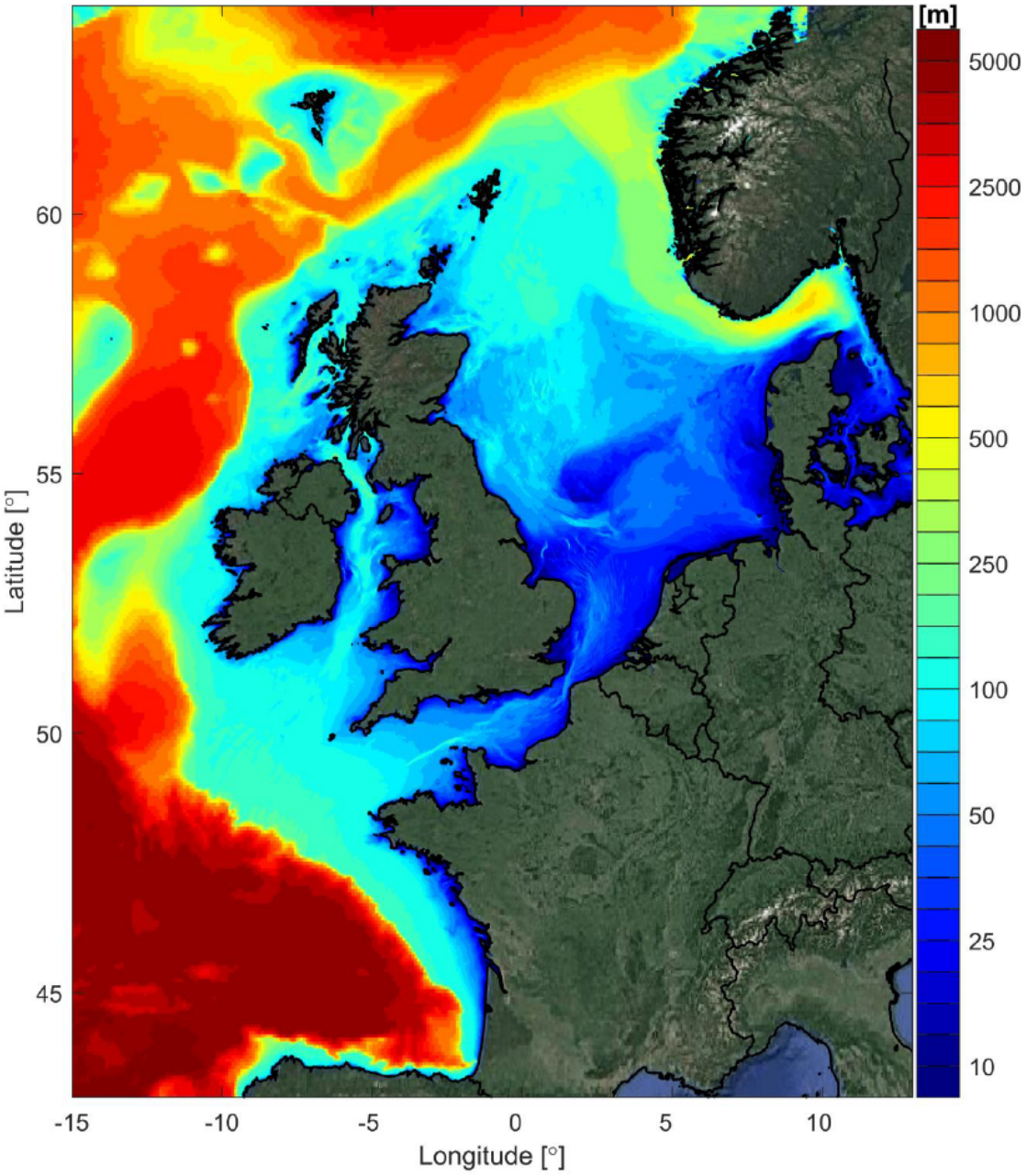

Figure C.2: The 3D DCSM-FM model bathymetry (relative to MSL) (Zijl and Veenstra, 2018).

C.1.2.3 Lateral forcing

The model forcing mechanisms can be separated into two distinct categories, lateral forcing and surface forcing. The lateral forcing mechanisms are imposed at the boundaries three boundaries of the model (the northern, western and southern boundaries). At these boundaries the tide, temperature, salinity and surge are accounted for.

Tide

The main form of lateral forcing is the tidal forcing. This is done by defining open water level boundaries in the north, west and south of the model domain. Amplitudes and phases of 33 harmonic constituents are included, mostly obtained from the global tide Finite Element Solution 2012 (FES2012) model. The three boundaries are divided into several stations, all with unique constituent amplitudes and phases. In between these stations, the water levels are linearly interpolated to complete the entire boundary.

Inversed Barometer correction

To make sure that the surge is well represented in the model, the (non-tidal) effect of local pressure cannot be neglected. Wind set-up at the boundary can be neglected because of the large water depths, however the effect of local pressure cannot. The effect of local pressures is included in the form of a so called inversed barometer correction (IBC). This is included in the tidal water levels of the all the boundary stations, and is similarly interpolated to complete the entire boundary length.

Temperature and salinity

The temperature and salinity are included as lateral forcing in the model. The offshore boundary forcing of these properties are based on the data of the World Ocean Atlas 2013 (WOA2013). The WOA2013 is a collection of six in-situ objectively analysed climatologies for the world ocean. It consists of horizontal distributed maps of temperature and salinity at standard depths of the ocean (Locarnini et al., 2013)

The temperature and salinity forcing are included in the model as a time series of mean monthly fields, between which the rest of the values are interpolated. This data set consists of 107 depth levels. These values are interpolated to the correct horizontal location, and 50 equally spaced water depths.

In D-Flow FM, the transport of matter (in this case salinity and temperature) is defined as Equation C.1.

$$\frac{d}{dt}\int_{V(t)} cdV + \int_{\delta V(t)} c(u-v)\cdot ndS = \int_{\delta V(t)} (K\nabla c)\cdot ndS + \int_{V(t)} sdV \tag{C.1}$$

Here the property $V(t)$ describes a three-dimensional volume, with a concentration c representing temperature and salinity, dependent on flow velocity field u and vertical volume movement v. K represents a diagonal matrix with coefficients of diffusion and s depicts any source or sink of the corresponding transported matter.

C.1.2.4 Surface forcing

Other than the boundary lateral forcing mechanisms, the model also utilises imposed surface forcing fields. These fields all consist of 1485 points over the modelling area between which the time-varying values are interpolated linearly in time and space.

Tidal potential

Numerical models for rivers, estuaries or smaller coastal areas usually do not included the direct effect of tide generating forces, the tide is then only imposed as an open boundary forcing since the area contains a relatively small amount of water mass. A sufficient accuracy can be obtained without the inclusion of tidal potential.

In case of a larger modelling area like seas or even oceans, the amount of water mass becomes considerably large, making the tidal potential of gravitational forces on the fluid motion non-negligible. For this modelling domain, the tidal potential must be taken into account. FM can be used to included tide generating forces in combination with spherical grids, since it defines the exact location of each computational cell. The FM suite applies the Fortran subroutines by E.J.O. Schrama to describe tide generating forces. The FM user manual includes more information about the derivation of this tidal potential (Deltares, 2018).

Coriolis force

The Coriolis force is be included in the model by specifying the space varying Coriolis parameter known as f. This is done by selection of the applicable coordinate system (in this case WGS 64) and turning on the *Spherical Coordinate* option. The Coriolis force is then determined with the use of the earth's angular rotation speed ω and the geographical lattitude ϕ in as seen in Equation C.2.

$$f = 2 \cdot \omega \cdot sin\phi \tag{C.2}$$

Heat fluxes

D-Flow FM models the surface heat exchange by combining all seperate effects like short wave (solar) and long wave (atmospheric) radiation, back radiation, convection and evoporation. This model set-up uses the so-called *heat flux model 5* or *Ocean heat flux model* of D-Flow FM, which is based on Gill (1982) and Lane (1989) and is specially calibrated for the North Sea (but can be applied to large lakes aswell).

In order to use this heat flux model, the relative humidity, air temperature and cloudiness must be defined as input. For this model, a specially varying external forcing file is used which specifies these parameters with a time step of 180 minutes.

The heat losses caused by convection and evaporation, are functions of the defined wind speed and air pressure. These are also given as spatially varying external forcing files, with a time step of 180 minutes. The meteorological data are taken from the ERA-Interim analysis, which is a global atmospheric forecasting system (Berrisford et al., 2011). The used ERA-Iterim air pressures by ECMWF (Europees Centrum voor Weersverwachtingen op Middellange Termijn) follow from a combination between an atmospheric and an ocean-wave model.

Delft3D-FM calculates the effective back radiation as well as the heat losses due to convection and evaporation. It even accounts for free convection of latent and sensible heat in case air density and water density facilitate free convection.

Wind

In order to include the effect of wind on the flow field, it must be included as an external influence. The wind exerted force is included in the water movement equations as shear stress. In order to determine the magnitude of the exerted windforce, a quadratic equation is used (Wilson, B.W., 1960) that describes the shear stress as function wind speed, air density and a non-dimensional drag coefficient:

$$|\tau_s| = \rho_a C_d U_{10}^2 \tag{C.3}$$

with:

ρ_a = the air density
C_d = the drag-coefficient which depends on U_{10}
U_{10} = the wind speed at 10 meters above the water surface

The drag coefficient depends on the wind speed and can be determined with several methods. For this model set-up, the Charnock (1955) dependency is used. For further explanations on the different methods, the Delft3D-FM user manual can be consulted. Table C.2 summarises the models surface forcing properties.

Table C.2: Summary of surface forcing fields.

Forcing type	Units	Timestep	Longitude points	Latitude points
Dewpoint	C	180 min	45	33
Air temperature	C	180 min	45	33
Cloud area fraction	%	180 min	45	33
Northward wind	m/s	180 min	45	33
Eastward wind	m/s	180 min	45	33
Air pressure	Pa	180 min	45	33

C.1.2.5 Freshwater discharges

The modelling domain is fitted with almost 900 fresh water discharges around the North Sea. These discharges are base on E-HYPE data, which is a hydrological model that forecasts large-scale water balances with a daily time step. This pan-European water model calculates (amongst others) the daily discharges for the European continent. In this model, monthly (depth averaged) means are used based on data for the years 1989 until 2013. Moreover, the data includes the specific river water temperatures and a constant salinity value of 0.001PSU is used to depict fresh water.

Six of these E-HYPE discharges are replaced by actual discharges obtained from Waterbase to improve the accuracy of these important water sources. Instead of monthly means, these are given with an interval of 24 hours. The temperature data are not available for these six discharges, so a constant value of 11C° is used. The six replaced discharge data sets are given below.

- Den Oever Buiten
- Haringvlietsluizen Binnen
- Ijmuiden Binnen
- Kornwerderzand Buiten
- Maassluis
- Schaar van Oude Doelen

C.1.2.6 Time frame

The time zone of 3D-DCSM-FM is set to GMT+0 hours. All the phases of the prescribed boundary conditions are also prescribed relative to GMT+0 hours making all the output of the same time zone.

Computational time

Using Deltares' h6 cluster, the model set-up takes around 29 hours to compute one calendar year of output using five nodes with four cores each. The maximum time step is set to 200 seconds leading to an average time step of 196 seconds. For computations with adjusted grids around the island, the computational time step could be reduced if necessary.

Spin-up and initial conditions

For the original model, the initial water level is set to zero elevation with stagnant flow conditions throughout the domain. The salinity is set to 35.1PSU and the temperature is set to 5.5°C for the whole domain. Through testing, a spin-up time of one complete calendar year was deemed sufficient for southern North Sea predictions.

C.2 Boundary instability

In order to produce reliable case study results, instabilities may not be present as it will be unclear whether the impact results are actually a consequence of the island, or the instability.

During the initial impact testing, unexpected high effects of the island were computed in the northern North Sea, indicating the possibility of small instabilities.

Because the output variables did not seem to 'explode', the error did not seem to be the result of a local Courant-Friedichs-Lewy condition violation, which guards the numerical stability for a grid cell. Velocity magnitude maps were used to identify the location of instability that causes faulty results in the northern North Sea. Through these velocity magnitude maps, instabilities were explored at the southern model domain boundary.

Figure C.3 shows the near-bed velocity magnitude near the southern boundary and the unusual jet-like structures. Some of the grid cells in these jets produced velocity magnitudes of up to 5m/s. Such velocities magnitudes and jet-like phenomena are highly unlikely near the bed and indicate a form of numerical instability. The original model is only meant to be used for shelf investigations. However, this instability outside the shelf is likely the reason for unrealistic results on the northern part of the shelf.

There will almost always be a transition zone near the boundary since there are mismatches between the lateral boundary forcing values and the values calculated by the model itself. Especially at boundaries with high water depth that have little dissipation, these mismatches are more likely to escalate. Most models have such mismatches, however for this boundary with water depths up to five kilometres the mismatch seems to grow out of proportions.

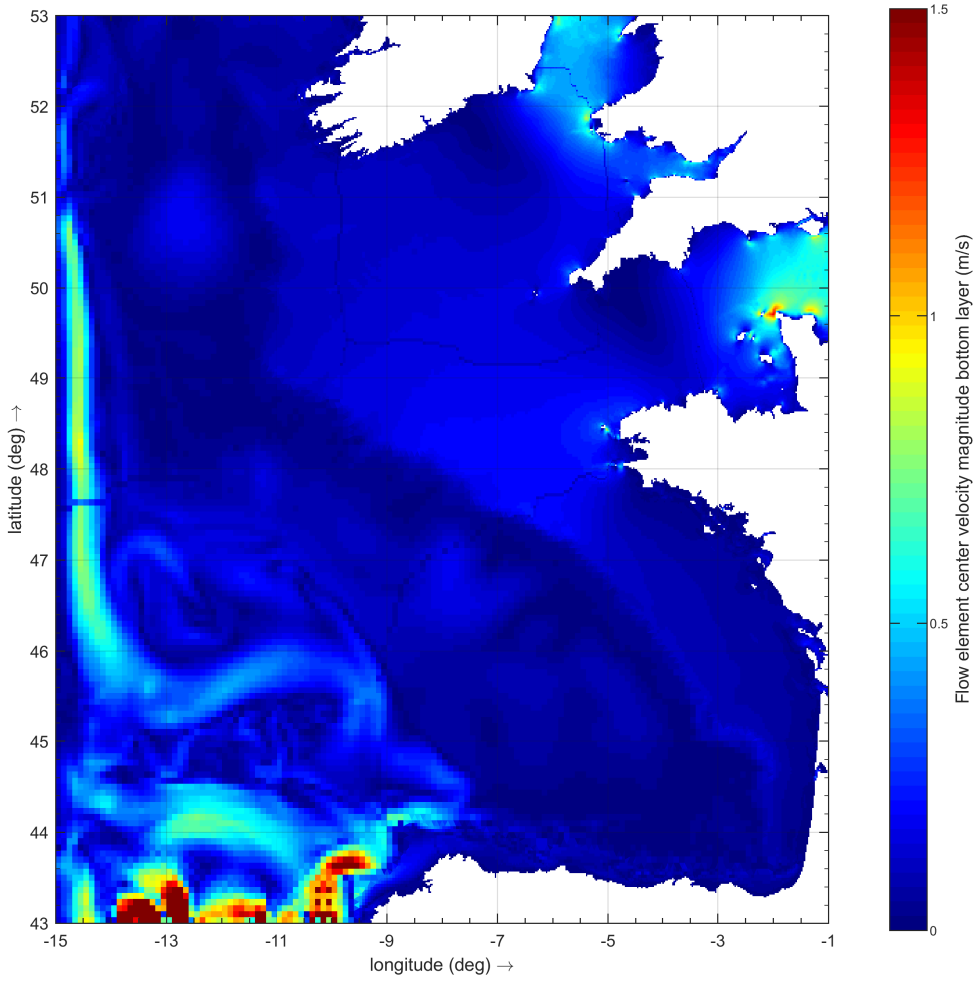

Figure C.3: The near bed velocity magnitude profile at the southern boundary of the original model set-up after two years of spin-up.

In order to reduce this boundary instability, model adjustments had to be made. In the original set-up, some extra dissipation is already present at all boundaries in order to prevent escalating mismatches. This is done through the presence of strokes with enlarged viscosity values. These strokes have a width of two cells along all boundaries and impose a local viscosity of 2000Pa·s, compared to the viscosity of 0.1Pa·s in the rest of the domain.

To improve the model, several test runs have been made with different model interventions to find the most suitable work-around or model improvement. An overview of these adjustments can be found in Table C.3.

Table C.3: Adjustments made to reduce southern boundary instability.

Model adjustment	Description
1	Boundary advection = 0
2	Southern boundary viscosity = 20.000
3	Southern boundary viscosity of 2.000 extended to 5 cells
4	Decreasing the maximum time step to 100 sec
5	New boundary temperature and salinity forcing conditions
6	Combinations of the other adjustments

First, an extra conditions was added at every boundary. This boundary condition imposes zero advection through the boundary. Even though this intervention did not solve the instability, it did slightly improve validation results on the southern North Sea.

Tests were carried out with the boundary strokes of increased viscosity. Several test were carried our with higher viscosity values up to 20.000 $Pa \cdot s$, and with an expended width of up to 5 grid cells. Extending the width did not have much impact, but the increase of viscosity up to 20.000 $Pa \cdot s$ did seem to suppress most of the boundary instability. Moreover, the maximum time step was reduced to 100 seconds, but this did make any noticeable difference.

During the testing phase, an improvement was made to the D-Flow FM module. This improvement allows the user to impose temperature and salinity conditions at any specific water depth, as opposed to the old version which required equally spaced conditions along the water depth. These conditions for the old module were obtained through interpolation of the original data at particular depth. Tests were also carried out with the new D-Flow FM module, imposing temperature and salinity conditions at standard depths instead of equally spaced depths. This new form of boundary forcing greatly improved the model performance at the southern boundary.

Since the change in lateral temperature and salinity forcing can be seen as a model improvement compared to the increased boundary viscosity which is more of workaround, it is the favoured adjustment out of the two options.

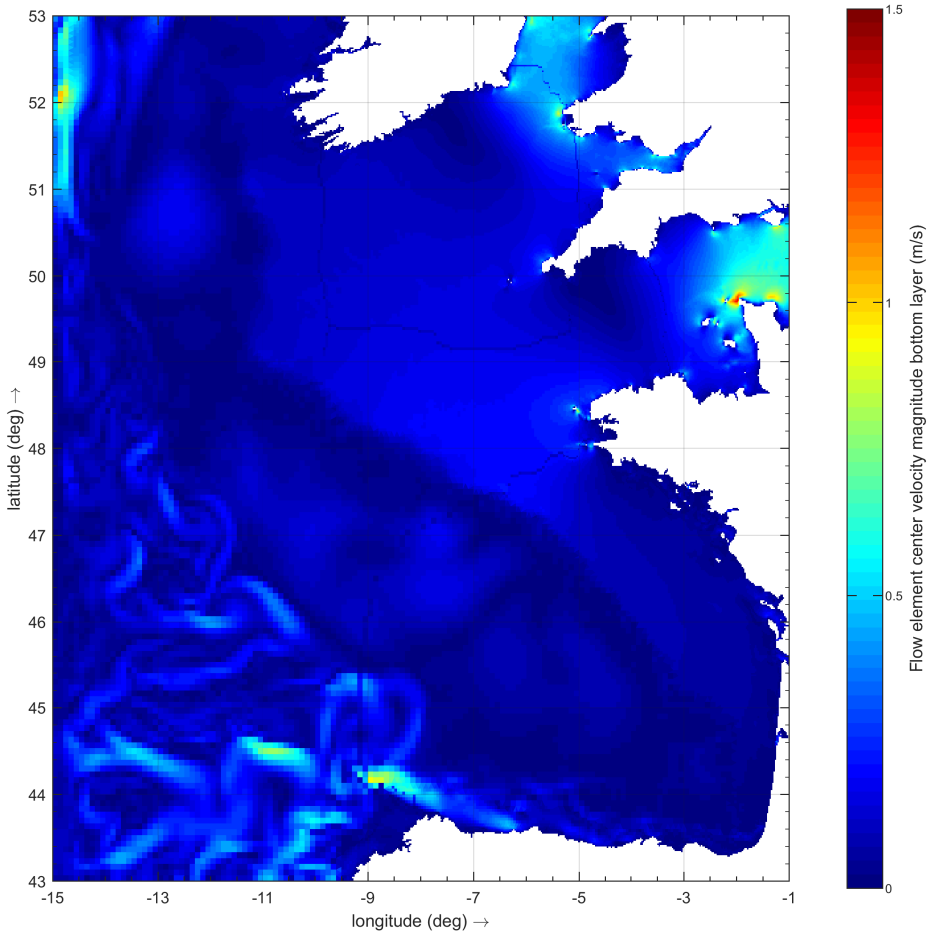

Figure C.4: The near bed velocity profile at the southern boundary with the new boundary conditions.

Combinations of all the adjustments were also made, leading to a final model adjustment including improved lateral boundary forcing and an additional boundary condition imposing zero advection. The new near bed velocity magnitudes are plotted in Figure C.4, showing much more probable velocity magnitudes around the southern boundary. No more jet-like phenomena are present.

The model has been revalidated for the southern North Sea measurements, showing improved results for water levels, sea surface temperatures and salinity, and stratification. This full revalidation has been carried out by Zijl and Veenstra (2018) for the new model set-up. No further quantitative validation will be carried out in this report. The northern shelf area now shows converging outputs and this model set-up is deemed sufficiently accurate for the intended case study of artificial islands.

C.3 Modelling spin-up

In numerical simulations, spin-up is an important phenomenon that needs to be taken into account. Numerical models (such as Delft3D-FM) require both initial conditions and boundary conditions in order to start and generate estimations for future scenarios after the model's start date. Due to intrinsic issues such as numerical simplifications and interpolated boundary conditions, the model will initially produce unreliable results. During the initial phase, the model will need to stabilise and converge to its own preferred statistical equilibrium. This is known as a model's spin-up period. Once the spin-up period has passed, the model can be used to retrieve accurate predictions.

If a model were to be extremely accurate and if it had perfectly accurate initial conditions and boundary conditions, the spin-up time would not exist. In reality however, this is almost never the case. The spin-up time mostly depends on the time that is needed for boundary enforced disturbance to travel across the modelling domain. Simultaneously, the spin-up time also depends on the damping of numerical wiggles induced due to large differences between the boundary and initial conditions.

While the travelling velocity of enforced disturbances can be predicted rather easily (for instance using the shallow water equation for the tidal propagation), the damping of numerical wiggles is much harder to predict. This depends on many factors such as numerical damping, physical damping and the type of boundary condition.

To make sure the spin-up time taken for this case study set-up is sufficiently long, tests were carried out for several locations on the shelf. Since density stratification is dominated by temperature and salinity, spin-up tests were carried out for both parameters. The locations far from the shore are mainly thermally stratified, while near shore locations also experience high salinity fluctuations due to river influences.

Figure C.5 shows that the temperature spin-up time for off-shore locations such as the Dogger Bank is around two years. After one year, the largest portion of the difference between the two runs has been overcome. After two calendar years it seems no further convergence takes place.

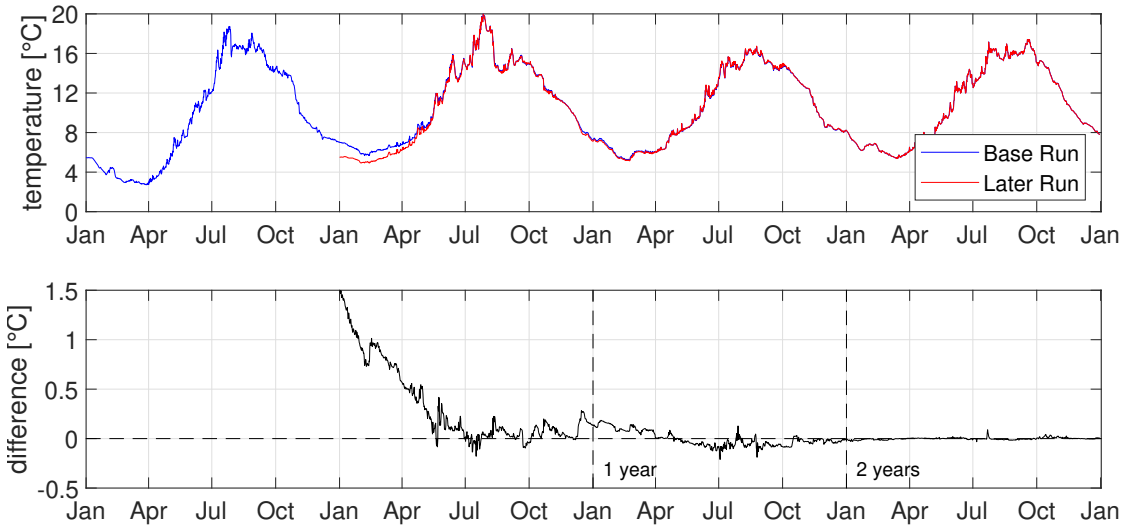

Figure C.5: Temperature comparison at location Terschelling 235km (Dogger Bank) between two runs with equal initial conditions but different start dates.

Whilst water temperatures are mainly dependent on heat exchanges between the atmosphere, salinity is mainly dependent on the interaction between oceanic and river inputs. The time it takes for salinity influences to reach the middle of the North Sea is much longer than for near shore areas. Nevertheless, Figure C.6 shows that the spin-up time for salinity is also around two calendar years.

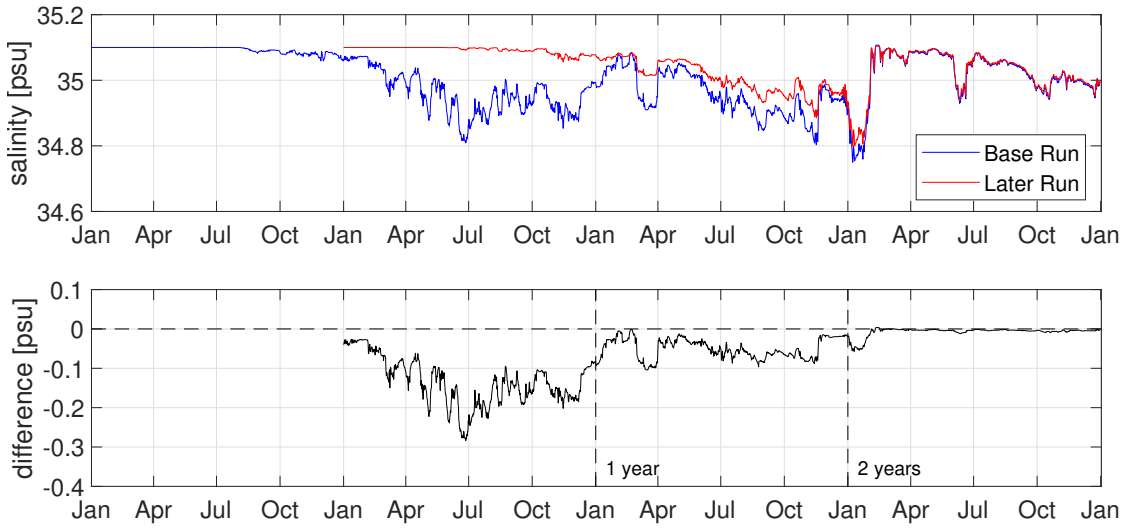

Figure C.6: Salinity comparison at location Terschelling 235km (close to the Dutch shore) between two runs with equal initial conditions but different start dates.

Closer to the shore the convergence happens slightly faster for salinity and temperature, since they are mostly dependent on river inputs located nearby.

Two years of spin-up time is deemed enough for this research objective with artificial islands near the Dutch coast and around the Dogger Bank. Do however notice that the difference between two runs never quite becomes zero. This is the result of chaotic behaviour, either numeric or physical. No further investigation will done into the cause of this chaotic behaviour. However, during the case-studies it is import to quantify the (location dependent) chaotic behaviour in order to separate it from the actual impact analysis.

C.4 Island implementation

After the adjustments to the basic model set-up were done, the model was further adjusted to facilitate the impact analyses. The implementation of an island in the model requires an adjusted grid with refinements in the area of interest. This makes sure that all relevant processes are correctly represented and allows for a circular profile of the 6km^2 island. This island size is based the island investigation carried out by Gerrits (2017).

C.4.1 Grid refinement

First, the grid was refined three times, with a factor of two. This leads to a total refinement of factor eight around the island areas. The capabilities of Delft3D-Flexible Mesh were utilised through the use of flexible grid compositions. Triangular and quadrilateral grid cells form the transitions from the original grid cell size towards the refinement, as can be seen in Figure C.7. This type of refinement is used for every single island location and stretches an area of ten by ten original grid cells.

For computational efficiency, the unstructured grid must satisfy the orthogonality requirements. This means that the corners of two adjacent cells are positioned on a common circle, while the centre of each cell falls within its boundaries. The grid refinement of Figure C.7 has been checked on orthogonality and uses the minimal amount of triangle possible to refine the required area in order to keep the computational efficiency as high as possible.

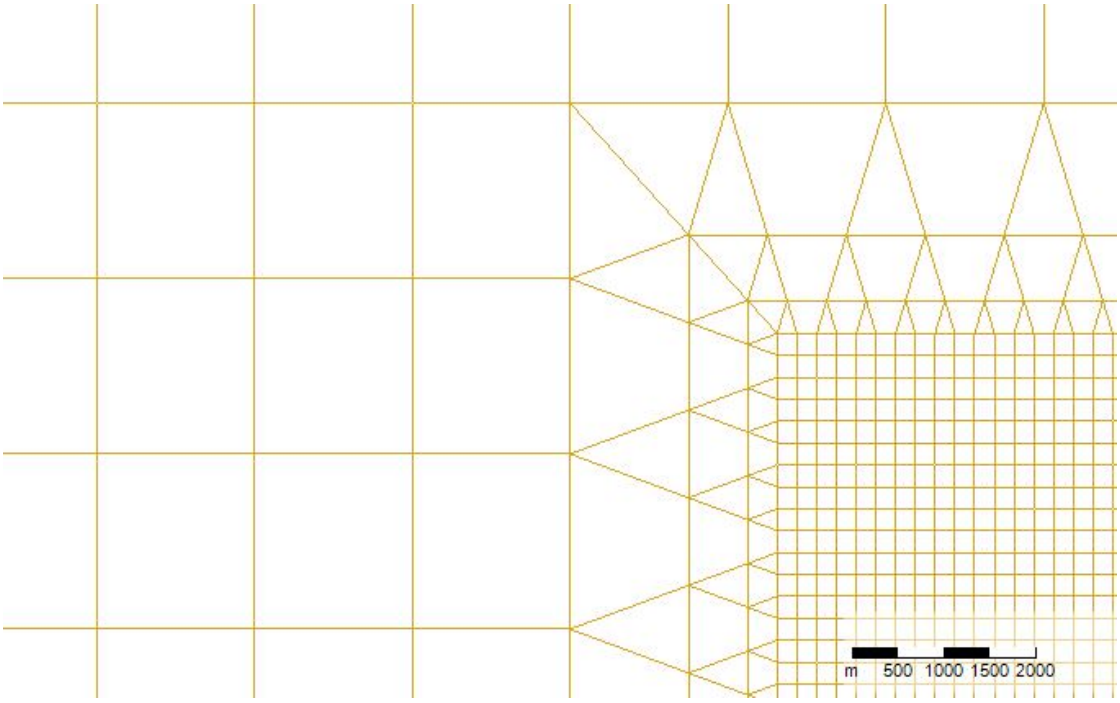

Figure C.7: Transition from the finest original grid size (1nm) to the refinement of factor eight used around island locations.

Since the bathymetry was defined with samples at each grid node, the refinement creates new nodes without depth values. To determine the depth of each new node within the refinement area, the samples of the original bathymetry were used for triangular interpolations. This way, each new node received its own depth value to form the new and very similar bathymetry profile of the model.

The grid refinement leads to an increase in computational burden. On one hand, the amount of grid cells is increased leading to a higher computation time. On the other hand, this refinement creates grid cells with a much smaller size which leads to a demanded decrease in the computational time-step as the Courant criterion for hydrodynamic modelling must still be satisfied. This Courant criterion indicates the maximum times step to prevent numerical instabilities. With the new grid refinements applied, the burden for an one calendar year computation increased from around 29 hours to almost 80 hours. Because of this, no further refinement was applied.

C.4.2 Observation points

A full year analysis can not be carried out with full map files for this research project with small output time steps, as the created files will be too large for the available storage space. To do an impact analysis without maps files, a profile of observation points around the islands is made. To do so, the flow ellipses of Section 4.4.2 are used to define the main direction of the tidal flow. The directions most interesting to the analysis are parallel to the flow main flow direction and perpendicular to the main flow direction. Table 4.2 summarise the chosen main direction of interest.

Through exploratory modelling runs, an impact range of around 15km away from the artificial island was expected. A deliberation between storage space and accuracy determined the use of 32 observation points for each island. An observation point was placed at every 2.5km in each direction of interest, with two additional observation points close to the islands edge.

Figure C.8 visualises this basic set-up of observation points (in this case for North-South and East-West directions), with similar observation point spacing in each direction. It coincides with the set-up of islands B and E, which have the same main directions of interest. For other the other islands, the observation points are all rotated 45 degrees, in order facilitate the correct directions of observation points.

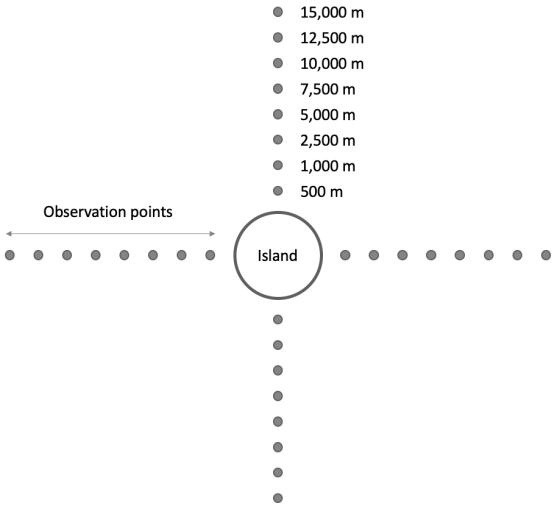

Figure C.8: The basic set-up of observations points used for the impact analysis.

D Additional output figures

This chapter contains additional post-processed model output, supplementary to the output of in Chapter 5. It contains z,t-diagrams of the temperature and salinity at each location, and the stratification and chaotic behaviour over the year. Moreover, the timing differences at 2.5km at location C and the residual current maps are included.

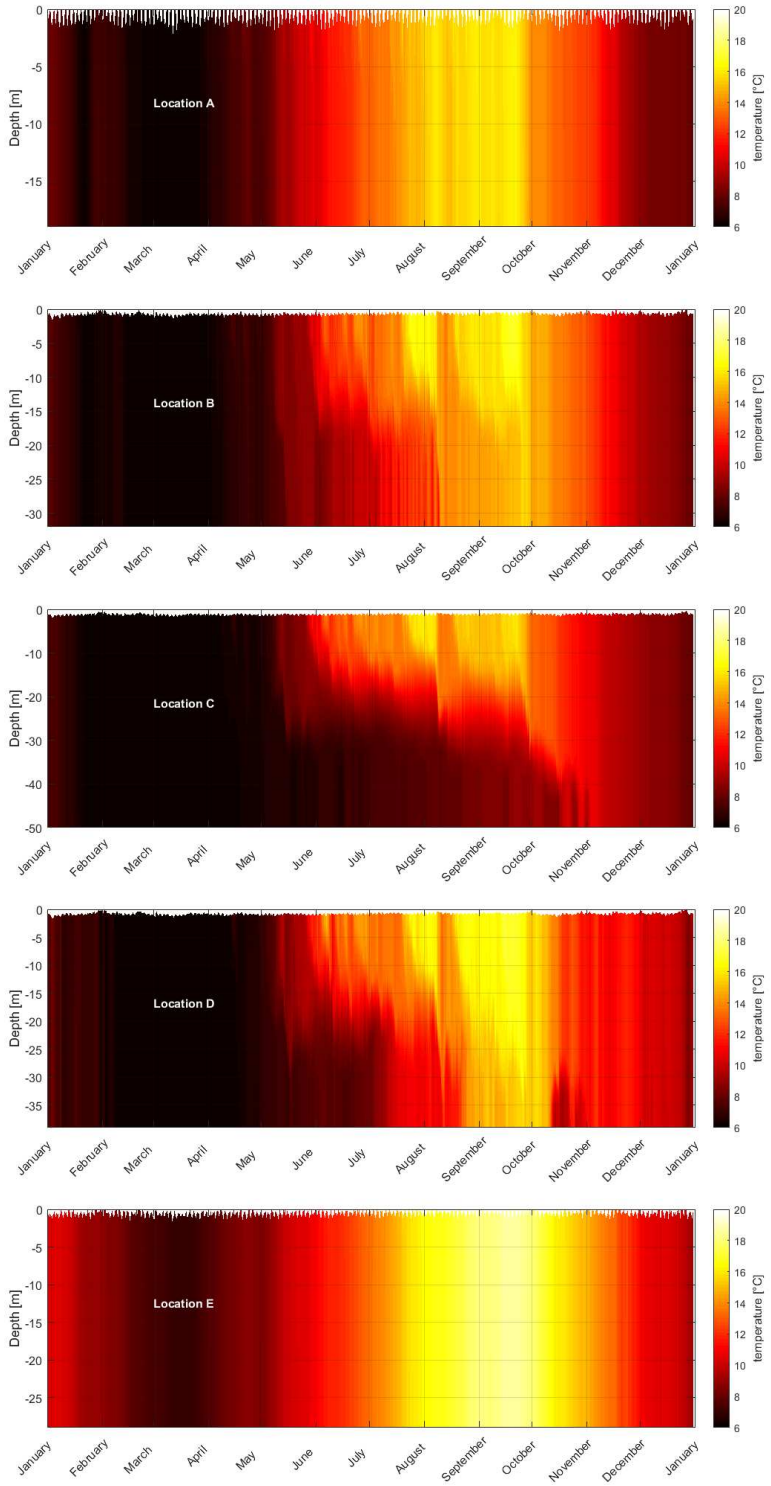

Figure D.1: The temperature distribution over depth, at each location for one calendar year (2016).

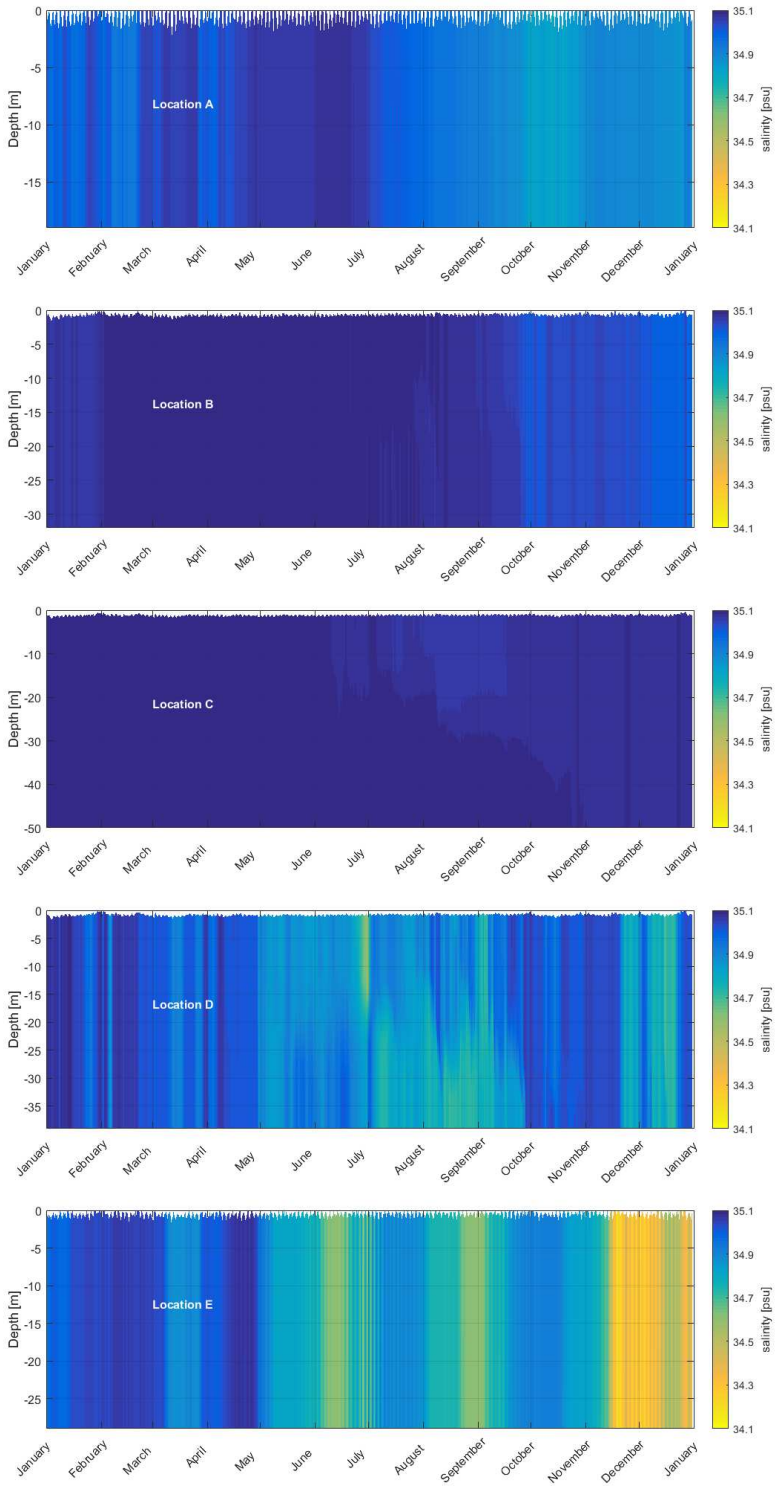

Figure D.2: The salinity distribution over depth, at each location for one calendar year (2016).

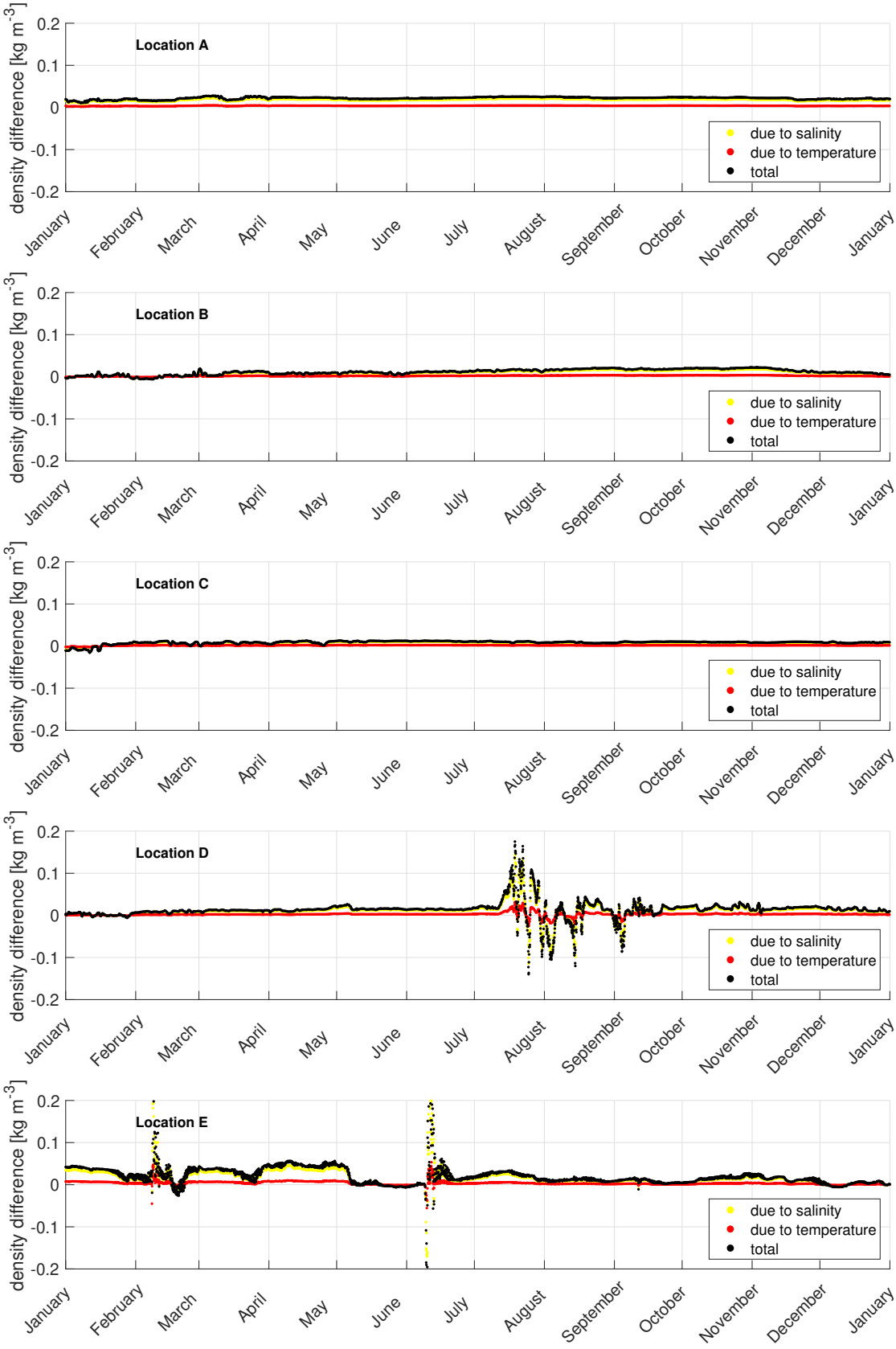

Figure D.3: Chaotic behaviour of density for all locations for the calendar year 2015.

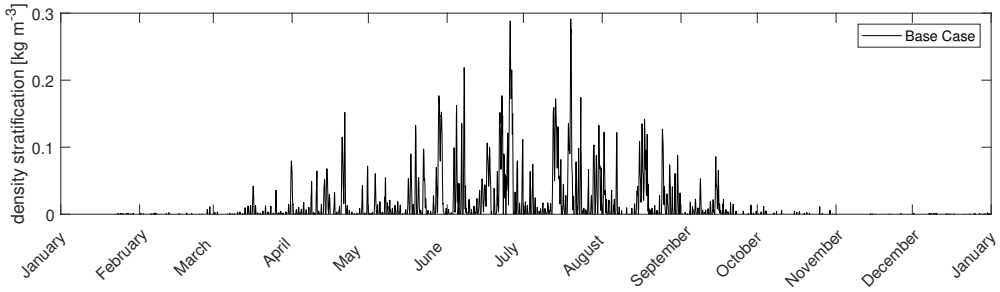

(a)

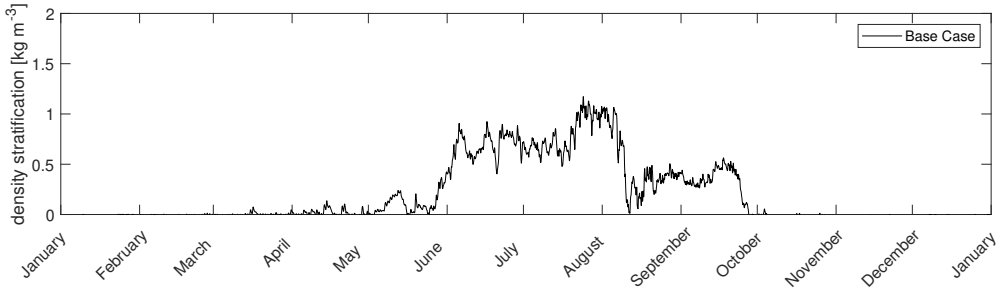

(b)

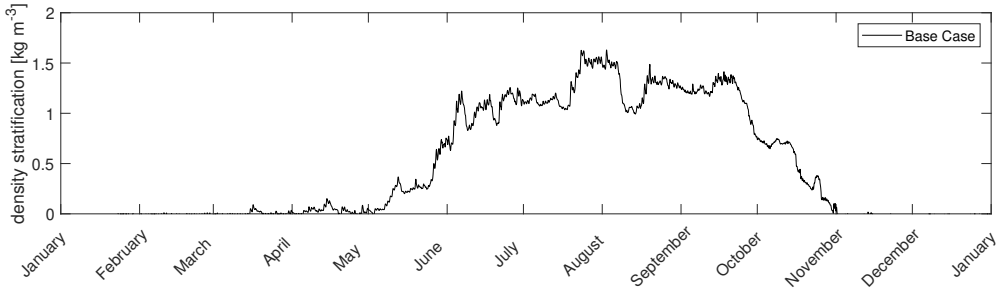

(c)

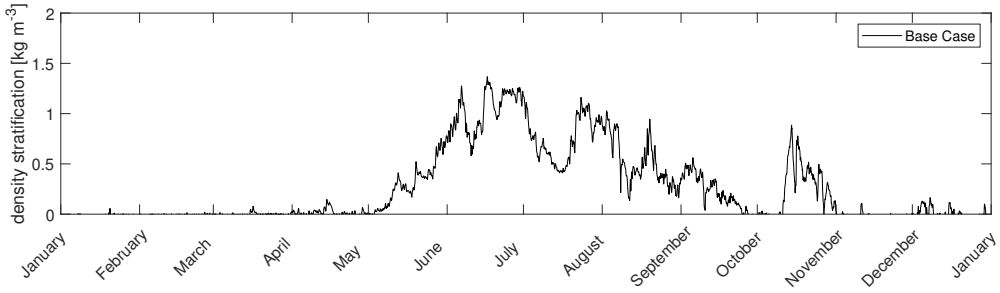

(d)

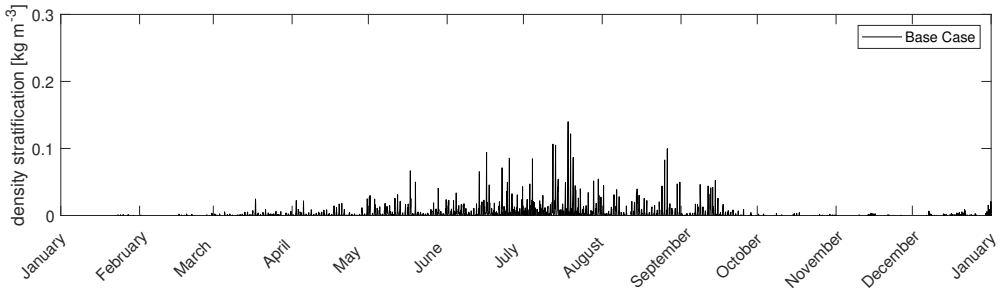

(e)

Figure D.4: The density difference between the water surface and bottom for all location. Notice the different scale for stratification.

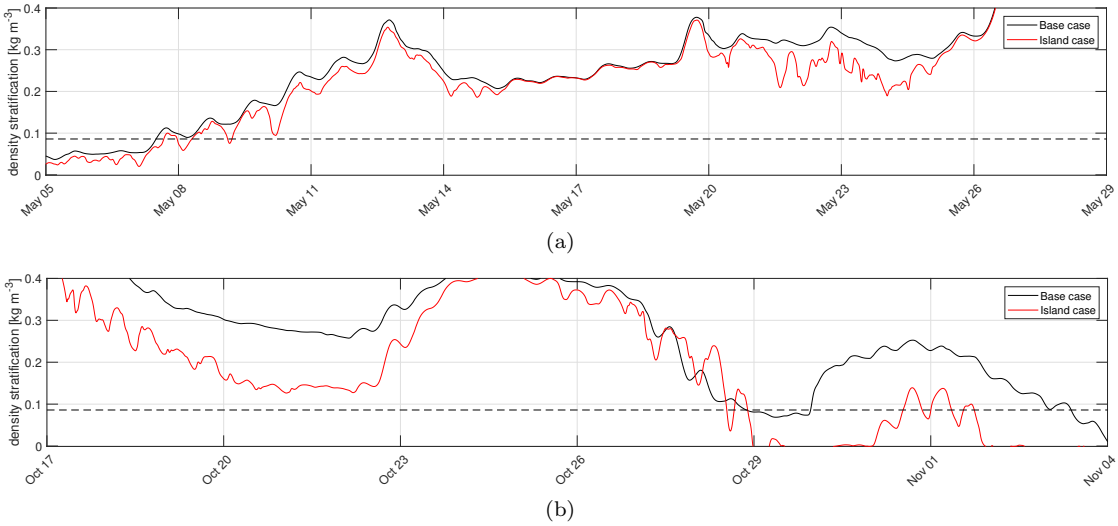

Figure D.5: Density stratification for the base case and island C case at 2500 metres to the East. (a) The commence of the extended stratified period. (b) The conclusion of the extended stratified period.

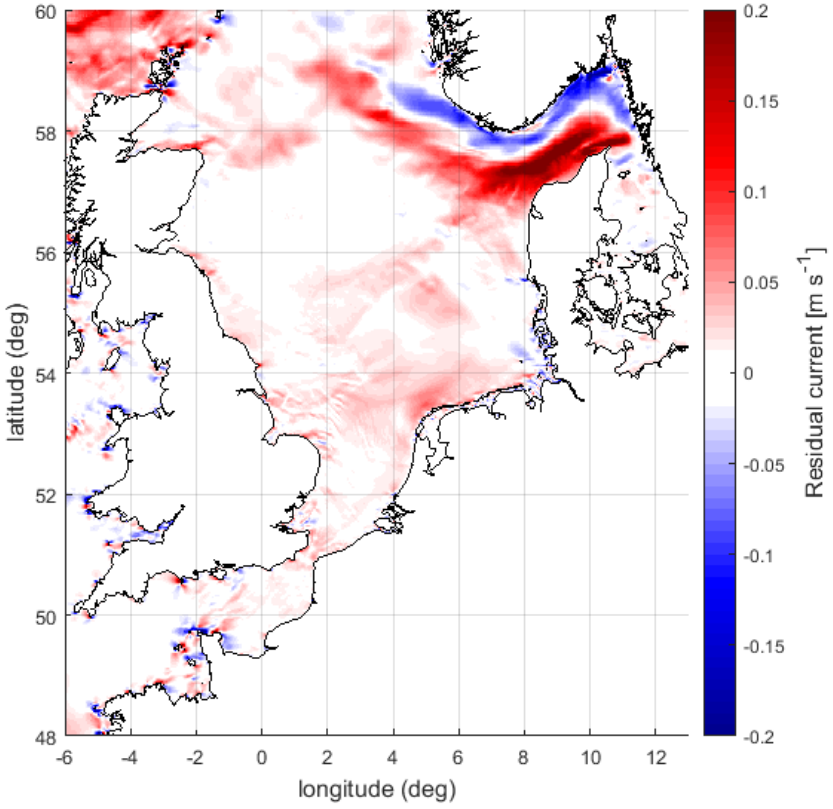

Figure D.6: Baseline depth-averaged x-component of the residual flow velocity in 2016. Positive values indicated a residual current in the positive northern y-direction.

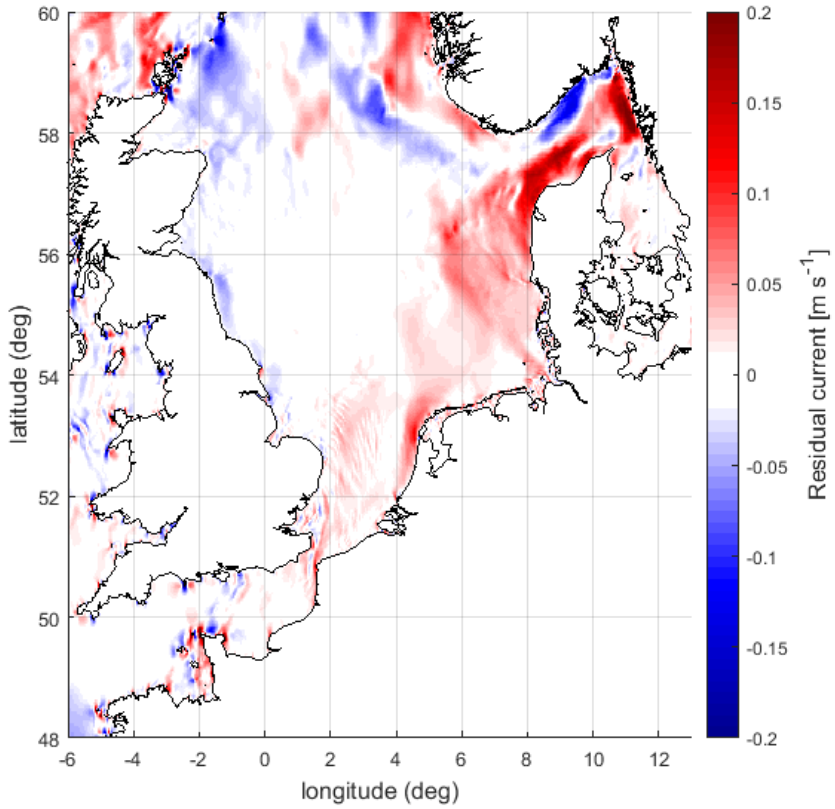

Figure D.7: Baseline depth-averaged y-component of the residual flow velocity in 2016. Positive values indicated a residual current in the positive eastern x-direction.

E Additional literature figures

This chapter includes additional figures from literature. The baroclinic residual currents, biological regime consequences and origin of non-organic nutrients are included.

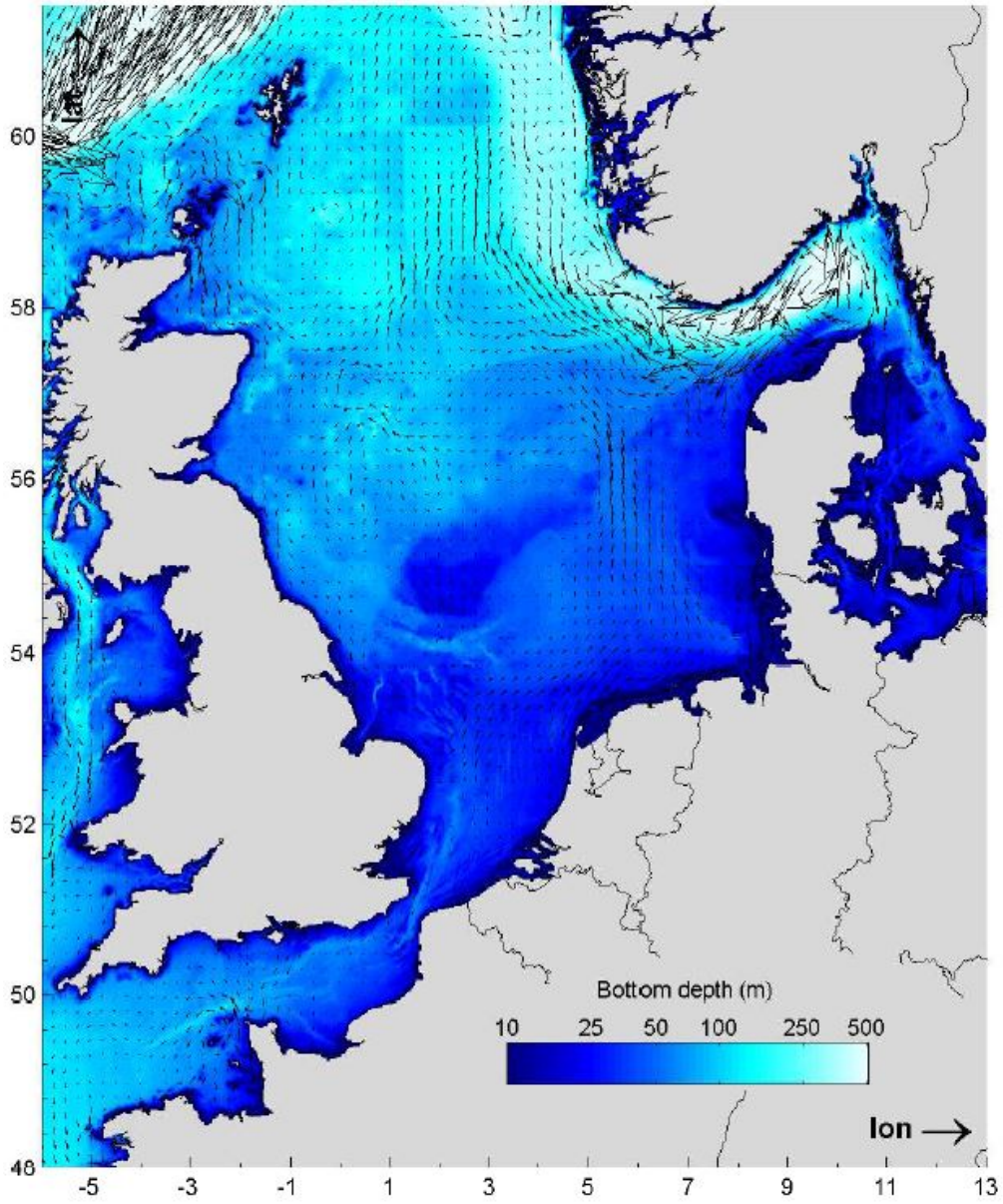

Figure E.1: Annual mean, depth integrated, horizontal velocities for baroclinic flow. For clarity only vectors are shown at every tenth grid cell. Magnitude is indicated with the vector lengths, while the bottom depth is plotted on a logarithmic scale (Linden, 2014).

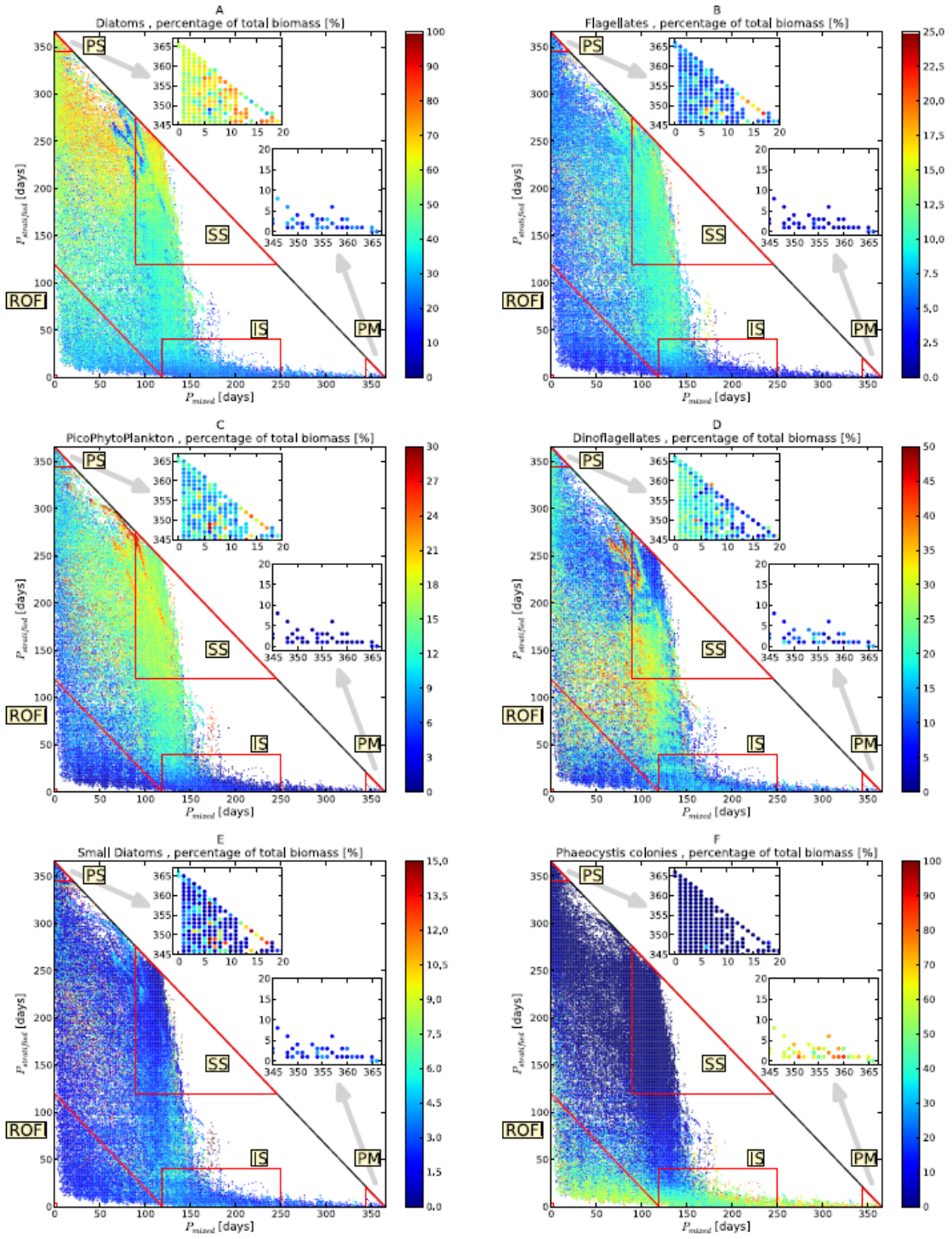

Figure E.2: Distribution of phytoplankton with respect to the different regimes, in percentage of total biomass. (a) Diatoms, (b) flagellates, (c) picophytoplankton, (d) dinoflagellates, (e) small diatoms, and (f) Phaeocystis. Adapted from Leeuwen et al. (2015).

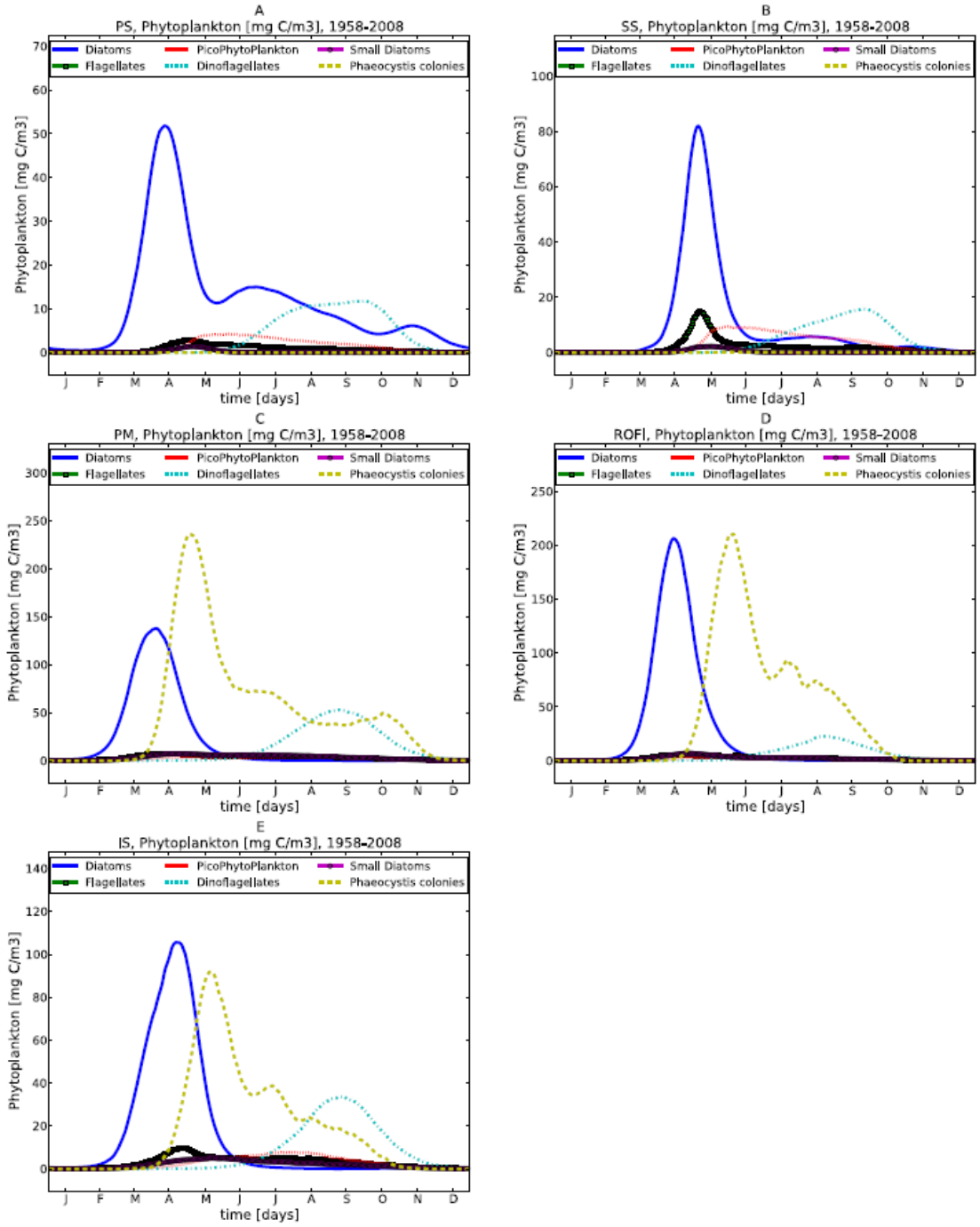

Figure E.3: Annual mean phytoplankton dynamics for the five different regimes. Mean seasonal cycle based on spatially and depth-averaged values for the ERSEM-BFM phytoplankton groups for the largest polygon in each regime. (a) Permanently stratified area, (b) seasonally stratified area, (c) permanently mixed area, (d) ROFI area, and (e) intermittently stratified area. Adapted from Leeuwen et al. (2015).

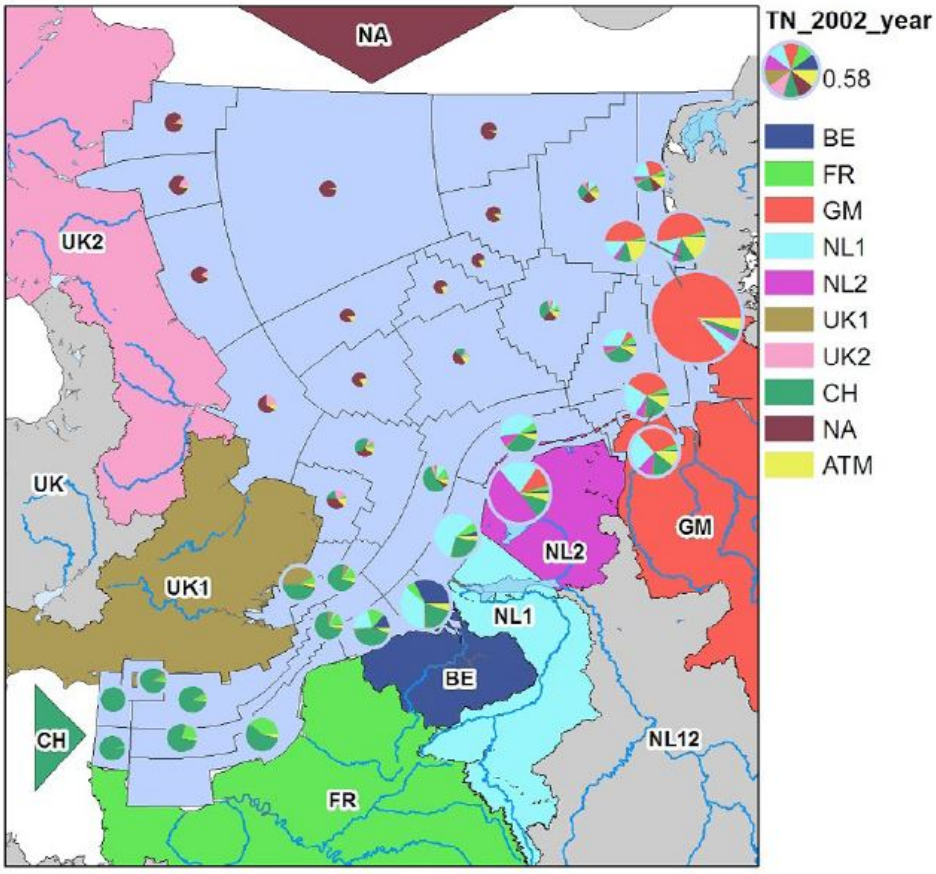

Figure E.4: The origin of nitrogen nutrients in different parts of the North Sea (Los et al., 2014).